CHANNEL CHANGES OF THE SAN XAVIER REACH OF THE SANTA CRUZ RIVER, TUCSON, ARIZONA 1971 - 1988

by

Albert Lynn Guber

A Thesis Submitted to the Faculty of the

DEPARTMENT OF GEOGRAPHY
AND
REGIONAL DEVELOPMENT

In Partial Fulfillment of the Requirements
For the Degree of

MASTER OF ARTS
WITH A MAJOR IN GEOGRAPHY

In the Graduate College

THE UNIVERSITY OF ARIZONA

1988

STATEMENT BY AUTHOR

This thesis has been submitted in partial fulfillment of requirements for an advanced degree at The University of Arizona and is deposited in the University Library to be made available to borrowers under the rules of the Library.

Brief quotations from this thesis are allowable without special permission, provided that accurate acknowledgment of source is made. Requests for permission for extended quotation from or reproduction of this manuscript in whole or in part may be granted by the copyright holder.

SIGNED: 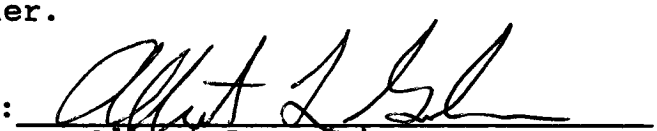
Albert Lynn Guber

APPROVAL BY THESIS DIRECTOR

This thesis has been approved on the date shown below:


Dr. Richard W. Reeves
Professor of Geography

9 Dec 1988
Date

ACKNOWLEDGEMENTS

Throughout my college education, many people have taught and supported me in my study of geography, and in the production of this thesis in particular. Special thanks is extended to Professor Richard Reeves, my thesis director, for devoting long hours of review and comment to the many preliminary drafts of this thesis. Without his guidance and expertise in the field of fluvial geomorphology, this project would not have been possible. I also thank my other committee members, Professor D. Robert Altschul and Professor Thomas F. Saarinen for their suggestions and advice. Dr. Robert Webb of the Hydrology Division of the United States Geological Survey in Tucson was instrumental for providing the funding necessary to purchase expensive aerial photography which made this project possible.

Professor Charles F. Hutchinson and Professor Robert Schowengerdt deserve credit for allowing me to train on and use the computer facilities at the Arizona Remote Sensing Center in the Office of Arid Land Studies. Michael Sicurello, John Regan, and Douglas Kliman provided technical assistance on the use of the Office computer systems and software packages necessary for map generation and analysis in this project.

Finally, special thanks goes to my parents for their on going support of my academic studies from the beginning.

Albert L. Guber
Tucson, 1988

TABLE OF CONTENTS

LIST OF FIGURES

LIST OF FIGURES (CONTINUED)

LIST OF TABLES

ABSTRACT

Aerial photographs of the San Xavier reach of the Santa Cruz River near Tucson, Arizona, were used to interpret four planimetric surface classes and to generate hydraulic variables for analysis of channel change. Variables were regressed to determine the extent to which channel form is controlled by "catastrophic" flows. Channel width analysis, in combination with channel overlay maps provided the means of assessing spatial variations in channel form through time. Results indicate that the study reach is dominantly controlled by equilibrium conditions rather than catastrophic events as determined in previous studies in arid and semi-arid climates. The definition and implementation of the braid index variable as a measure of channel pattern in this study account for measurement errors inherent in defining hydraulic variables in a channel which changes pattern through time. Such errors may be critical sources of inconsistency in previous studies of channel change in fluvial systems.

CHAPTER 1

INTRODUCTION

> "In reality, the fluvial system is a physical system with a history. Present form is the product of past and present processes and conditions..."
> -Knighton, 1984 p.162

The purpose of this study is to determine the extent to which the channel of the Santa Cruz River near Tucson, Arizona, is a result of catastrophic floods. Studies of channel morphology in arid and semiarid climates indicate that catastrophic floods are primarily responsible for determining channel form. Channel relaxation (recovery) periods following catastrophic events in these climates may require decades or, perhaps, centuries of time. In contrast, results of studies in humid regions indicate that channel form is adjusted to frequent, moderate flows through the fluvial system. Further, relaxation periods are measured in weeks or months, relatively short time frames by comparison to channels in dry regions. This study examines channel

changes and responses of an ephemeral reach of the Santa Cruz River to a series of discharge events between 1971 and 1988.

Catastrophic floods are discharge events whose forces act to redefine the form of a river channel through extensive bank erosion, creating a post-flood channel different in form than pre-flood conditions. Most fluvial systems in arid and semi-arid regions are characterized by relatively easily eroded banks due to the sparsity of vegetation and low cohesiveness of coarse grained alluvial sediments comprising both bed and banks of these channels (Leopold and Miller, 1956; Schumm, 1961). Flow events, often associated with thunderstorm activity, are generally of short duration but high intensity relative to normal no flow conditions. Thus, catastrophic channel changes are prone to, and in fact do, occur in arid and semi-arid regions more easily than humid regions as a result of inherently lower catastrophic thresholds in dry climates.

In channels similar in form to that within entrenched "arroyo" reaches of the Santa Cruz River in Southern Arizona, catastrophic thresholds are reached when the volume of water routed through the system is sufficient to over top channel banks (cause flooding) and precipitate extensive floodplain and lateral channel

erosion (Pearthree and Baker, 1987, p.1). The resulting channel from such events is controlled by a new-post flood channel form which determines a new set of hydraulic variables within the system. In this respect, catastrophic events represent abrupt interruptions to the development and/or stability of a fluvial system in time (Graf, 1979, p.14).

Recent studies of river systems in dry climates similar to the present day Santa Cruz River indicate that catastrophic events result in extensive channel widening and channel aggradation due to large amounts of suspended sediment transported and deposited by these flows (Nordin and Beverage, 1965; Burkham, 1972). Post-flood periods are subsequently characterized by channel degradation and narrowing due to the 'overfit' nature of the flood-widened channel to transport the relatively small post-flood flows (Dury, 1964). Further narrowing of the channel occurs as vegetation develops on the sides of the channel thereby increasing the probability of sediment deposition in these areas (Schumm and Lichty, 1963; Pearthree and Baker, 1987).

Four abnormally high discharge events along the Santa Cruz River near Tucson, Arizona, between 1971 and 1988 should have resulted in channel changes similar to those outlined above. In this model, each event should

cause extensive channel widening and floodplain destruction. Deposition should result as the flood recedes and the discharge is no longer able to transport large quantities of suspended sediment. Subsequent channel recovery periods should be characterized by gradual revegetation of channel surfaces ultimately leading to channel narrowing and degradation within the reach.

The study reach of the Santa Cruz River, as it exists today, is an arroyo which has developed over the past century. During this period the reach was transformed from a shallow stream interrupted by cienegas (marshes) in the upstream reaches into an arroyo with walls typically between 20 and 30 feet high (Cooke and Reeves, 1976; Waters, 1988). The present day arroyo is comprised of arroyo walls, a floodplain (consisting of terraces representing previous discharges), and the primary, or active, channel for the river system (Leopold et al., 1966, p.203). Flows within the channel are ephemeral and vary in intensity based upon the local precipitation regime.

The Santa Cruz River generally routes flow only during times of precipitation primarily associated with late summer monsoon and winter rainfall seasons characteristic of southern Arizona. Storms associated with the late summer monsoon season account for

slightly more than 50 percent of annual precipitation totals. These storms are typically convective thunderstorms which produce intense, short duration (rarely more than 30 minutes) rainfall events (Sellers et al, 1985). These events generally produce the annual peak discharge for years of normal (non-flood) flow. Contrasting, cyclonic winter storms, associated with low pressure systems during November, December, January, and February are typically less intense and last much longer in duration (several hours to a few days) than the summer events. On average, winter rainfalls amount to slightly less than 50 percent of the annual precipitation (Sellers et al, 1985). Two of the four highest annual peak discharges recorded in Tucson during the past 17 years, were generated by major winter storms within the Santa Cruz River basin (Webb and Betancourt, 1987). The remaining two large flows were associated with a deteriorating tropical storm and a hurricane, both occurring in October of different years. These flows surpassed thresholds of channel bank erosion and caused change, either minor or catastrophic, within the fluvial system.

This study examines recent channel changes along a 4.5 mile reach of the Santa Cruz River located south of Tucson near the San Xavier Mission (henceforth

called the San Xavier Reach) (Figure 1). Twelve years of aerial photographic coverage are used to identify four classes of ground surface within the limits of the arroyo walls. Each class represents a different stage of vegetation development and indicates the age of a surface relative to the other surface classes in the arroyo. Observation of changes in the classification of surface areas through time may provide information about previous locations of the channel as well as the limits of erosion and/or deposition during recent flood events. Of these surface classes, the primary channel, the unvegetated surface which routes all non-flood flows, is measured to generate hydraulic variables for analysis in this study.

Primary channel variables of width, sinuosity, wavelength, area, and an index of braiding are measured and then analyzed in a LOTUS spreadsheet program to identify and compare symptoms of channel change within the study reach. Measurements of variables are related to antecedent peak discharges by means of regression analysis, and trends in the data through time are compared to model expectations. A braid index is defined and included as a measure of channel pattern in subsequent regressions to adjust for systematic errors resulting from measurements of variables in a braided

Figure 1

San Xavier Study Reach Location

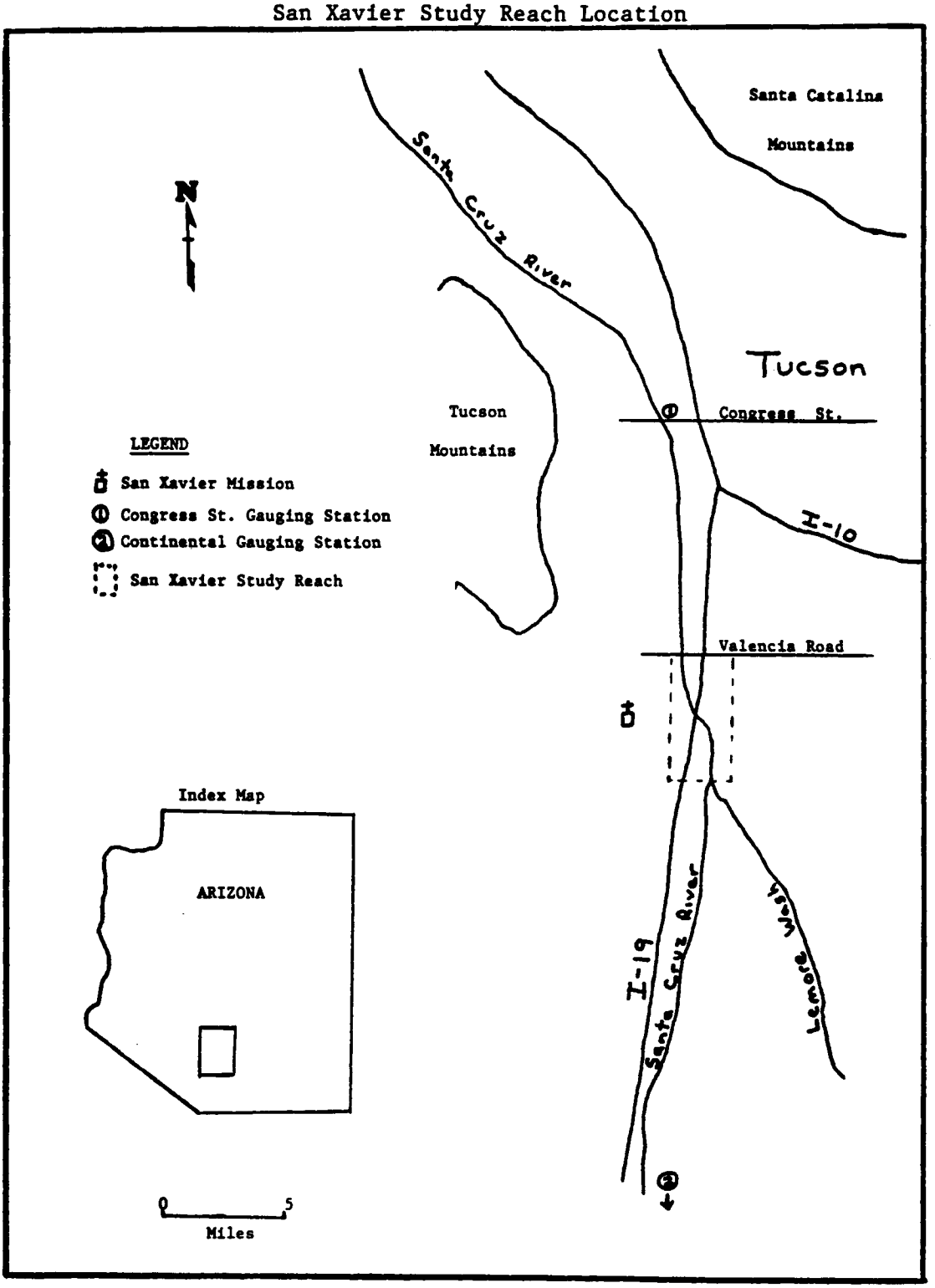

system. The braid index standardizes hydraulic variables to a single channel system thereby reducing errors associated with definition and measurement of variables for a channel which fluctuates between a single channel and braid pattern through time.

Assuming traditional models of channel change apply, major increases in channel width should result from flood events exceeding the threshold for channel bank erosion in the ephemeral system. Subsequent years of 'normal' flow should be characterized by channel narrowing as described above until some state of quasi-equilibrium (Leopold and Miller, 1956) between discharge and channel variables is achieved. The period of channel recovery (response) following a flood event should last more than ten years according to traditional models (Baker, 1977). Since planimetric area of a channel is ideally an integral measure of channel width, changes in channel area should follow the same pattern as, and be highly correlated to, channel width. Sinuosity and wavelength measures are, ideally, inversely related. As sinuosity increases, wavelength decreases. High discharges (floods) should straighten channel patterns due to extensive lateral bank erosion associated with these flows (Schumm and Lichty, 1963, p.80). Consequently, a primary channel of low sinuosity should be associated with large

prior discharges. As vegetation becomes reestablished in the flood-widened channel over time, the channel pattern should become more sinuous (Schumm and Lichty, 1963; Leopold et al., 1966). Therefore, sinuosity of the primary channel at a particular time should be inversely and wavelength positively correlated to the magnitude of preceding peak discharges. I hypothesize that the hydraulic relationships described above typify recent changes in the morphology of the Santa Cruz River system during the past 17 years of channel history (1971 - 1988).

In this study, a geographic information system (GIS) is used generate primary channel cross section and area data, and to register and overlay channel surface interpretations for 12 sets of photographs spanning the 17 year period. A GIS is a computer cartographic tool used to tie a database of information, in the form of attributes, to a system of polygons, points, and lines comprising digitized maps. Using a GIS, the ability to locate channel cross sections accurately from year to year, the ability to quickly obtain precise area measurements for the primary channel, and the opportunity to overlay several years of channel data, is facilitated and may help reduce measurement errors in this type of study.

CHAPTER 2

BACKGROUND AND LITERATURE REVIEW

Within the context of systems analysis, catastrophism and equilibrium theory provide frameworks for analysis of channel change in river systems. Typically frameworks of catastrophism best describe channel changes in arid and semi-arid regions while concepts of equilibrium seem best suited to studies of humid systems. Climatic factors characteristic of arid and semi-arid regions result in irregularity of both frequency and magnitude of flow in fluvial systems. In humid regions, the alternate situation often applies as perennial channels route flow throughout the year (Wolman and Miller, 1960). Although these climatic differences create situations in which one framework is often better suited for problem solving than the other, neither theory should be considered mutually exclusive of the other (Schumm and Lichty, 1965).

Catastrophism provides a framework for analysis of changes associated with individual events and how

these events ultimately impact on form and, thus, on process in geomorphologic systems. Three types of equilibrium defined by Schumm and Lichty (1965) - dynamic, steady state, and static equilibrium - on the other hand, perceive change in systems as continuous through time. The state of balance or stability between components (variables) of a system defines equilibrium in the truest sense of the word. The movement of a system toward this state by way of negative feedback (self-regulation) through time (relaxation time) provides the major focus of equilibrium theory. Thus, catastrophism provides a framework for the analysis of events which move systems away from stability while equilibrium focuses on periods of system movement toward stability. Since natural processes do not remain static through time, integration of both frameworks is necessary to understand the nature of channel changes through time in studies of fluvial systems.

Catastrophism

Catastrophism in fluvial geomorphology is used to study sudden abrupt changes in channel morphology (Graf, 1979). These changes redefine the form, and thus the processes, within a fluvial system. Schumm and Lichty (1965) provide two prerequisites for a catastrophic event: (1) The event must occur infrequently, and (2) at

a great enough magnitude to exceed thresholds for the equilibrium state of the system. Thus, catastrophic channel changes are frequently associated with abnormally high discharge events (floods) within fluvial systems. Catastrophism focuses on analyzing the effects of single events rather than gradual changes through time.

In arid and semi-arid climates, catastrophism is often the dominant framework for explanation of channel morphology. Thresholds for channel bank erosion are exceeded more frequently in dry than humid climates due to the absence of dense vegetation, the low cohesion of alluvial sediments, and the irregular nature of channel flows in these systems. When arid and semi-arid channels are redefined by catastrophic events, relaxation periods of channel adjustment may last in excess of 50 years since channel flows occur infrequently. Because the time necessary for these channels to readjust to 'normal' flow conditions may last as long, or longer, than the frequency with which catastrophic events occur, morphologies of these systems are said to be dominated by the rare catastrophic event.

In a study of the response of central Texas stream channels to floods, Baker (1977) demonstrates that regions with highly variable flood magnitudes seem to

have a great potential for catastrophic channel changes. He determines that in regions where flood events occur frequently, the threshold 'for meaningful work' (catastrophic threshold) decreases as a function of coarsening sediment loads. Baker attributes this condition to the fact that channel flows in arid and semi-arid climates are primarily controlled by overland flow as opposed to inflow of groundwater sources. Thus, he concludes that unique combinations of climatic and physiographic controls in these regions increases the potential for catastrophic floods.

Stewart and LaMarche (1967) hypothesize that the pattern of erosion and deposition resulting from a 1964 flood event in Coffee Creek, California, indicate that the channel morphology is dominantly controlled by catastrophic events. The flood caused extensive bank erosion destroying meadowlands and forests neighboring the channel and deposited coarse gravel not transportable by more frequent normal flows through the channel. Stewart and LaMarche conclude that the channel is unable to readjust to frequent flows and remains essentially fixed in form for long periods until reshaped by a subsequent catastrophic event.

Equilibrium Theory

For fluvial systems, Schumm and Lichty (1965) define three types of equilibria - dynamic, steady state, static - according to relative time frames within which different states of system balance are achieved. Concepts of dynamic equilibrium are based upon a cyclic time period spanning the age of the classic "erosion cycle" for a given drainage system. The foundations for dynamic equilibrium lie in the work of G. K. Gilbert, who, during the latter part of the nineteenth century, identified a cause-effect relationship between form and dominant processes over extensive intervals of geologic time. Concepts of dynamic equilibrium during cyclic time consider only time, geology, relief, and climate as independent variables which determine channel form.

Steady state equilibrium is maintained in systems during graded time periods lasting between 100 and 10,000 years. Concepts of steady state equilibrium consider changes within a fluvial system as fluctuations about or approaches to a steady state (average) condition (Chorley, 1962). Negative feedback (self-regulation) mechanisms causes a system to fluctuate about rather than move consistently away from the steady state condition. The graded time span is considered a subset of the longer cyclic time frame in that the pattern of long

term fluctuations about the steady state comprise gradual progressive change within the framework of cyclic time.

Conditions of static equilibrium pertain to time frames which last between instantaneous time and 100 years in length. Within these short time frames only water and sediment discharge are independent variables of channel form. Therefore, static equilibrium is a constant state through time in which dependent variables of erosion and deposition are maintained in a state of balance to determine channel form.

Leopold and Miller (1956) apply concepts of static equilibrium to ephemeral channels, hypothesizing that channel form is adjusted to imposed sediment load and discharge to maintain a state of quasi-equilibrium. Quasi-equilibrium is later defined by Langbein and Leopold (1964) as the most probable state of channel form based upon tendencies of a system to minimize total work expenditure (maximize entropy) and evenly distribute energy throughout the system. They argue that since quasi-equilibrium is a probable rather than predefined state, a system will constantly seek equilibrium using feedback mechanisms controlled by interrelationships among hydraulic variables. Therefore, change in a independent variable results in changes to all dependant variables and is followed by a response, or

recovery period, toward the most probable quasi-equilibrium state for the system.

The relaxation period is especially important to equilibrium studies since this period represents the time necessary for a fluvial system to return to quasi-equilibrium following disruptions within the system. The relaxation periods necessary for channels to achieve a state of equilibrium is a function of the number of annual flows within the channel. Since channel flow in arid and semi-arid climates is limited to very few days of the year, flood events generally occur more frequently than the time necessary for the channel to achieve equilibrium. Comparisons of relaxation periods for both humid and arid/semi-arid climatic regions indicate that major discrepancies between regions occur as a result of differing frequencies of flow through typical river channels.

In a study of the effects of two extreme flood events on the form of the Patuxent River in the Maryland Piedmont, Gupta and Fox (1974) determined that channel form rapidly readjusts itself to typical discharge events. The floods, one a 50-year event and the other exceeding a 100-year event, caused temporary widening of the channels and destruction of floodplain vegetation. Low and medium flows following each flood

quickly narrowed the flood-widened channel by depositing fine sediments on gravelly point bar remnants of the pre-flood channel. Within weeks, the channel completely readjusted to the apparent quasi-equilibrium state. On the other hand, A study of the Gila River, Arizona, by Burkham (1972) indicates that recovery periods for arid and semi-arid ephemeral channels may last in excess of 50 years. A series of large winter floods between 1905 and 1917 caused extensive channel widening and straightening along the Gila River. After 1917 flow conditions were low to normal and the channel responded by gradually narrowing and becoming more sinuous until near pre-flood average channel widths were reestablished 47 years later. Since flood events generally occur more frequently then 47 years in arid and semi-arid climates, quasi-equilibrium states may rarely, if ever, be achieved in these ephemeral systems.

Channel Pattern Development

Studies of channel pattern changes in arid and semi-arid river systems following catastrophic events indicate a cyclic nature of channel development within these systems. The three channel patterns -- meandering, straight, and braided -- are characteristic of different phases of ephemeral channel recovery. Each is a result of erosion and deposition within the ephemeral system.

During flood flows in systems similar to the present day San Xavier Reach, large quantities of suspended sediment are routed through and eventually deposited within the primary channel. The tendency for such flows to cause lateral channel erosion rather than channel down cutting in arid and semi-arid climates (Schumm and Lichty, 1963) leads to aggradation (deposition) within the channel during the early stages of the receding flood. As discharge decreases and is no longer able to transport a large suspended sediment load, deposition results. The widened post-flood channel tends to be less sinuous than the pre-flood channel. Thus the channel defined by the flood event can be classified as straight relative to the initial channel form.

Low to moderate flows following major floods are unable to fill the newly defined primary channel. These flows are restricted to braid channels located within a series of alternate bars deposited by the most recent flood event (Maddock, 1969). Pearthree and Baker (1987) note that these braided channels, often thought to be overloaded with sediment, may in fact be in equilibrium with the discharge and sediment load transported through the system. These channels narrow by depositing sediment on the bars until the channel is no longer able to contain the flows through the system.

At this point the channel must either widen or downcut to accommodate the flow conditions. As the alternate bars begin to revegetate, deposition on the bars is enhanced and often leads to the stabilization of bar position in the channel and ultimately abandonment of braid channels (Schumm and Lichty, 1963). Braided channel patterns are characteristic of recovery periods immediately following major flood flows.

As the alternate bars within the braid belt revegetate and abandonment of braid channels continues, the fluvial system tends toward a sinuous, single channel pattern. Eventually, the abandoned channel and alternate bar will completely revegetate and attach to the lateral channel banks. This process is demonstrated by Schumm and Lichty (1963) as controlling channel narrowing (floodplain construction) along reaches of the Cimmaron River in Kansas following the inception of a catastrophic flow.

Chapter 3

METHODS

In this study a set of aerial photographs were used to differentiate surfaces along the Santa Cruz River and create a data set of hydraulic variables for analysis of channel changes along the San Xavier Reach. Photo interpretation focused on identification of four distinct vegetation surfaces within the arroyo limits. Results of classification were then entered into a digital GIS format. Hydraulic variables of channel width, total channel area, sinuosity, meander wavelength, and a braid index were determined to be measurable and, when combined with peak discharge records, provided the data set for analysis. Variables were then correlated against one another to determine covariation, especially with peak discharge, and to test for expected trends in the data through time. A set of GIS overlays were generated to graphically depict channel changes as they occurred and to determine relative stability of channel subreaches during the time frame of this study.

Study Reach Selection

The San Xavier Reach was selected for study based on the availability of repeat aerial coverage and prior knowledge of arroyo change within the reach. Cooper Aerial Survey flies missions of the region on a yearly to semi-annual basis as part of a contract to the city of Tucson. The photography needed was readily available and purchased for my analysis by Robert Webb of the U. S. Geological Survey, Tucson Hydrology Branch. Upon receipt and inspection of the photography it was determined that the study reach be subdivided into two subreaches based on relative amount of artificial control on the channel.

The San Xavier study reach is located at approximately 32°07'N 110°59'S, just south of Tucson, Arizona, and extends nearly 4.5 miles in length (Figure 1). Discharges through the reach flow from south to north. The upstream boundary of the reach is located at the confluence of the Santa Cruz River and Lemore Wash (also known as Brickyard Wash and, historically, as Spring Branch) (Betancourt and Turner, 1985; Haynes and Huckell, 1986). From this point, the reach extends northward, is deflected around the west side of Martinez Hill where it passes beneath the Interstate 19 and San Xavier Mission Road bridges, and culminates as the

channel passes beneath the Valencia Road bridge crossing to the north (Figure 2). The reach can be subdivided into south and north sub-reaches based on the amount of artificial control on the channel.

The south subreach is located between the confluence of Lemore Wash and the Santa Cruz River on the south and the Interstate 19 bridge crossing approximately 2.5 miles to the north (downstream). A drainage canal empties into the arroyo from the east about a half-mile south of Martinez Hill. The reach lies entirely on Tohono O'odham Indian reservation land and there is no bank reinforcement along its length. Thus, the channel within this reach is allowed to respond naturally to both flood events and subsequent channel relaxation periods.

The north subreach lies between the Interstate 19 bridge on the south (upstream) and Valencia Road bridge on the north (downstream). Extending about two miles in length, this reach is characterized by channel bank reinforcement at three bridge crossings (I-19, San Xavier Mission Road, Valencia Road) and bank reconstruction within the limits of a gravel mining district. A drainage canal empties into the channel near the southernmost boundary of the gravel mining district. Also, about a quarter mile upstream from the mining

Figure 2
Map of Study Reach

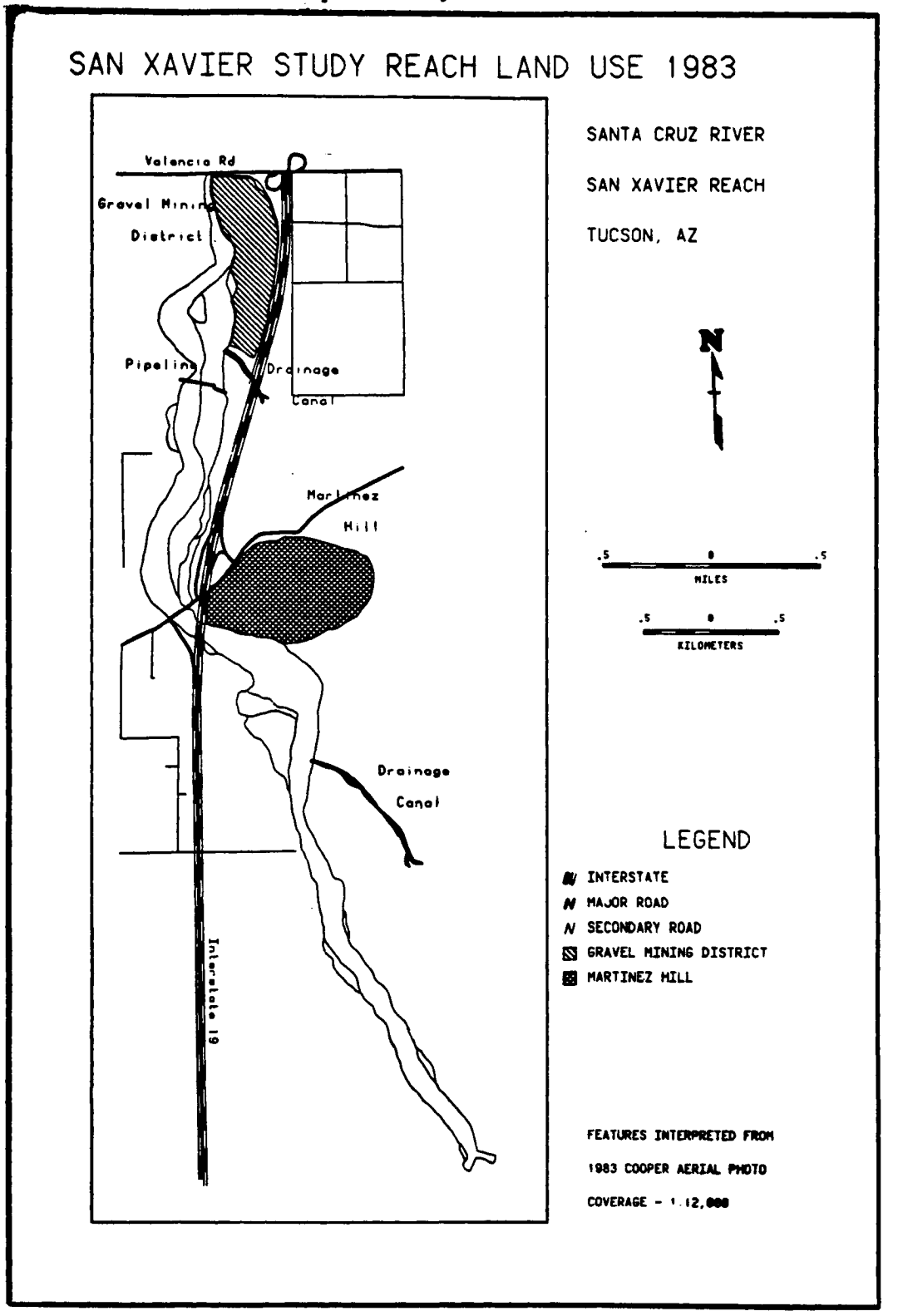

operation, a pipeline crosses the arroyo above the floodplain surface. The channel morphology along the reach may be strongly controlled by human activity, most prominently in the gravel mining district where channel rerouting occurred following the 1983 flood.

Aerial Photography

Areal photography was acquired for twelve separate years of coverage between 1971 to 1988. The photos range in scale from 1:12,000 to 1:40,000 and cover the entire study reach except in 1971 and 1984 when coverage ended approximately 1.5 miles south of I-19 bridge (Table 1). With the exception of a 1983 photo blueprint, all photos were nine inch by nine inch black and white prints.

Table 1

Listing of Aerial Photography

Date of Flight	Scale	Comments	Stereo
1/7/71	1:12,000	Shortened Coverage	Partial
4/8/72	1:30,000	None	None
11/8/74	1:20,500	None	Partial
9/7/76	1:20,500	None	Partial
9/8/78	1:21,500	None	Partial
12/7/79	1:12,000	None	Total
4/11/80	1:20,500	None	Partial
2/28/82	1:30,000	None	Partial
10/10/83	1:12,000	Blueprint Photo	None
7/31/84	1:15,000	Shortened Coverage	Total
12/23/86	1:24,000	None	Total
3/26/88	1:40,000	None	Partial

Stereoscopic photo pairs were obtained whenever possible to improve interpretation of channel terraces and arroyo

walls. Parallax, linear displacement of images on vertical aerial photos (Ambrosia and Whiteford, 1983), was obvious when flight lines of photography were mosaiced. However, this source of planimetric error was accounted for in GIS map registration discussed below.

Photo Interpretation

Four categories of vegetation surface within the Santa Cruz arroyo were interpreted by overlaying frosted mylar on each photo and outlining the boundaries of distinct surface classes with a fine tip drafting pencil (.5 mm lead width). Interpretations were done on a light table so that photo features were visible through each mylar sheet. Whenever stereo photo pairs were available, a Bauch & Lomb zoom stereoscope was used to improve interpretation of surface classes on the photos. Stereo interpretation proved especially useful in differentiating individual terraces from one another within the confines of the arroyo. Unfortunately, accurate measurements of bank and terrace heights were not possible due to the sporadic stereo coverage and the relatively large scale of much of the photography. Location of 25 ground control points (tics) for each year of coverage was the final step of the photo interpretation. Control points were located at the intersections of roads and at field corners along the study reach, as these locations remained unchanged

throughout the study time period (Figure 3). All control points were marked and labeled on each mylar sheet for later reference in GIS map registration.

Automation of Data

Once all years of photographic coverage were interpreted, the data were entered into an ARC/INFO GIS by manually digitizing the mylar classifications. Most of the GIS work was done using the personal computer (PC) ARC/INFO system at the Arizona Remote Sensing Center in the Office of Arid Land Studies. The system, supported by a CALCOMP 9100 digitizer calibrated to 1/1000 of an inch resolution and a CALCOMP 1024 pen plotter, provided the means for data entry and map production. The digitizing process involved two basic steps; coverage registration and data entry.

Before digitizing the interpreted photos, each coverage was registered to the same tic, or ground control, scheme to transform all interpretations to a consistent map scale. The tic-base coverage was generated from the ground control interpretation of the 1971 photography. The 1971 coverage was chosen for the tic-base since it represented the smallest scale photography used in the study. Tic marks for all subsequent years of data were then registered to the 1971 tic scheme to provide a transformation of the data

Figure 3

Map Registration Control Points

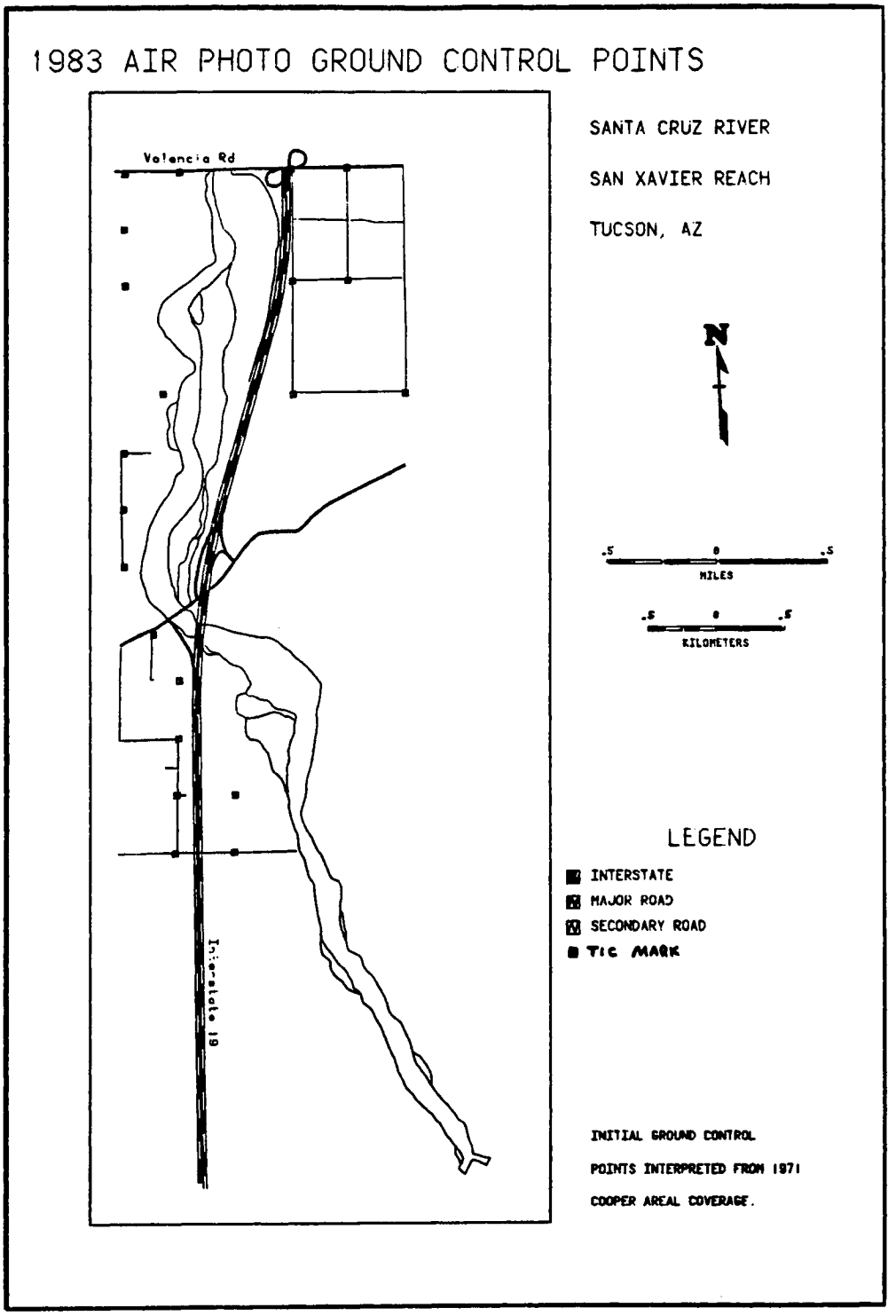

from the digitizer into the scale and registration of the 1971 coverage. A measurement of error involved in transforming the individual coverages to the 1971 base was provided by the system in the form of a residual mean square (RMS) error. A low RMS error indicated a good registration fit, and a high RMS error a poor registration fit. Tic entry was repeated for each coverage until a close to optimal RMS error was achieved. An RMS error of .003 is considered an optimal value for land use mapping (Environmental Systems Research Institute, 1987). However, due to the parallax inherent to the photography, this value was unrealistic and any RMS value less than .01 represented an adequate registration fit for this study. Final RMS values are indicated in table 2 below. Once the tic marks were adequately registered, the coverage was ready to be digitized.

Table 2

GIS Map Registration
Residual Mean Square Error Values

Photo Year	RMS Error
1971	.001
1972	.008
1974	.006
1976	.008
1978	.007
1979	.009
1980	.004
1982	.007
1983	.008
1984	.007
1986	.005
1988	.004

Coverages were digitized into the GIS by entering nodes and vertices through a hand-held digitizer keypad. Since ARC/INFO is vector based data entry, the nodes, starting and ending points of a line (arc), had to connect for all lines in the coverage in order to create polygon topology (attribute information associated with individual polygons). To aid in this process, a node snap distance (Environmental Systems Research Institute, 1987) of .015 inches was pre-set into the system. The snap distance allowed any node digitized within .015 inches of an existing node to snap (connect) with the existing node. Thus, node placement had to be accurate to within 15 feet of actual ground distance for the arc to be properly entered. This tolerance helped to insure digitizing accuracy. Once all arcs were digitized and the nodes properly snapped, polygon codes associated with the surface classes were entered into the GIS, again through the digitizer keypad. These codes provided the attribute information necessary to access and overlay primary channel classes for different years of coverage. Finally, the initial GIS data entry culminated with the construction of polygon topology for the coverage using the ARC/INFO 'BUILD' command (Environmental Systems Research Institute, 1987). At this stage, plots (maps) were generated for each year of classification and

checked against the respective mylar interpretation overlays for errors.

Generation of Hydraulic Variables

With the exception of peak discharge, the hydraulic variables analyzed in this study were generated directly by and indirectly from the GIS coverages described above. Variables of primary channel cross sectional width, channel sinuosity, channel wavelength, and the braid index were measured directly from plots of the primary channel for each year. Primary channel area measurements were determined internally by the ARC/INFO GIS. All variables were ultimately tabulated and analyzed using LOTUS database software. All resulting measurements of hydraulic variables are presented in Appendix 1.

Area measurements for the primary channel were generated by the GIS as part of the database topology information. The system calculated areas in square inches at the scale of the digitized coverages (1:12,000). Each coverage was 'clipped' (Environmental Systems Research Institute, 1987) into two separate subcoverages corresponding to the north and south subreaches defined above. By clipping each coverage by the same two polygons (clip coverages), the area values were made consistent for all twelve years of data excepting the

south reach in 1971 and 1984 when complete photo coverage was lacking. The primary channel area measurements were entered into the LOTUS database and converted from digitizer square inches to actual square feet measurements.

A series of thirty-four channel cross sections were generated for each year of digitized data. All cross sections were located using a cross section index grid created in ARC/INFO. This grid consisted of 34 horizontal lines spaced .66 inches (660 feet) apart at the 1:12,000 scale of the digitized coverages. The grid was then registered to the map coverages and clipped (Environmental Systems Research Institute, 1987) by the primary channel polygon for each year. A plot was then generated of the primary channel boundary overlain by the associated index grid at a scale of 1:12,000 (Figure 4). The plot of the index grid was used to locate channel cross sections for measurements of channel width and braid index.

Channel cross sections were located on the plots by marking the bisector point of each index grid line. The channel cross sections were then drawn by passing a line through the bisector point perpendicular to the centerline of the primary channel (Figure 5).

Figure 4

Cross Section Location and Number Map

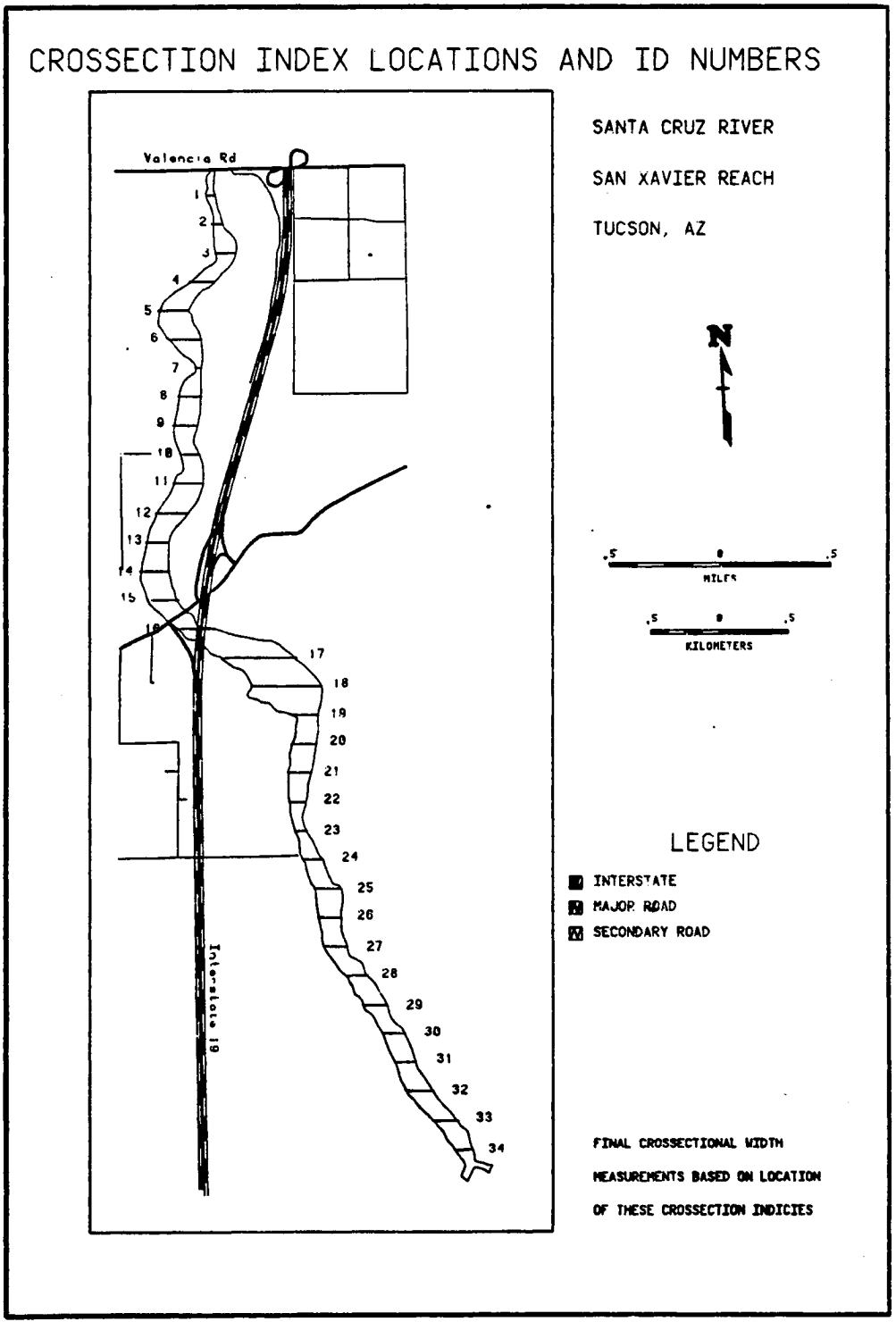

Figure 5

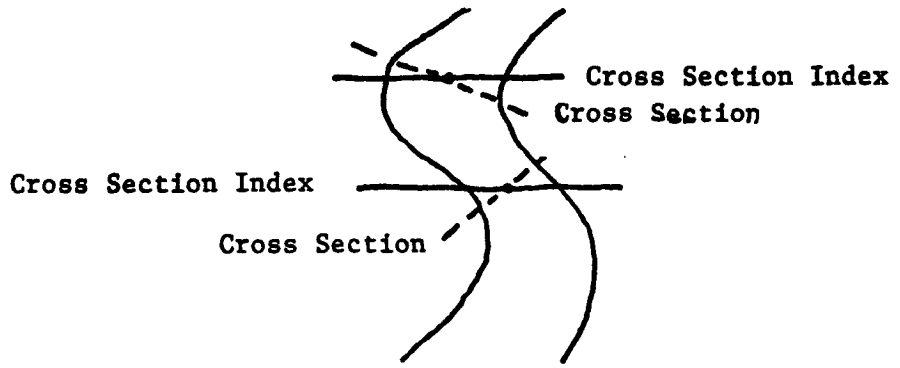

Cross Section Derivation from Cross Section Index

The length of each cross section, channel width, was then measured using an engineer's scale accurate to within 0.0083 inches, or eight feet of actual ground distance. These lengths were converted to ground distance in feet and entered into the LOTUS database for analysis.

Once channel cross sections were located, the braid index was easily determined. The braid index was measured by locating the calculated channel cross sections on the air photos for each year. Within the primary channel, the number of braid channels which intersected each cross section on the photography were counted and assigned to that cross section as a braid index value. These index values for all cross sections within the study reach were averaged to generate a mean braid index value for each year. This variable provided a

measure of the amount of braiding that occurred in the study reach within the confines of the primary channel for each year of analysis. For example, the mean braid index for the heavily braided 1984 primary channel is 1.97 channels/cross section. This contrasts to single channel systems like those in 1971, 1972, and 1983 which have a mean braid index value of 1.0 channel/cross section. Again, these data were entered into LOTUS for analysis.

Channel wavelength and sinuosity were also measured from the 1:12,000 plot of the primary channel. Channel wavelength was measured as the linear distance between every second meander inflection point along the centerline of the primary channel (Figure 6)(Leopold et al., 1964). Wavelengths were measured both north and south away from an origin point at the Interstate 19 bridge crossing. This origin was chosen due to its importance in separating the north and south study reaches as well as the fact that the location served as a meander inflection point for all years. An engineers scale was again used to measure distances on the map. Individual wavelength data and average wavelength data for the entire study reach were obtained, converted from inches to feet, and finally entered into LOTUS for analysis.

Figure 6

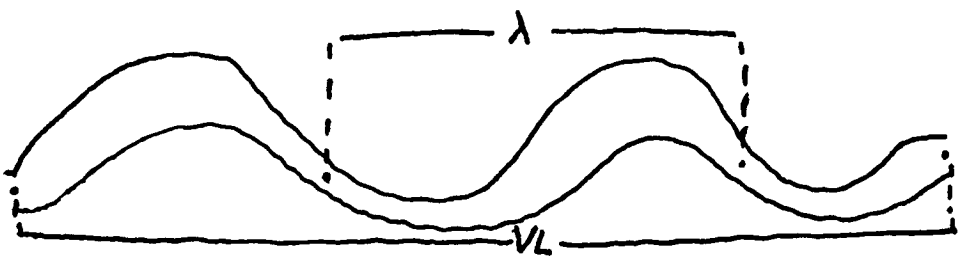

Schematic Diagram of Wavelength and Sinuosity Parameters

Channel sinuosity was the last variable acquired from the primary channel plots. Sinuosity was measured using a Fullerton map measurer to determine both stream length (measured along the east and west banks of the primary channel) and valley length (measured along the straight line channel axis) (Figure 6). An average value of both the east and west bank lengths was used in the numerator of the sinuosity equation (Equation 1) to account for discrepancies between lengths of opposite banks. Measurements were obtained separately for both the

EQUATION 1. Sinuosity = ((E+W)/2) / VL

E = East bank length
W = West bank length
VL = Valley length

north and south reach and then averaged together to generate an average sinuosity value for each year. All

average sinuosity values were then entered into LOTUS.

Peak Discharge

Peak discharge data for the Santa Cruz River were obtained from records of two U.S. Geological Survey river gauging stations: the Tucson gauging station (at the Congress Street bridge crossing) and the Continental gauging station (located near Green Valley, Arizona) (See Figure 1). The highest peak discharge value immediately preceding the date of aerial photographic coverage was used to represent the effective discharge for that primary channel (Table 3). Since the records from the Tucson station may have been influenced by city runoff (Jens and McPherson, 1964), data from both gauging stations were averaged to represent the flow through the study reach whenever peak discharge data were available for the same date at both stations. When dates did not coincide, the Tucson value was used to represent the reach. Since the Tucson station was washed out by the October 1983 flood, the 1986 discharge value was derived from the Continental station records. Peak discharge data corresponding to the 1984 and 1988 primary channel were not available from U.S.G.S. records. In these cases, peak discharge values were acquired from Robert Webb (U.S. Geological Survey, Tucson, personal commun. 1988) as probable estimates for each year. All

Table 3

Peak Discharge and Photo Data

Peak Discharge & Gauging Station Data

Peak Discharge in cf/sec & Photo Dates				STATION T = Tucson
YEAR	DISCHARGE	DATE	PHOTO DATE	C = Continental
1971	6880	7/19/70	1/7/71	T
1972	8000	8/17/71	4/8/72	T
1974	7930	7/8/74	11/8/74	T
1976	2760	7/12/76	9/7/76	T
1978	25100	10/10/77	9/8/78	(T+C)/2
1979	14750	12/19/78	12/7/79	(T+C)/2
1980	5760	8/15/79	4/11/80	T
1982	2660	9/5/81	2/28/82	T
1983	48850	10/2/83	10/10/83	(T+C)/2
1984	1900	1/8/84	7/31/84	C
1986	11600	12/28/84	12/23/86	C
1988	2000	-	3/26/88	T&C

Note: 1988 peak discharge value and date not yet available. Estimate from personal communication with Robert Webb (USGS).

discharge data were finally entered into the LOTUS spreadsheet to complete the database for analysis.

Analytic Methods

ARC/INFO plots of arroyo classifications and channel overlays as well as numerous LOTUS graphs and regressions provide the output data from which results are obtained in this study. Each type of analysis provided information about channel changes from a different perspective. Trends in the hydraulic variables through time provided the basis for regression analysis in the study (Knighton, 1977). Average channel changes for the entire reach were depicted by plots of hydraulic variable trends through time. Analysis of the variability of channel change as a function of spatial location within the study reach serves as the foundation for at-a-section analysis of width and generation of primary channel overlay plots.

LOTUS graphs of peak discharge, average channel wavelength, channel area, channel sinuosity, average channel width, and mean braid index versus year were generated to indicate years when major changes in the hydraulic data occur. Excepting the braid index, scatterplots of all variables versus peak discharge were created to determine the relative scatter of data around a regression trend line. Peak discharge is used as a

independent variable in this study as it was anticipated that discharge, at least above some threshold, is the major force in determining channel form. Simple regressions were run on all variables using peak discharge as the independent variable to determine an R squared measure of correlation and the regression line equation for all relationships. Residual values were derived by subtracting actual data values from those predicted by the regression equation. Graphs of residuals versus year were generated to determine when the regression model failed to explain data trends. To account for the effects of the braid index on the regression model, a multiple regression, using both peak discharge and braid index as independent variables, was also run for each dependant variable. Residuals for each multiple regression were determined and plotted on the same graphs as the simple regression residuals for each relationship. It was anticipated that the multiple regression analysis would account for the effects of the changing channel pattern during the time period of this study.

While regression analysis provided a way to analyze relationships between variables through time for the entire study reach, at-a-section analysis of channel widths and overlay analysis of different years of primary

channel coverage provided useful information about when and where within the study reach major morphological changes occurred. Six graphs of cross-sectional width versus cross section location are generated to indicate where sub-reaches of channel widening, channel narrowing, and little channel change are located within the study reach. Two years of width data were plotted on each graph corresponding to the earliest and latest years of channel relaxation periods (1971-1976, 1979-1982, 1983-1988) and both pre- and post-flood years for major discharge events (1976-1978, 1978-1979, 1982-1983). Thus, changes in width during relaxation periods and changes resulting from each flood are indicated by the distance between the two curves at individual cross section locations. Large changes in primary channel width are represented by greater distances between curves than during periods of cross section stability when only small width changes occur.

Further information concerning the spatial variability of change within the study reach is derived from primary channel overlay plots. Primary channel overlay plots were generated to correspond to the relaxation periods and flood events defined above. Another plot depicted changes which resulted from the 11,600 cfs peak discharge between 1984 and 1988. These

plots provide descriptive information concerning changes in meander geometry through time for both short and long subreaches of the study reach.

Chapter 4

RESULTS

Change in Surface Classes

Interpretation of aerial photography resulted in the definition of four planimetric surface classes in this study: primary channel, newly vegetated terrace, scrub surface, and maturely vegetated surface. Each is defined by the type and age of vegetation lying between the arroyo walls. Within the arroyo, vegetation varies from sparse grasses to more mature brush growth to established areas of tree cover. Each surface class provides information about the relative resistance of the surface area to erosion and length of time since the area was subjected to an event of extreme erosion. Observations of surface class changes through time indicate areas which have been subjected to erosional processes during recent discharge events.

The primary channel serves as the fundamental surface class for analysis of hydraulic variables in this study. The primary channel is the surface area within

which non-flood flows through the arroyo are contained. For this reason, the primary channel lacks vegetation cover as young plants are easily uprooted by relatively frequent small discharge events associated with summer monsoon and winter precipitation seasons. Generally, a well defined bank delineates the primary channel from neighboring surface classes. The bank heights vary from about one foot to the full height of the arroyo wall in situations when the primary channel abuts the boundaries of the arroyo. In these respects, the primary channel is similar to the "active channel" (Leopold et al., 1966; Pearthree and Baker, 1987) and the "low flow" channel (Graf, 1981) defined in previous studies of arroyo change. However, due to the changing nature of channel pattern from straight to braided through time along the San Xavier reach, the definition of the primary channel is extended to accommodate different channel patterns.

Between the years 1971 and 1976 a single unvegetated channel is observable on the photography as the route through which flows had occurred. Through this time period, this single channel is defined as the primary channel. However, from 1978 to 1988 the channel pattern becomes braided as a response to the large amounts of easily erodible sand deposited by major discharge events in 1977, 1978, 1983, and 1984. For this

period the primary channel is defined as the area delimited by the unvegetated lateral limits of the braid belt. This definition is derived to simplify otherwise complex measurements of sinuosity and wavelength in a braided system. To accommodate for this change of primary channel definition, the braid index variable is defined, as discussed above, to measure the relative amount of braiding that occurs in the primary channel for each year of study.

The newly vegetated terrace, the second surface class defined in this study, lies adjacent to the primary channel and represents a recent relict of the primary channel. As areas of the primary channel are abandoned, they slowly revegetate through time. Revegetation increases the resistance of these areas to erosion thus helping to stabilize the route of the primary channel. Thresholds for the primary channel bank erosion increase as the densities of vegetation on the newly vegetated terraces also increase. Therefore, assuming thresholds for the primary channel are not exceeded, primary channel downcutting occurs more easily than lateral cutting once the revegetated areas have been established and continue to mature. Revegetation begins with the development of grasses and shrub seedlings within the arroyo. Typical examples of these vegetation types include ephemeral

gramma grasses (Bouteloua sp.) and seedlings of creosotebush (Larrea tridentata) and saltbush (Atriplex sp.). Clusters of these plant species define the limits of the newly vegetated terrace.

The third surface class, the scrub surface, represents older relict primary channel than the newly vegetated terrace. Because the scrub surfaces have been abandoned for longer periods of time than newly vegetated terraces, scrub surfaces are represented by more mature vegetation cover. Within scrub surface areas, species of the newly vegetated terrace are more fully developed. Scattered trees begin to appear within the scrub surface areas. Typical tree species include mesquite (Prosopis juliflora) and saltcedar (Tamarix pentandra). A discernable terrace is occasionally visible on the photography between the newly vegetated terrace and the scrub surface. However, the density of vegetation on the scrub surface often hinders the interpretation of this terrace. Thus, identification of vegetation change from young to mature shrubs provides the most reliable means of determining the boundaries of the scrub surface.

The final surface class is the maturely vegetated surface. This surface represents either remnants of very old primary channel, or areas where the arroyo wall has

collapsed, been replaced by a talus slope (Ritter, 1986, p.147), and revegetated to maturity. These areas are defined by either relatively dense clusters of trees which have been allowed to mature as they have not been affected by large channel flows in recent history, or by recently formed talus slopes in early stages of vegetation development.

Like any generalized classification scheme, exceptions to these surface class definitions occur. When a surface did not fit within the defined scheme, the surface was grouped into the class with which it was functionally most similar. For instance, bare soil surfaces clearly separated from the primary channel were grouped into the classes with which they seemed most closely related to in age, or terrace height. The accuracy of interpretations is strongly influenced by the scale of the photography. Large scale photography (1:12,000) provided better resolution (detail) than small scale (1:30,000) coverages. Minor changes in interpretations through time are often a function of the varying scales of photography used in the study. GIS maps of interpretations of the four surface classes (arroyo surfaces) are presented in Appendix 2.

Identification of major changes in surface classes through time provides information about the spatial limits

of erosion and deposition during flood events and recovery periods. During years of primary channel narrowing, abandoned primary channel areas revegetated into newly vegetated terrace. Likewise, established newly vegetated terrace surfaces matured into scrub surface, and scrub surfaces developed into maturely vegetated surface. This sequence of classification change is depicted during the channel relaxation period between 1972 and 1976. The sequence of maps from 1972 to 1974 and 1974 to 1976 (Appendix 2) indicate that a mile long reach between .5 miles south and north of I-19 bridge underwent gradual channel narrowing during this period, resulting in the production of newly vegetated terrace along the banks of the primary channel. Further, the area of scrub surface increased as newly vegetated terraces matured. Between 1983 and 1988 (Appendix 2), also a relaxation period, channel narrowing resulted in development of newly vegetated terrace along the southern-most reach of the channel. The newly vegetated areas are alternately positioned on the east and west sides of the primary channel thereby causing increases in sinuosity as these areas grow. This observation is consistent with studies by Schumm and Lichty (1963) and Pearthree and Baker (1987) which note the development of sinuosity in a channel as a function of vegetation

development.

Discharges in 1977, 1978, and 1983 caused primary channel widening and floodplain erosion which resulted in systematic changes in surface classes through time. Interpretations from 1976 and 1978 (Appendix 2) photography indicate substantial increases in arroyo surface area covered by newly vegetated terrace as a result of the 10/10/77 discharge. Surfaces which experienced reverse vegetation development (changed from maturely vegetated or scrub surface to newly vegetated surface and primary channel) were probably covered by water during the discharge event. Therefore, pre-flood vegetation was scoured out by erosional processes associated with the discharge. The same pattern of surface class change resulted from the 12/19/78 and 10/2/83 discharges as indicated by 1978, 1979, 1982, and 1983 maps of surface classes (Appendix 2). The most dramatic changes in classification resulted from the 10/2/83 event when nearly the entire arroyo was gutted of vegetation and redefined as primary channel.

Hydraulic Variable Trends Through Time

Trends of hydraulic variables through time provide information about both the degree of channel change by large flows and the rate of channel relaxation following such events. In accordance with the

hypothesized model of channel change, sudden increases through time of average channel width, channel area, and average channel wavelength should correspond to flood events. (See Figure 7 for peak discharge trends through time) Braid index should also increase following floods which deposit large amounts of coarse grained sediment. Ideally, more deposition will lead to a more braided channel. Channel sinuosity should respond by rapidly decreasing (becoming straighter) during the same flood events. Conversely, channel relaxation periods should be associated with gradual decreases through time of average channel width, channel area, average channel wavelength, and braid index. Sinuosity should increase through time. A rapid rate of channel recovery may indicate that forces of equilibrium are dominantly controlling channel form. Alternately, slow recovery rates favor catastrophism as the dominant control since floods may occur more frequently than equilibrium can be attained. Although traditional models of channel change in arid and semi-arid climates indicate recovery periods lasting several decades, the results from the San Xavier reach discussed below seem to manifest short periods of rapid recovery requiring only a few years.

Figure 7

Peak Discharge vs. Year

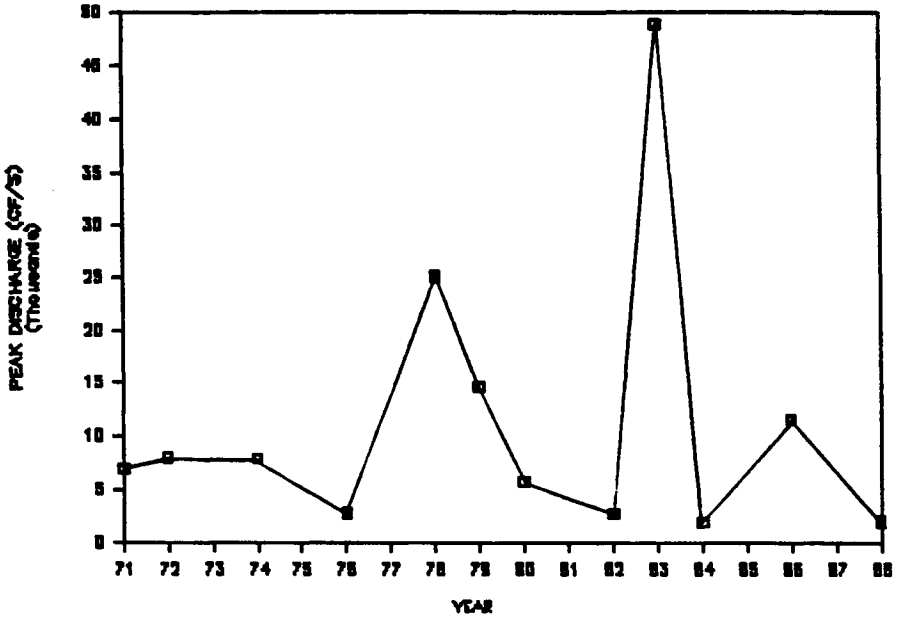

Figure 8

Average Channel Width vs. Year

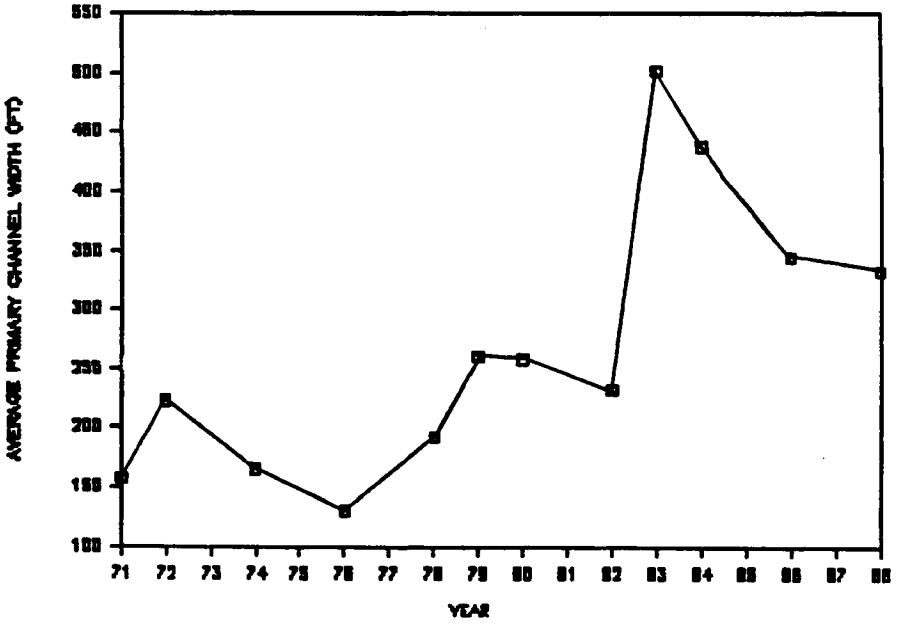

Average Channel Width

With the exception of 1971 data, average primary channel width decreased through time during relaxation periods. Increases in average channel width are associated with flood events of 10/10/77, 12/19/78, and 10/2/83 (Figure 8). The most dramatic change is associated with the 1983 flood which increased average channel width by slightly more than 260 feet. The flow of 12/28/84 (11,600 cfs) appears to have caused no major channel widening possibly due to increased thresholds for the primary channel defined by the 10/2/83 flood. The 1984 flow apparently did not exceed bankfull discharge for the primary channel as evidenced by trends in the average channel width data. Figure 8 shows that average channel width increased between 1971 and 1972. Since the peak discharge in 1972 of 8,000 cfs was probably lower then the bankfull discharge for the 1971 channel and not sufficient to precipitate channel widening, this change may be a result of the shortened photo coverage in 1971 which did not include narrow cross sections in the southern-most reaches of the study area. Because upstream reaches are narrower than downstream reaches, the 1971 width may be underestimated in comparison with subsequent years of channel data.

Channel Area

Trends in channel area data through time closely resemble those for channel width (Figure 9). Area and width variables are in fact so closely related that a simple regression of the two variables yields an R squared value of .9935 (Table 4 and Figure 11). Since area is an integral function of width, this strong relationship was expected and supports the assumption that the cross section locations are indeed representative of the channel reach. Trends in channel area are parallel those of channel width discussed above.

Sinuosity

Sinuosity measurements through time do not follow the expected trends as outlined by the general model of channel change discussed on pages 7 and 8 (Figure 10). The channel becomes relatively straighter between 1971 and 1978. The trend of decreasing sinuosity during the relaxation period between 1971 and 1976 was not predicted by the model as sinuosity should have increased during this period. As expected, the trend reverses between 1978 and 1982 as sinuosity increases during the recovery period following the 10/10/77 and 12/19/78 discharge events. In response to the 10/2/83 flood, the channel becomes relatively straight dropping

Figure 9

Channel Area vs. Year

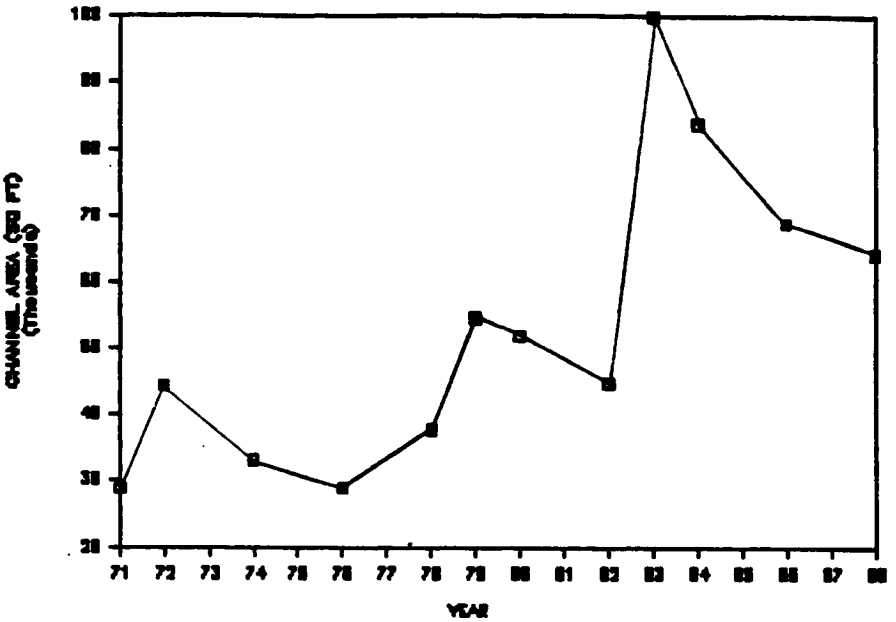

Figure 10

Channel Sinuosity vs. Year

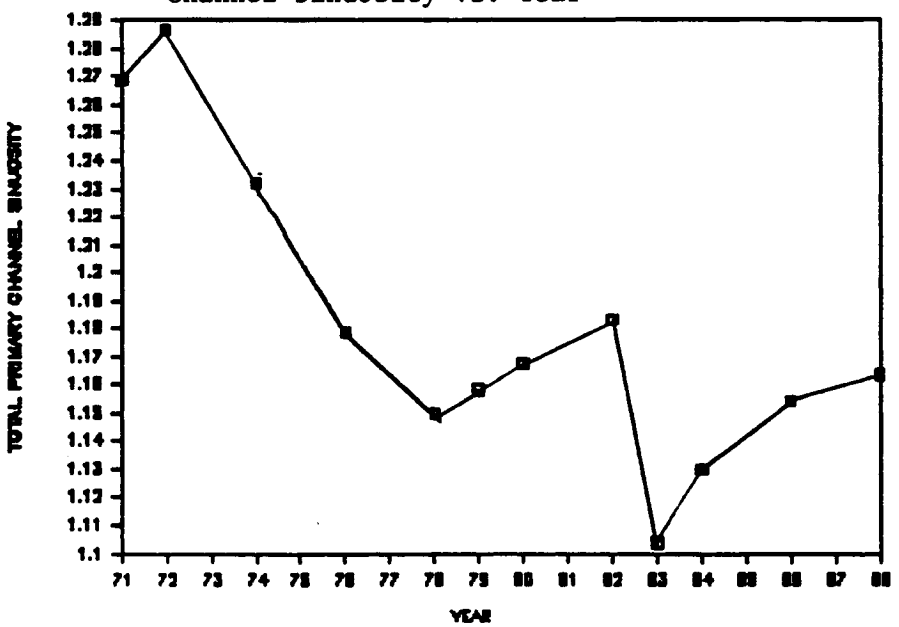

Table 4

Width (Ind.) vs Area
Regression Output:

Constant	1176.179
Std Err of Y Est	1876.594
R Squared	0.993548
No. of Observations	12
Degrees of Freedom	10
X Coefficient(s)	193.8804
Std Err of Coef.	4.940497

PRED	RESI
31714.85	2848.803
44377.29	-171.314
33125.11	14.00600
26416.66	-2402.78
38492.97	694.3671
51723.08	-2825.53
51102.23	-856.100
46223.35	1508.079
98424.00	-1506.54
86096.72	2298.113
67858.86	-849.472
65458.64	1250.307

Figure 11

Channel Width vs. Area Residuals

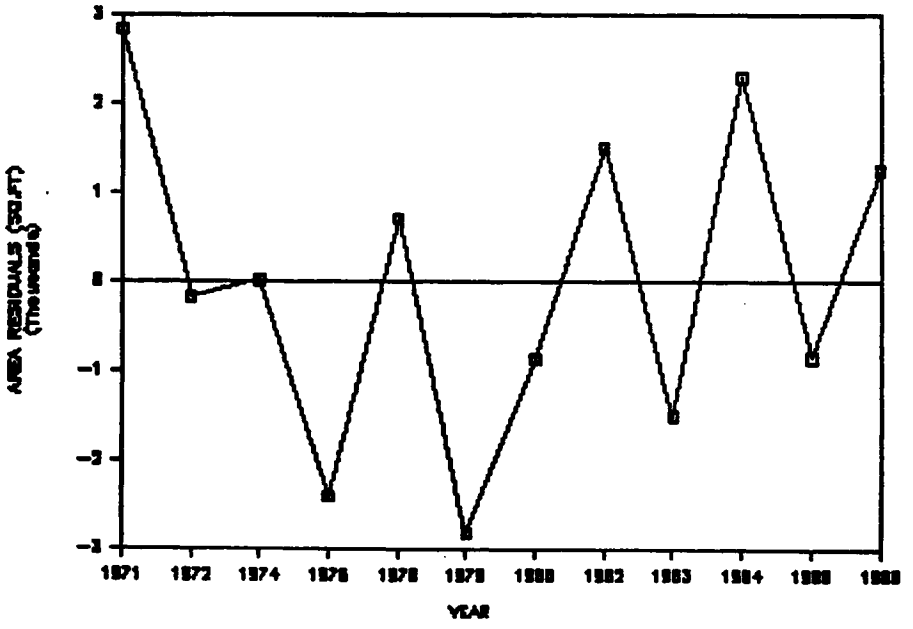

from a sinuosity of 1.183 in 1982 to 1.103 in 1983, the most dramatic sinuosity change during this study. Following 1983, sinuosity again increases as the meandering pattern is slowly reestablished through revegetation of the bars and abandonment of braided channels. Since highly sinuous braided channels are not accounted for in the definition of the primary channel, these raw sinuosity data are insufficient descriptors of channel form. The braid index variable compensates for these data in the multivariate regression analysis discussion below.

Average Channel Wavelength

Average channel wavelength data are also weakly related to discharge events through time (Figure 12). Before 1982, the wavelength data fluctuates up and down following no consistent trend through time. Only a small (210 feet) increase in wavelength results from the 25,100 cfs discharge in 1977. A greater increase occurs between 1972 and 1974 (320 feet) when the expected trend was a decrease in wavelength. However, in 1983, the most dramatic increase (1140 feet) in wavelength occurs, again in response to the 10/2/83 discharge. Wavelength again increases in 1984 followed by decreases between 1984 and 1988. The increase in wavelength between 1983 and 1984

Figure 12

Average Wavelength vs. Year

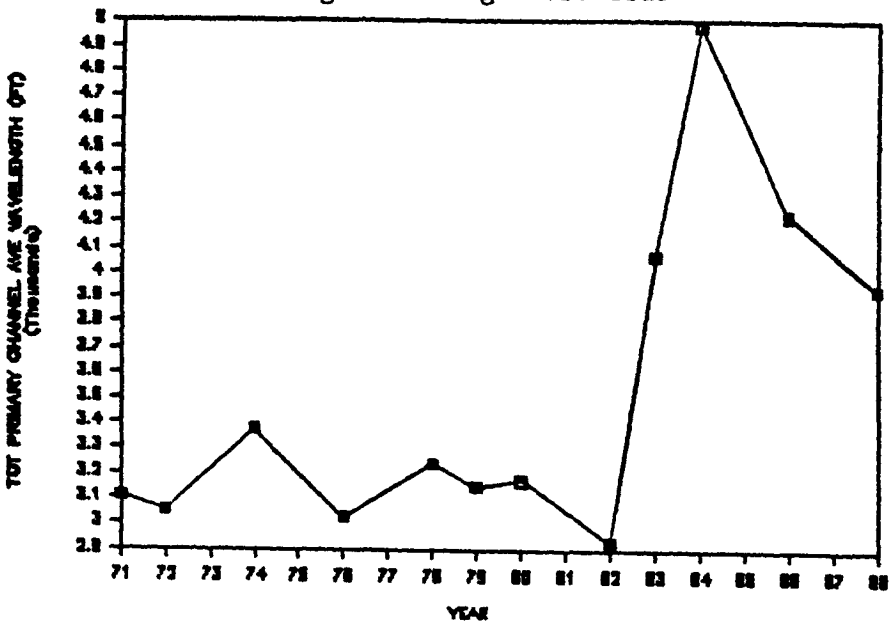

Figure 13

Braid Index vs. Year

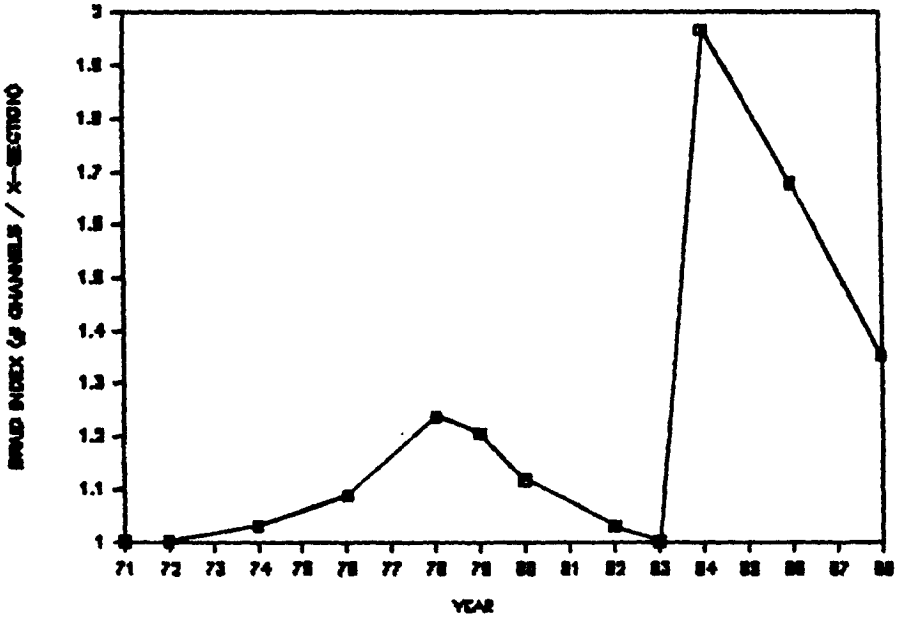

is probably due to measurement error: the abbreviated photo coverage in 1984 did not include relatively short wavelengths of the upstream reaches. As in the sinuosity data, wavelength results show that expected trends through time generally do not exist in the raw data. However, it is again important to note that without accounting for the braid index variable, the raw wavelength data are relatively poor descriptors of channel form.

Mean Braid Index

The mean braid index trends through time are strongly related to the 10/10/77 and 10/2/83 channel flows (Figure 13). In response to the 1977 discharge (25,100 cfs), the braid index increased by .15 channels/cross section. This increase is probably due to sediment deposition during the flood resulting in a braided channel, especially downstream from the meander cutoff immediately south of I-19 bridge. Between 1978 and 1982, a relaxation period, the braid index decreased from 1.235 to 1.029 channels/cross section. This short period of 5 years permitted the establishment of a single channel throughout nearly all of the study reach until its redefinition again in 1983. In 1983 the channel was redefined by the 48,850 cfs flow as a wide single

channel. By 1984, sufficient time had passed for a very complex braid network to be established within the limits of the primary channel. Again, development of the braided pattern is probably a response to extensive deposition in the channel during the 1983 flow. Between 1984 and 1988, the primary channel pattern -- as defined by the braid index -- rapidly adjusted toward a single channel, decreasing in braid index from 1.97 to 1.35 channels/cross section. The readjustment of the 1978 and 1984 channels from braided toward a single channel pattern seems to occur much more rapidly than the period derived in Burkham's (1972) work on the Gila River.

Regression Analysis

Regressions of the dependent variables (width, area, sinuosity, and wavelength) versus the independent variable of peak discharge should indicate the degree to which equilibrium is controlling channel form within the study reach. Strong relationships between hydraulic variables through time (high R squared values) should indicate the presence of some equilibrium state for the system. In other words, even through a time frame with a diverse range of peak discharges, a consistent relationship between hydraulic variables and peak discharge should exist. Thus, any catastrophic event is

either quickly readjusted to equilibrium, or, is not catastrophic at all (does not redefine hydraulic relationships). Conversely, a system characterized by weak hydraulic relationships through time (low R squared values) should be dominantly controlled by catastrophic flows followed by long relaxation periods. In essence, channel form is a product of only major discharges, and, for extended subsequent periods form and discharge are essentially unrelated.

Results of simple regressions on the hydraulic variables in this study identify moderate to weak relationships between hydraulic variables and discharge and indicate that the highest residuals consistently occur during years following major flows. Since the primary channel for these years is defined by the lateral limits of the braid belt, problems in defining hydraulic variables for these years resulted in systematic measurement errors. For instance, the channel width in the heavily braided system in 1984 actually includes, on average, two channels and an alternate bar. To rectify these measurement errors, the braid index is implemented as a second independent variable to describe channel pattern in subsequent multiple regressions.

Results of multiple regressions indicate that much more of the covariation between hydraulic variables

is explained by the combination of discharge and braid index than by discharge alone. In fact, relationships become so strong that it is difficult to avoid the conclusion that equilibrium is a dominant force in controlling channel form. Results of simple and multiple regressions for each hydraulic variable in this study are presented below.

Average Channel Width

The simple regression of width versus peak discharge yields an R squared value of .224 (Table 5 and Figure 14). Residuals indicate that the regression model is overpredicting width before 1979 (positive residuals) and underpredicting width (negative residuals) after 1982 (Figure 15). Greatest residuals occur in 1978 and 1984, years immediately following large flows through the channel.

In the multiple regression of average channel width on peak discharge and braid index, the R squared value increases to .633 (Table 6). This R squared value is an increase by a factor of nearly three over the simple regression results. The high residual value in 1984 for the simple regression is reduced by 170 feet in the multiple regression. Residual values for 1971, 1972, 1974, 1976, 1986, and 1988 are also reduced although not as

Table 5

Discharge (ind.) vs Average Channel Width
Regression Output:

Constant	223.1893
Std Err of Y Est	105.7777
R Squared	0.224485
No. of Observations	12
Degrees of Freedom	10

X Coefficient(s)	0.004017
Std Err of Coef.	0.002381

PRED	RESI
250.8262	93.31328
255.3253	32.50175
255.0441	90.25727
234.2762	104.0903
324.016	131.5427
282.4400	21.72828
246.3272	-11.1823
233.8745	1.529328
419.4197	-82.1669
230.8216	-207.183
269.7865	-74.1507
231.2233	-100.334

Table 6

Discharge and Braid Index (ind.)
vs Average Channel Width
Regression Output:

Constant	-93.6187
Std Err of Y Est	76.62333
R Squared	0.633760
No. of Observations	12
Degrees of Freedom	9

X Coefficient(s)	246.4383	0.005311
Std Err of Coef.	77.70737	0.001758

PRED	RESI
189.3592	31.8463
195.3076	-27.5159
202.1838	37.39698
189.2224	59.03659
344.1111	151.6378
281.8940	21.18229
212.4036	-45.1058
174.1948	-58.1503
412.2619	-89.3247
400.8508	-37.1539
381.1353	37.19811
250.4197	-81.1375

Figure 14

Width vs. Discharge

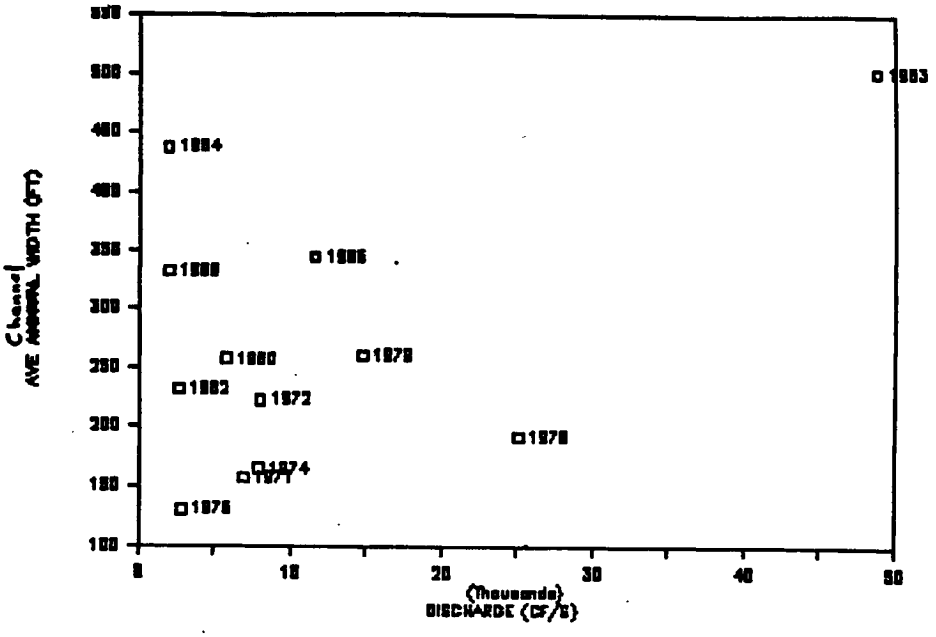

Figure 15

Width Residuals

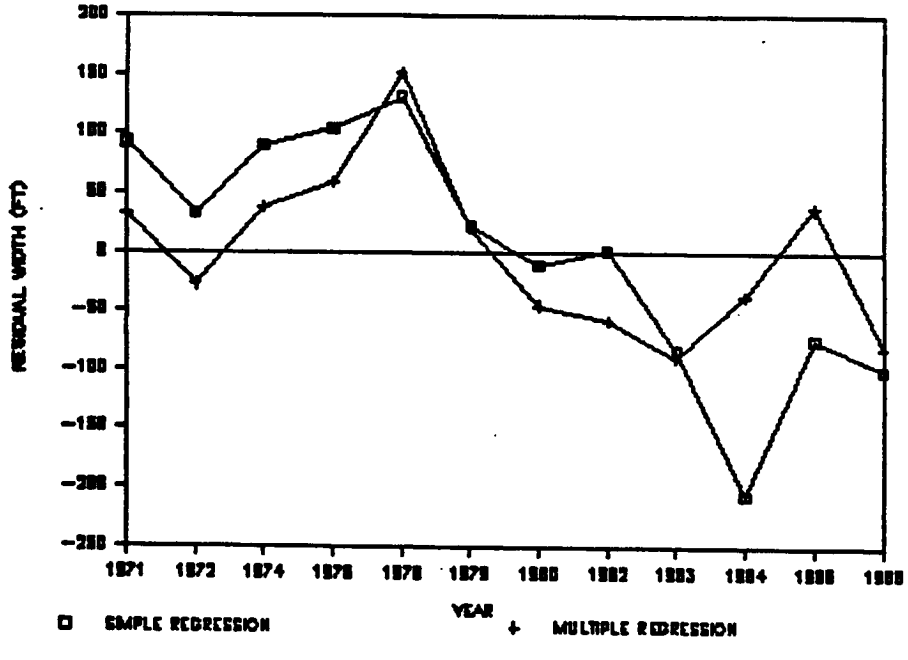

dramatically as in 1984. Further, the residuals for the simple regression become more evenly scattered about the regression line through time in the multiple regression analysis (Figure 15). The high residual value for 1978 in the simple regression is not improved by the multiple regression. The residual for 1978 shows that the regression is overpredicting width by 151 feet for the year. This residual indicates that another variable, possibly channel depth, is controlling channel form during this year. Since the primary channel banks were stabilized by mature vegetation along most of the study reach in 1976, channel widening may have followed an initial period of channel downcutting during the 10/10/77 event. Thus, energy required to widen the channel may have initially caused channel downcutting within the reach. However, channel depth measurements are needed to support this argument. Excepting 1978 data, the multiple regression analysis indicates that channel width is strongly related to peak discharge and braid index supporting arguments for equilibrium controls in the San Xavier reach.

Channel Area

Due to the strong relationship between channel width and channel area discussed above, results of both

the simple and multiple regressions for channel area mirror those for channel width. Tables 7 and 8 indicate that the R squared value for the simple regression (.249) increases by nearly a factor of three for the multiple regression (.640). Trends in the residuals also parallel those for channel width and follow the same discussion as for channel width regressions presented above (Figures 16 and 17).

Sinuosity

Results of the simple regression analysis of channel sinuosity versus peak discharge indicate that the two variables alone are poorly related to one another. An R squared value of only .1984 results from the simple regression (Table 9 and Figure 18). Residuals in 1971 and 1972 show that the simple regression model underpredicts sinuosity values for these years (Figure 19). In contrast, sinuosity in the heavily braided 1984 channel should be much higher based upon the regression results. Similar to channel width and area results, residuals for the simple regression for sinuosity follow a distinct trend through time. The regression model underpredicts sinuosity in 1971, 1972, and 1976 and overpredicts sinuosity for the remaining years.

Results of the multiple regression of sinuosity on

Table 7

Discharge (Ind.) vs Total Channel Area
Regression Output:

Constant	43931.44
Std Err of Y Est	20240.48
R Squared	0.249477
No. of Observations	12
Degrees of Freedom	10

X Coefficient(s)	0.823768
Std Err of Coef.	0.451825

PRED	RESI
49598.98	20730.90
50521.58	5972.972
50463.92	17352.80
46205.03	17385.59
64608.01	26809.40
56082.01	1533.406
48676.34	-3281.98
46122.66	1407.385
84172.50	-15758.0
45496.59	-38302.0
53487.14	-15221.1
45578.97	-18629.3

Table 8

Discharge and Braid Index (Ind.)
vs Total Channel Area
Regression Output:

Constant	-16266.7
Std Err of Y Est	14775.22
R Squared	0.640057
No. of Observations	12
Degrees of Freedom	9

X Coefficient(s)	46826.89	1.069696
Std Err of Coef.	14984.26	0.339083

PRED	RESI
37919.69	9051.642
39117.75	-5430.85
40420.10	7308.993
37644.32	8824.877
68427.64	30629.03
55979.01	1430.408
42230.68	-9727.65
34782.80	-9932.47
82814.83	-17115.7
77804.77	-5993.84
74645.64	5937.318
49226.71	-14981.6

Figure 16

Area vs. Discharge

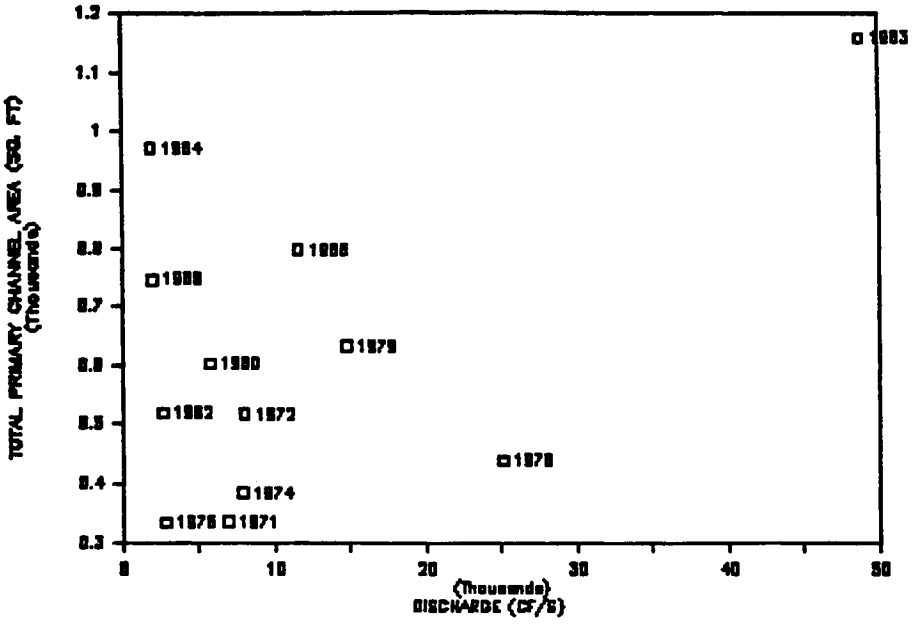

Figure 17

Area Residuals

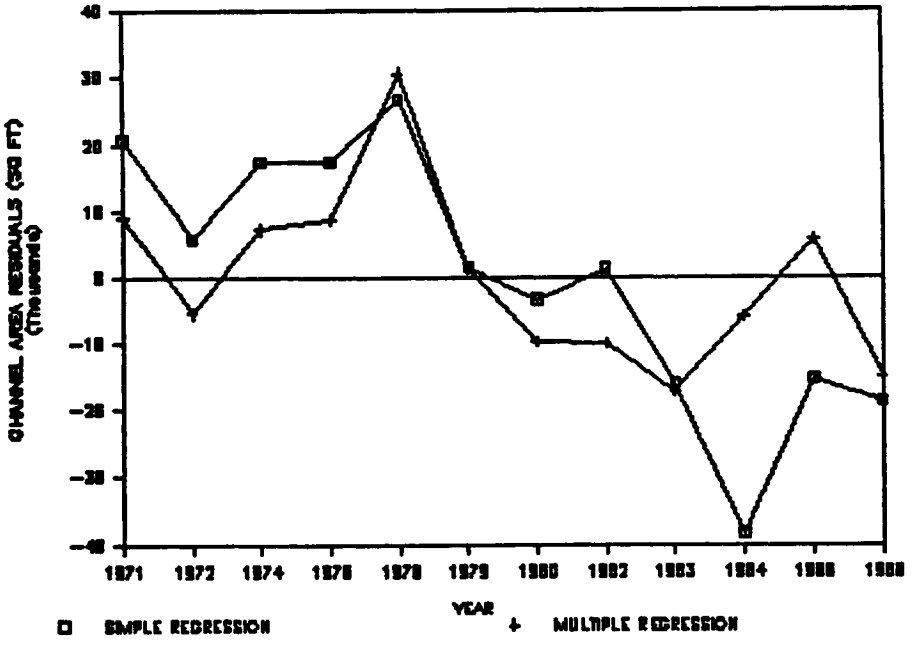

Table 9

Discharge (Ind.) vs Total Channel Sinuosity
Regression Output:

Constant	1.202224
Std Err of Y Est	0.051247
R Squared	0.198411
No. of Observations	12
Degrees of Freedom	10

X Coefficient(s)	-0.00000
Std Err of Coef.	0.000001

PRED	RESI
1.189841	-0.07913
1.187825	-0.09900
1.187951	-0.04419
1.197256	0.018446
1.157049	0.007019
1.175676	0.017221
1.191857	0.024057
1.197436	0.014436
1.114303	0.010563
1.198804	0.068604
1.181346	0.026936
1.198624	0.035049

Table 10

Discharge and Braid Index (Ind.)
vs Total Average Sinuosity
Regression Output:

Constant	1.341861
Std Err of Y Est	0.040540
R Squared	0.548535
No. of Observations	12
Degrees of Freedom	9

X Coefficient(s)	-0.10862	-0.00000
Std Err of Coef.	0.041114	0.000000

PRED	RESI
1.206583	-0.06239
1.202244	-0.08459
1.199320	-0.03282
1.212963	0.034163
1.110430	-0.03959
1.163727	-0.00472
1.198144	0.030344
1.219739	0.036739
1.043966	-0.05977
1.121004	-0.00919
1.114817	-0.03959
1.187165	0.023580

Figure 18

Sinuosity vs. Discharge

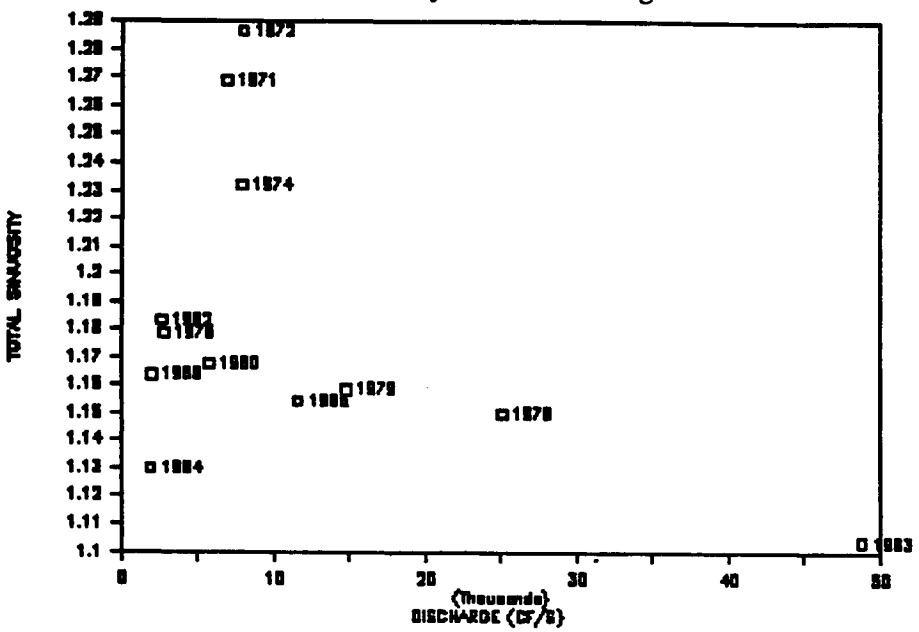

Figure 19

Sinuosity Residuals

peak discharge and braid index exhibit a stronger relationship between the hydraulic variables than that for the simple regression. The multiple regression yields an R squared value of .548, again nearly a three fold improvement over simple regression results (Table 10). Residuals for the multiple regression show that the greatest deviations from the regression line occur in 1971, 1972, and 1983, all years with a braid index equal to 1.0. The large residual in the braided channel of 1984 for the simple regression is reduced to nearly zero in the multiple regression. Also, the general trend in residuals through time for the simple regression disappears in the multiple regression analysis. The residuals for the multiple regression randomly fluctuate above and below the regression line through time. This implies that most of the covariation between the variables is explained by the multiple regression model. Again, the strong relationship between sinuosity, peak discharge, and braid index supports an argument that equilibrium controls the fluvial system.

If sinuosity develops over several years, as indicated by Schumm and Lichty (1963), sinuosity should not correlate well to rapidly adjusted variables in the channel (ie. discharge and wavelength). As discussed earlier, the sinuosity development in a channel is a

function of the rate of abandonment and revegetation of braid channels. Ideally, channel width also decreases at the same rate. Thus, channel width and channel sinuosity should adjust at similar rates and therefore display a strong inverse relationship to one another. Figure 20 (a scattergram of predicted sinuosity versus predicted width) indicates that the predicted channel sinuosity and predicted average channel width measurements calculated from the multiple regression model are in fact very strongly related to one another compared to relationships between the other predicted variables (Figures 21 and 22).

Average Channel Wavelength

The simple regression of average channel wavelength versus peak discharge indicates the poorest relationship between variables in this study. An R squared value of .019 depicts very little relationship between wavelength and discharge alone (Table 11 and Figure 23). The trend in the residuals through time again follows a rather distinct pattern (Figure 24). Between 1971 and 1982 the regression overpredicts wavelength by a relatively constant amount. Between 1983 and 1988 the regression underpredicts wavelength, most severely in the heavily braided channels of 1984 and 1986.

Figure 20

Predicted Sinuosity vs. Predicted Width

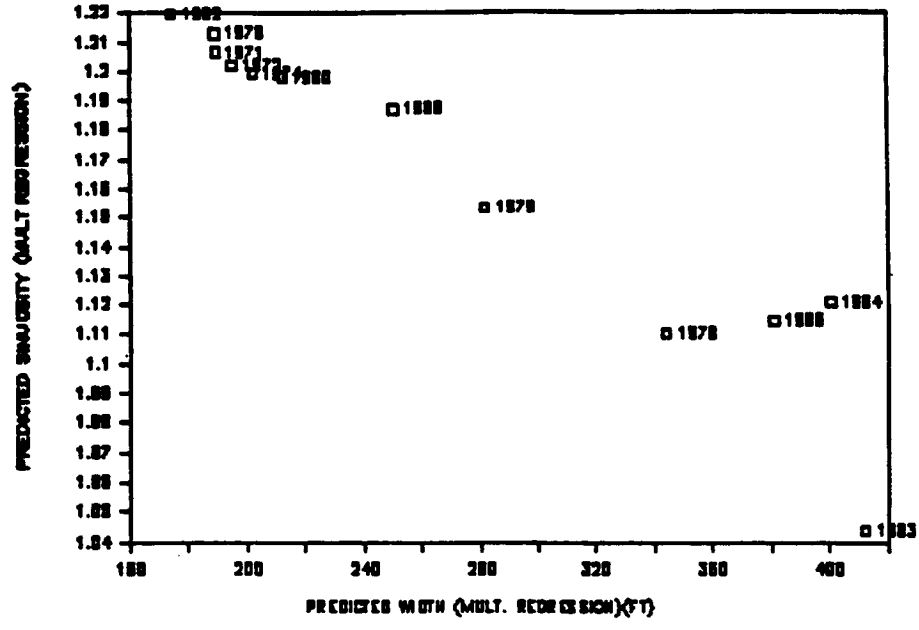

Figure 21

Predicted Wavelength vs. Predicted Sinuosity

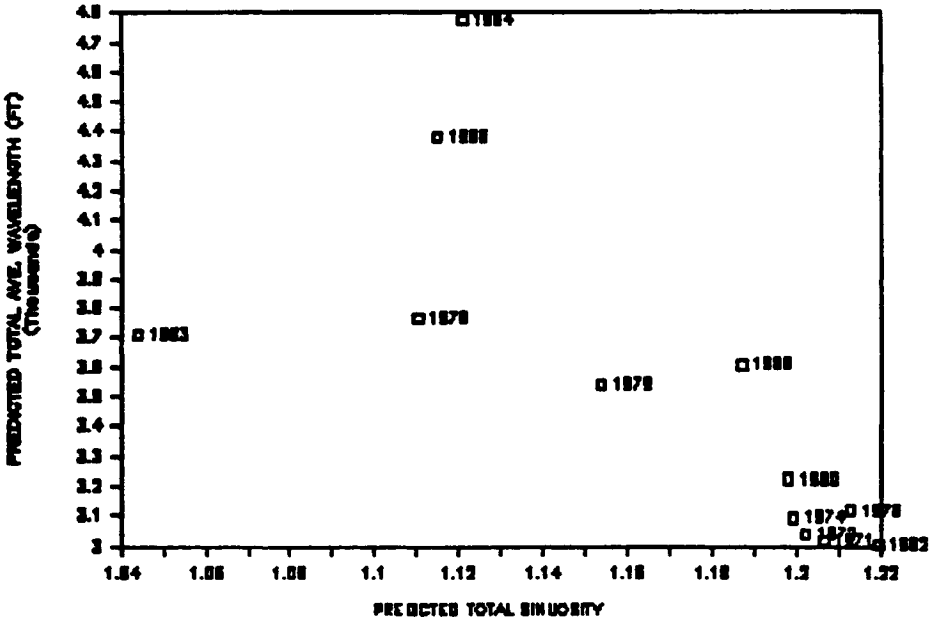

Figure 22

Predicted Wavelength vs. Predicted Width

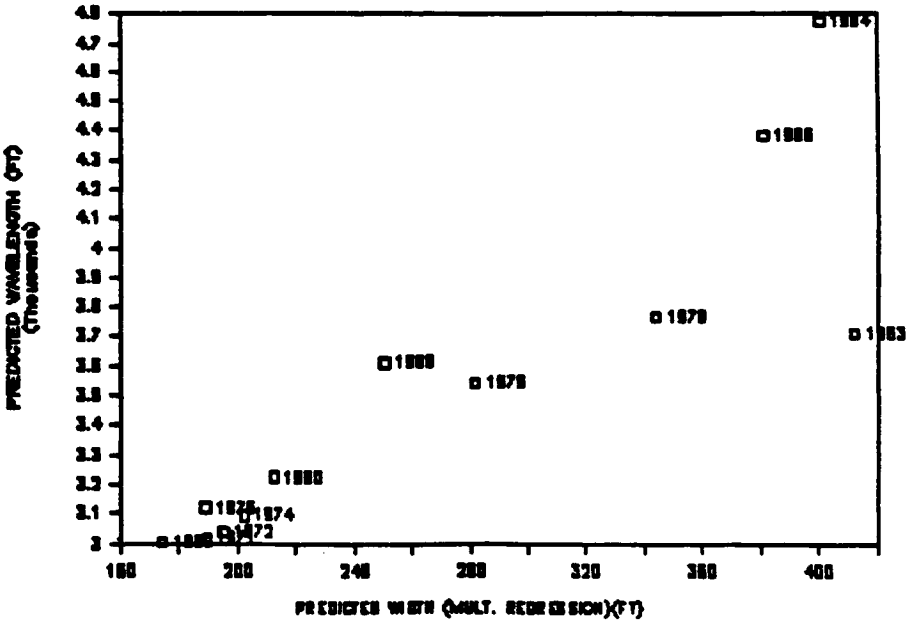

Table 11

Discharge (ind.) vs Total Ave. Wavelength
Regression Output:

Constant	3448.873
Std Err of Y Est	660.3930
R Squared	0.019308
No. of Observations	12
Degrees of Freedom	10

X Coefficient(s)	0.006541
Std Err of Coef.	0.014741

PRED	RESI
3493.875	382.7750
3501.201	449.101
3500.743	120.8389
3466.926	437.0011
3613.052	373.1229
3545.352	393.2610
3486.549	316.6616
3466.272	535.7012
3768.400	-302.365
3461.300	-1517.87
3524.748	-705.784
3461.955	-482.478

Table 12

Discharge and Braid Index (ind.)
vs Average Channel Wavelength
Regression Output:

Constant	1003.669
Std Err of Y Est	306.1491
R Squared	0.810313
No. of Observations	12
Degrees of Freedom	9

X Coefficient(s)	1902.072	0.016530
Std Err of Coef.	310.4804	0.007025

PRED	RESI
3019.467	-91.6326
3037.981	-14.119
3092.765	-287.138
3119.193	89.26812
3768.190	528.2609
3541.160	389.0692
3224.726	54.83936
3005.652	75.08180
3713.231	-357.535
4773.630	-205.544
4384.183	153.6503
3610.120	-334.313

Figure 23

Wavelength vs. Discharge

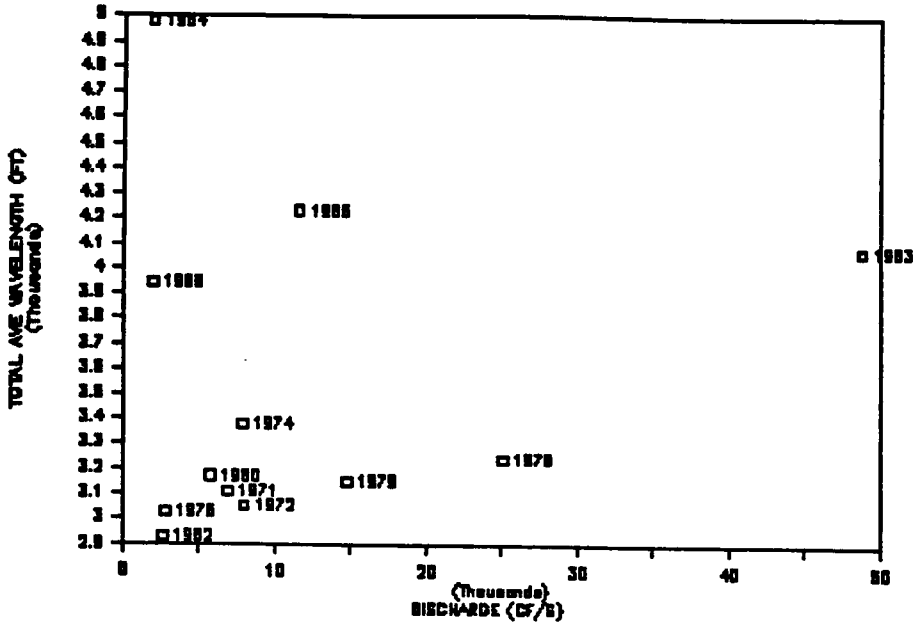

Figure 24

Wavelength Residuals

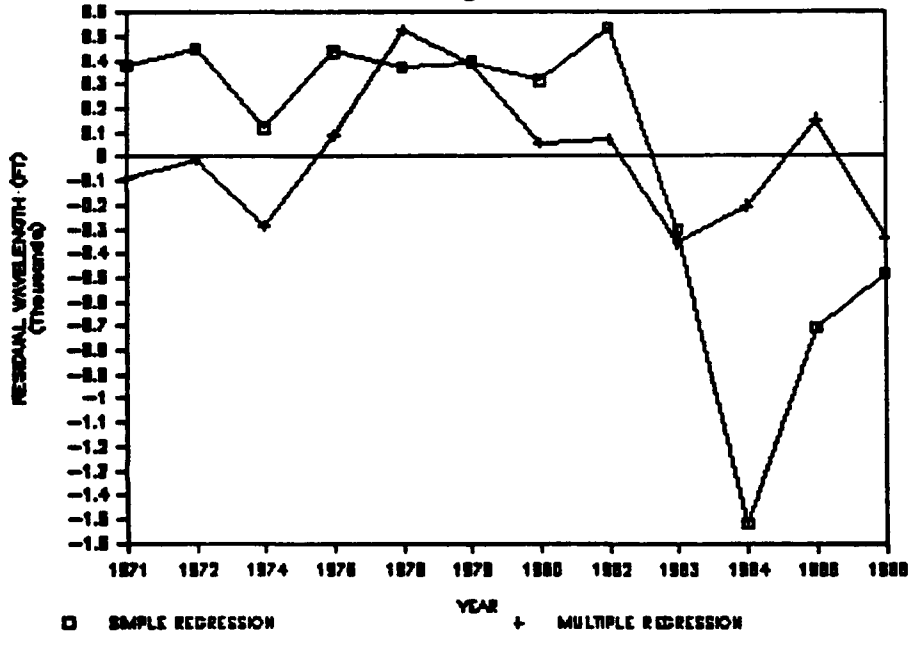

When the braid index is incorporated into the regression analysis as a measure of channel pattern, variables of wavelength, discharge, and braid index become very strongly related. The multiple regression yields an R squared value of .810 (Table 12). This high R squared value indicates that discharge and braid index in combination explain almost all of the covariation between these variables through time. Excepting 1978 data, all residuals fall within 400 feet of the regression line (Figure 24). A high residual wavelength in 1978 (528 feet) may be a result of some other fluvial process influencing the form of the 1978 channel as indicated in the discussion of channel width regressions above. Generally, however, the multiple regression model provides a very good fit to the raw wavelength data. Again, the relationship between variables remains constant through time despite the wide range of peak discharges moving through the system during the timeframe of this study.

Spatial Variation in Hydraulic Variables

Results of regression analysis are based upon average values for hydraulic variables and do not account for spatial variation of channel change within the study reach. For this reason, cross section analysis (at-a-section analysis) of channel width and primary channel overlay analysis should provide further support for

results of regression analysis if expected trends in the data exist. If actively changed sub-reaches exhibit major channel widening during floods followed by rapid channel narrowing during relaxation periods, the channel should be controlled by equilibrium conditions. Conversely, minor channel narrowing during relaxation periods following major flows should refute the argument that equilibrium conditions dominantly control channel form. Cross section numbers referred to in the subsequent discussion are indicated in Figure 4.

Changes in channel form resulting from both floods and relaxation periods are spatially variant within the San Xavier reach. Figure 25 depicts cross sections which have undergone the most change through time (deviated the most about their mean width). Much of the change seems to occur within three sub-reaches. However, since unusually dramatic changes in channel width resulted from the 10/2/83 discharge (48,850 cfs), most of the standard deviation in width is explained by that flood. For this reason, results of data corresponding to individual floods and subsequent relaxation periods are presented in chronological order below.

1972 - 1976

The channel relaxation period between 1972 and

Figure 25

Channel Width Standard Deviation vs. Cross Section

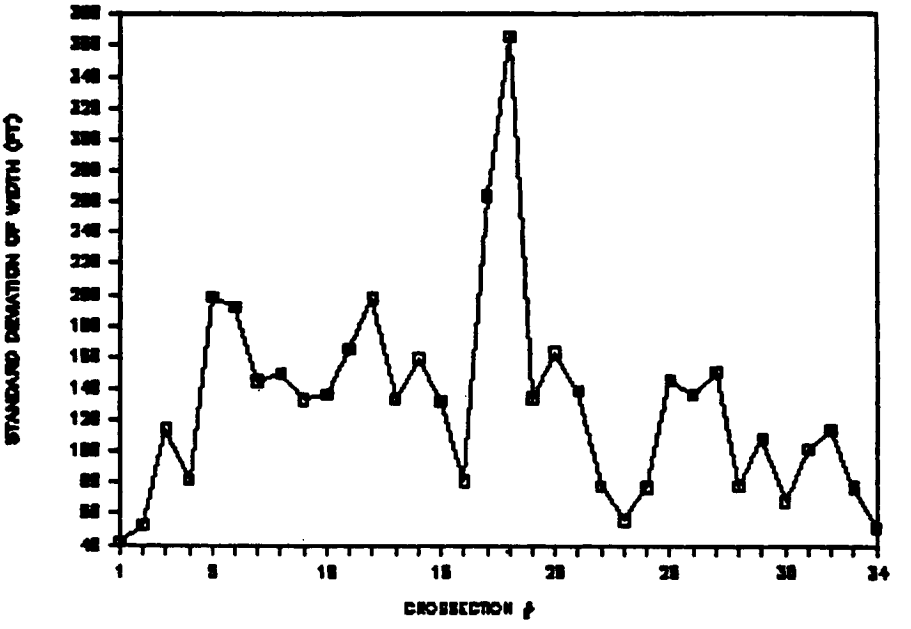

Figure 26

Channel Width Standard Deviation vs. Year

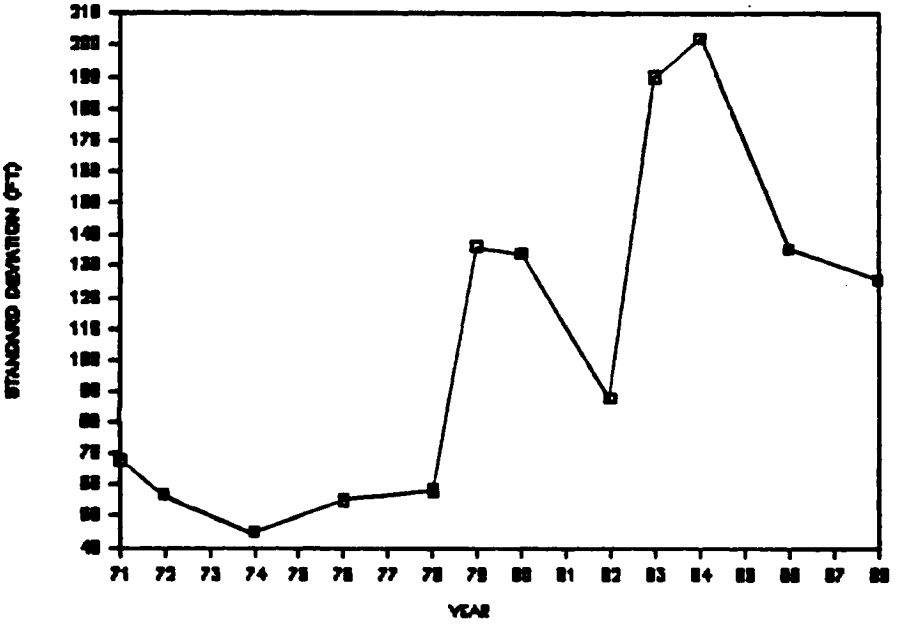

1976 is characterized by channel narrowing at almost all cross sections (Figures 27 and 28). Most significant narrowing between 1972 and 1976 occurs between cross sections 6 and 17 and between cross sections 26 and 32. Cross sections 5, 18, 21, 23, and 34 remain basically unchanged through this period. By 1976, channel widths in almost all subreaches are between 80 and 140 feet. This contrasts to the wide range of widths in 1972 between 140 and 340 feet. Standard deviations for these two years, however, do not indicate this trend (Figure 26). This is probably a function one unusually high width at cross section 33 (356 feet) in 1976. This width may be in error due to poor interpretation and/or measurement of the primary channel. The general tendency for channel widths in the 1976 system to seemingly approach a steady state near 100 feet supports the presence of an equilibrium condition throughout the system.

The 10/10/77 Flood

The discharge event of 10/10/77 (25,100 cfs) resulted in channel widening dominantly between cross section 17 and the southern limit of the mining district at cross section 6. Figure 29 indicates that only minor widening occurred outside this reach. However, Figure 30 shows that, while little primary channel widening

Figure 27

1972 and 1976 At-A-Section Widths

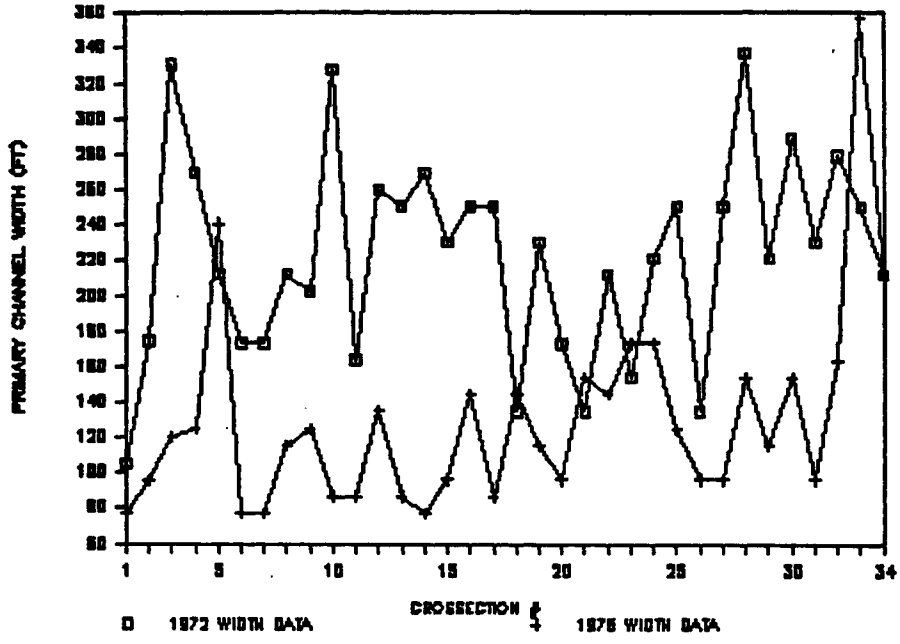

Figure 29

1976 and 1978 At-A-Section Widths

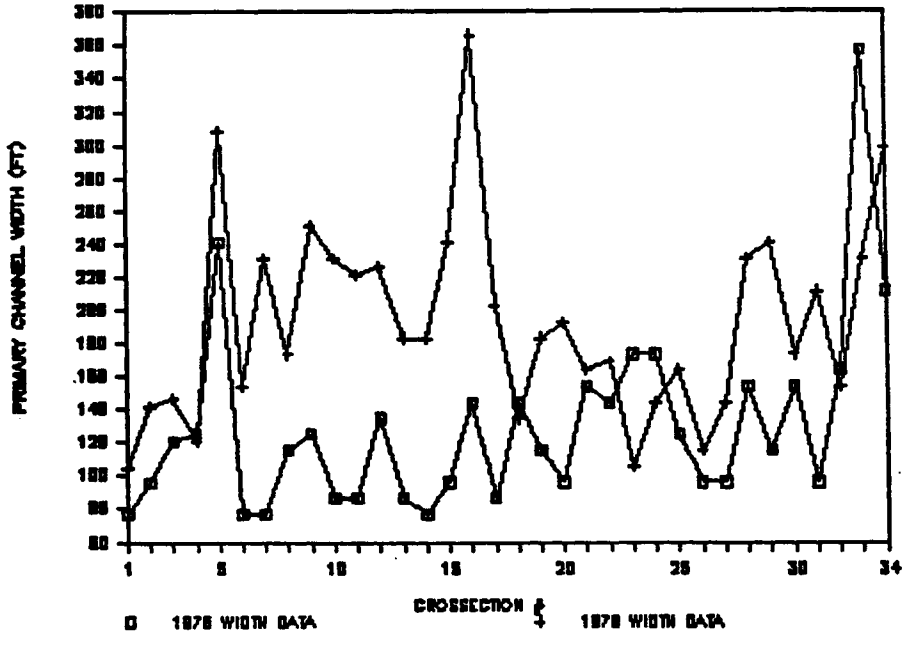

Figure 28

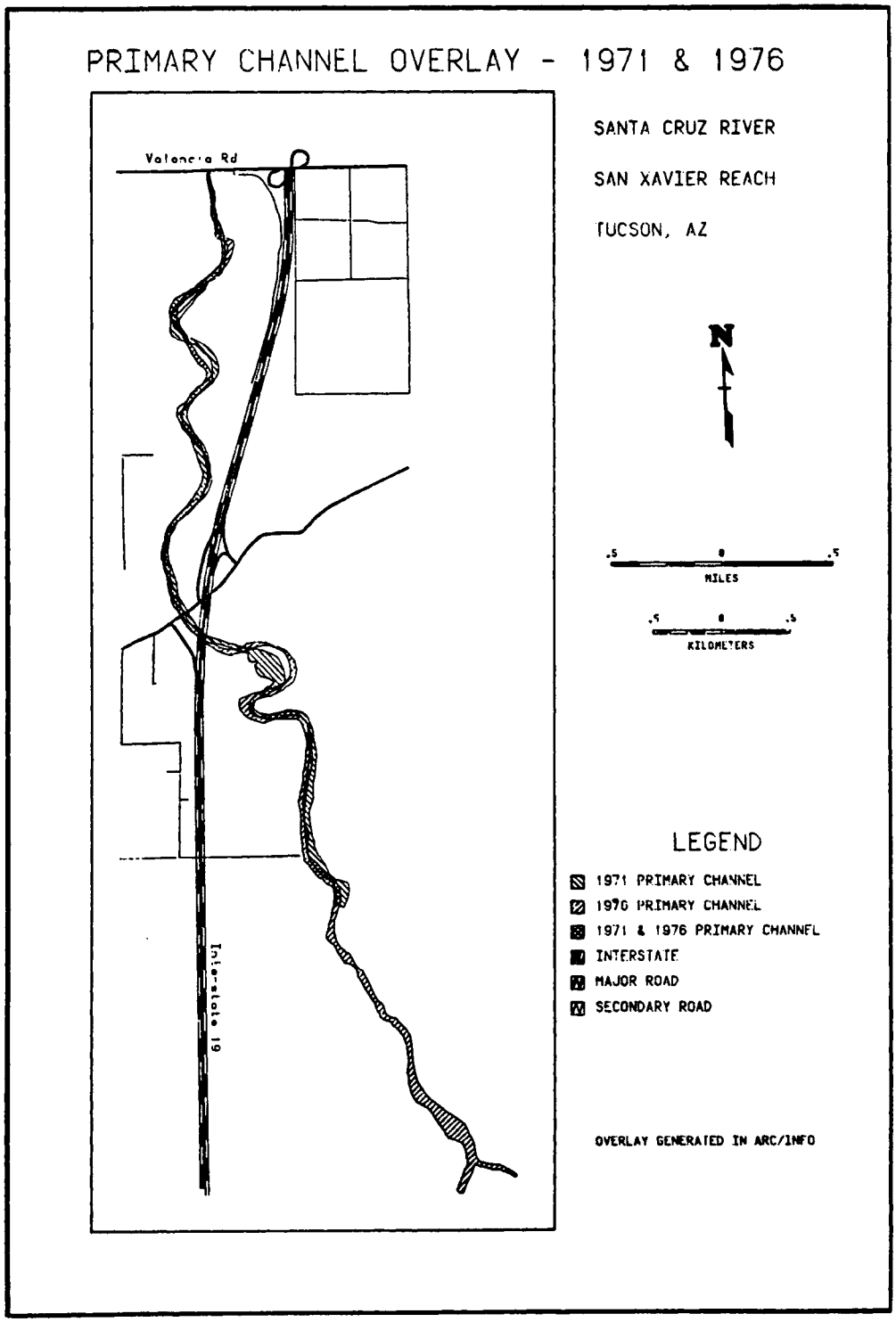
PRIMARY CHANNEL OVERLAY - 1971 & 1976
Valencia Rd
Interstate 19
SANTA CRUZ RIVER
SAN XAVIER REACH
TUCSON, AZ
N
.5 0 .5
MILES
.5 0 .5
KILOMETERS
LEGEND
1971 PRIMARY CHANNEL
1976 PRIMARY CHANNEL
1971 & 1976 PRIMARY CHANNEL
INTERSTATE
MAJOR ROAD
SECONDARY ROAD
OVERLAY GENERATED IN ARC/INFO

Figure 30

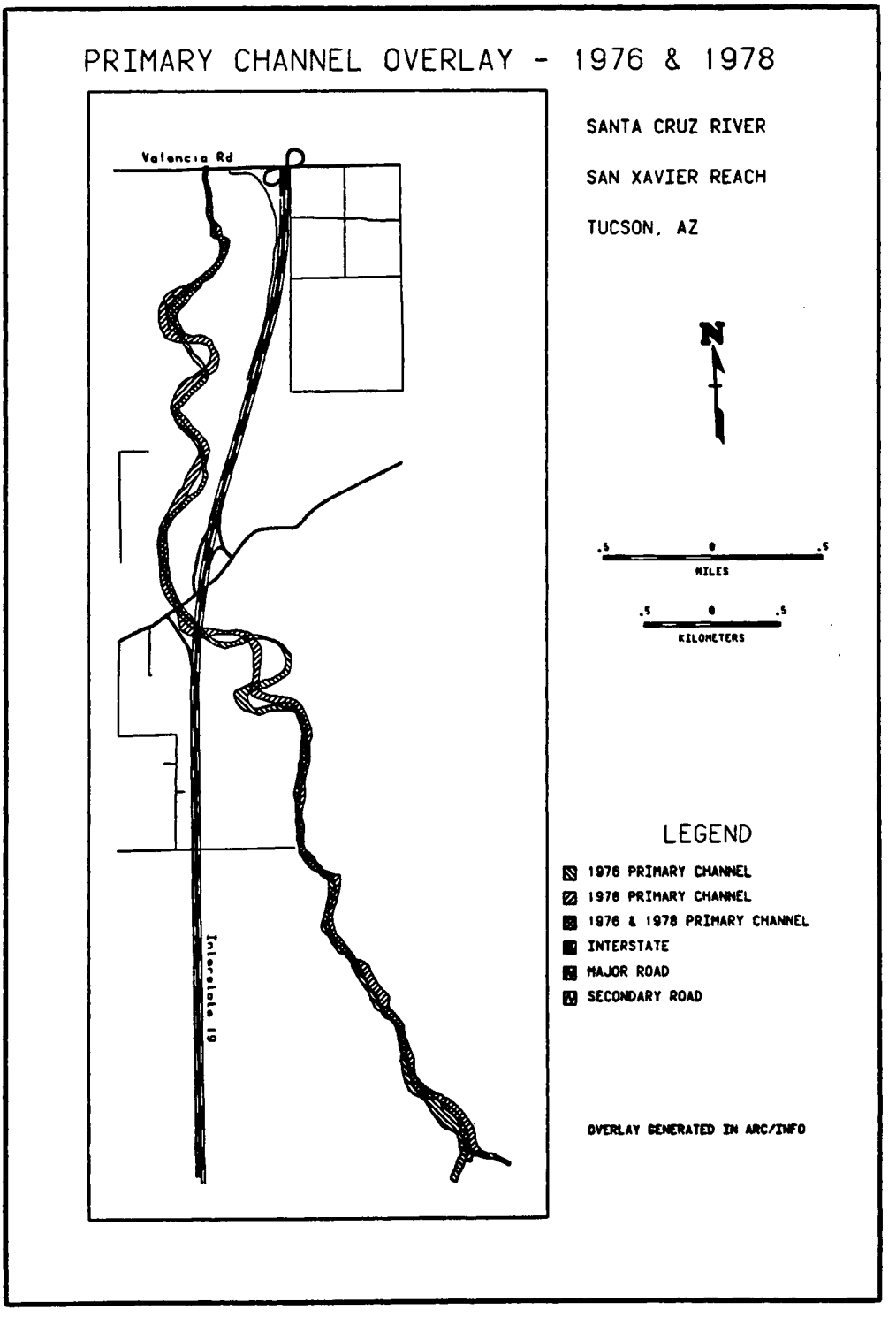
PRIMARY CHANNEL OVERLAY - 1976 & 1978
Valencia Rd
Interstate 19
SANTA CRUZ RIVER
SAN XAVIER REACH
TUCSON, AZ
N
.5 0 .5
MILES
.5 0 .5
KILOMETERS
LEGEND
1976 PRIMARY CHANNEL
1978 PRIMARY CHANNEL
1976 & 1978 PRIMARY CHANNEL
INTERSTATE
MAJOR ROAD
SECONDARY ROAD
OVERLAY GENERATED IN ARC/INFO

occurred in response to the flood, the reach between cross sections 19 and 17 immediately south of Martinez Hill was changed dramatically. A meander cutoff began to develop within this reach as a result of the flood. In this respect, the flood was catastrophic, at least through this subreach. Since little channel widening happened outside the indicated subreach, the standard deviation value for the 1978 channel increased only slightly over the 1976 value (Figure 26).

The 12/19/78 Flood

The flood of 12/19/78 (14,750 cfs) caused much more channel widening than the higher discharge a year earlier. Figures 31 and 32 indicate that most of the widening occurred within the three subreaches (cross sections 4 - 11, 17 - 19, and 24 - 27). The channel seems to be very stable through the gravel mining district, at the I-19 bridge crossing, and within very straight upstream sub-reaches. The standard deviation for the 1979 channel is 136.68 feet in comparison to the 1978 value of 58.54 feet (Figure 26). This sudden increase in standard deviation manifests spatially variable channel width increases within the study reach as a result of the 1978 flow.

Figure 31

1978 and 1979 At-A-Section Widths

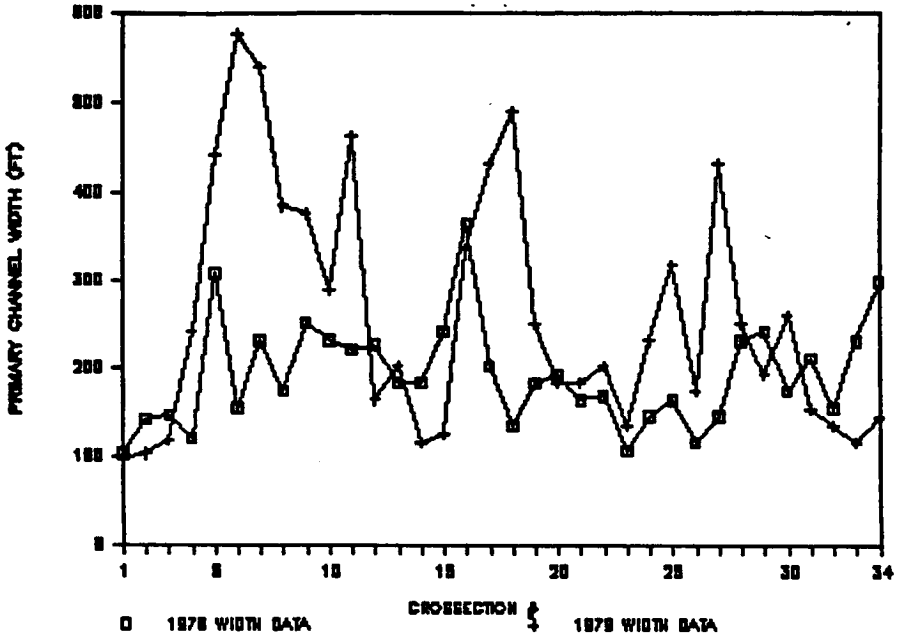

Figure 33

1979 and 1982 At-A-Section Widths

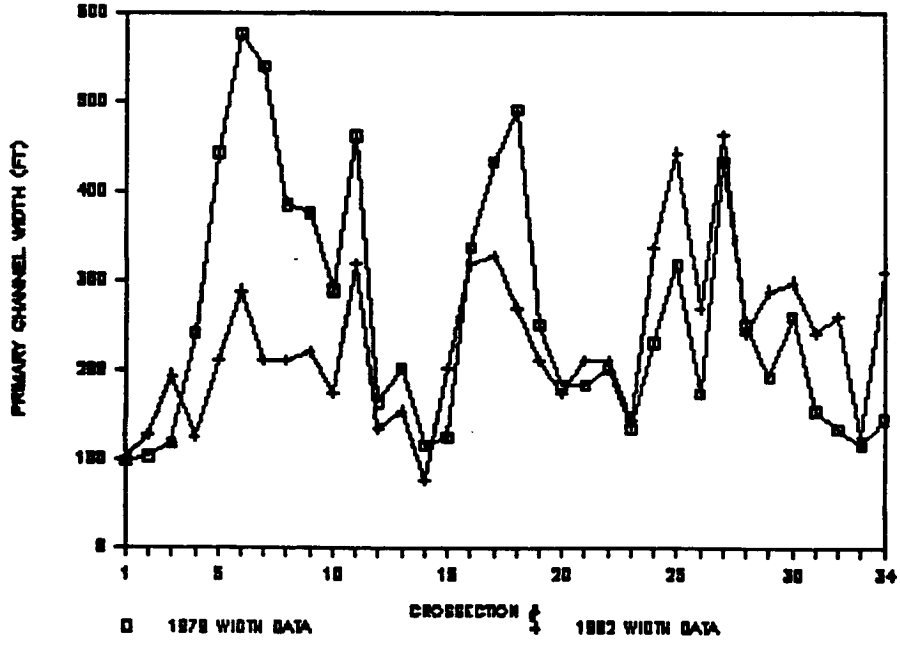

Figure 32

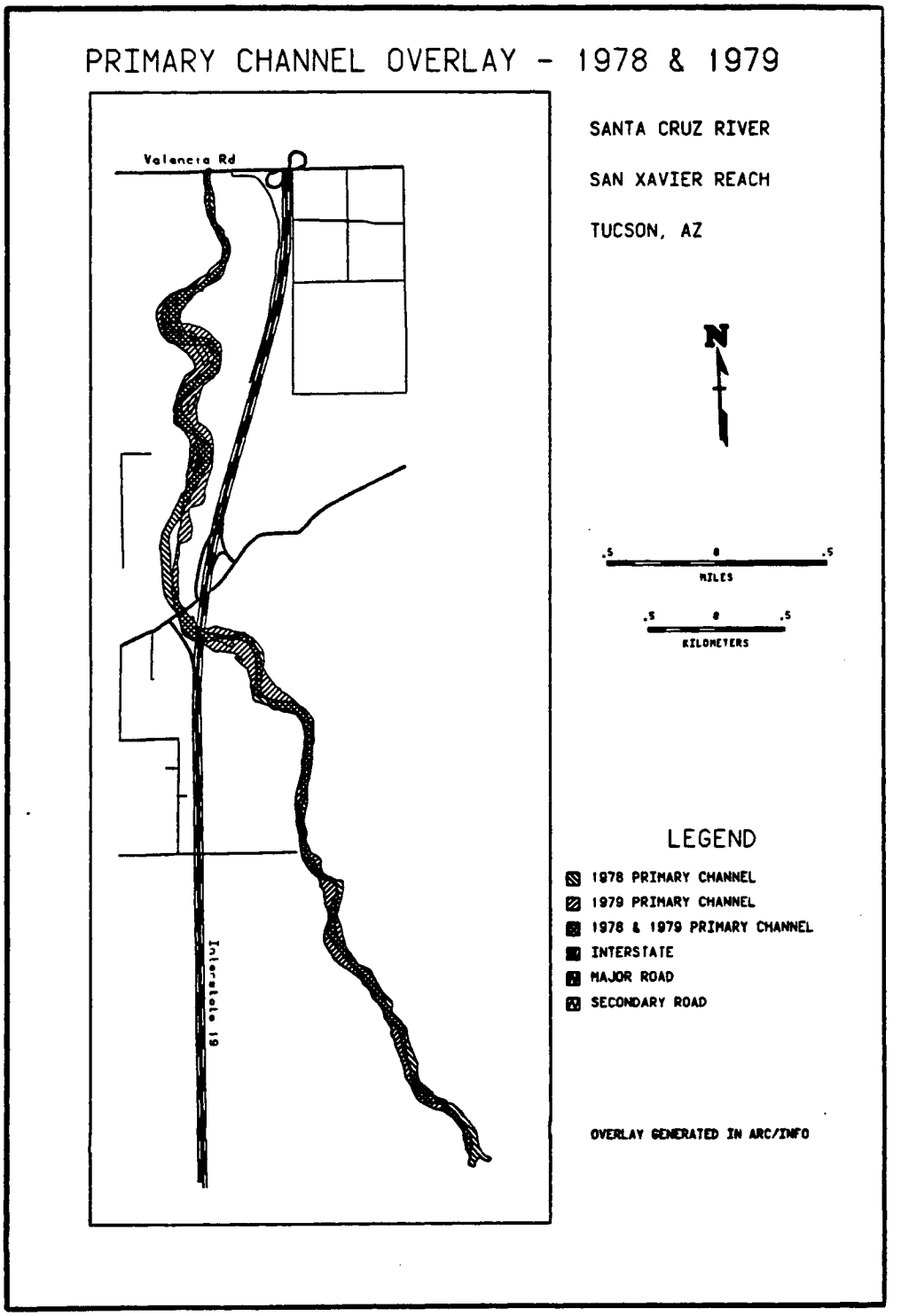
PRIMARY CHANNEL OVERLAY - 1978 & 1979
Valencia Rd
Interstate 19
SANTA CRUZ RIVER
SAN XAVIER REACH
TUCSON, AZ
N
.5 0 .5
MILES
.5 0 .5
KILOMETERS
LEGEND
1978 PRIMARY CHANNEL
1979 PRIMARY CHANNEL
1978 & 1979 PRIMARY CHANNEL
INTERSTATE
MAJOR ROAD
SECONDARY ROAD
OVERLAY GENERATED IN ARC/INFO

Figure 34

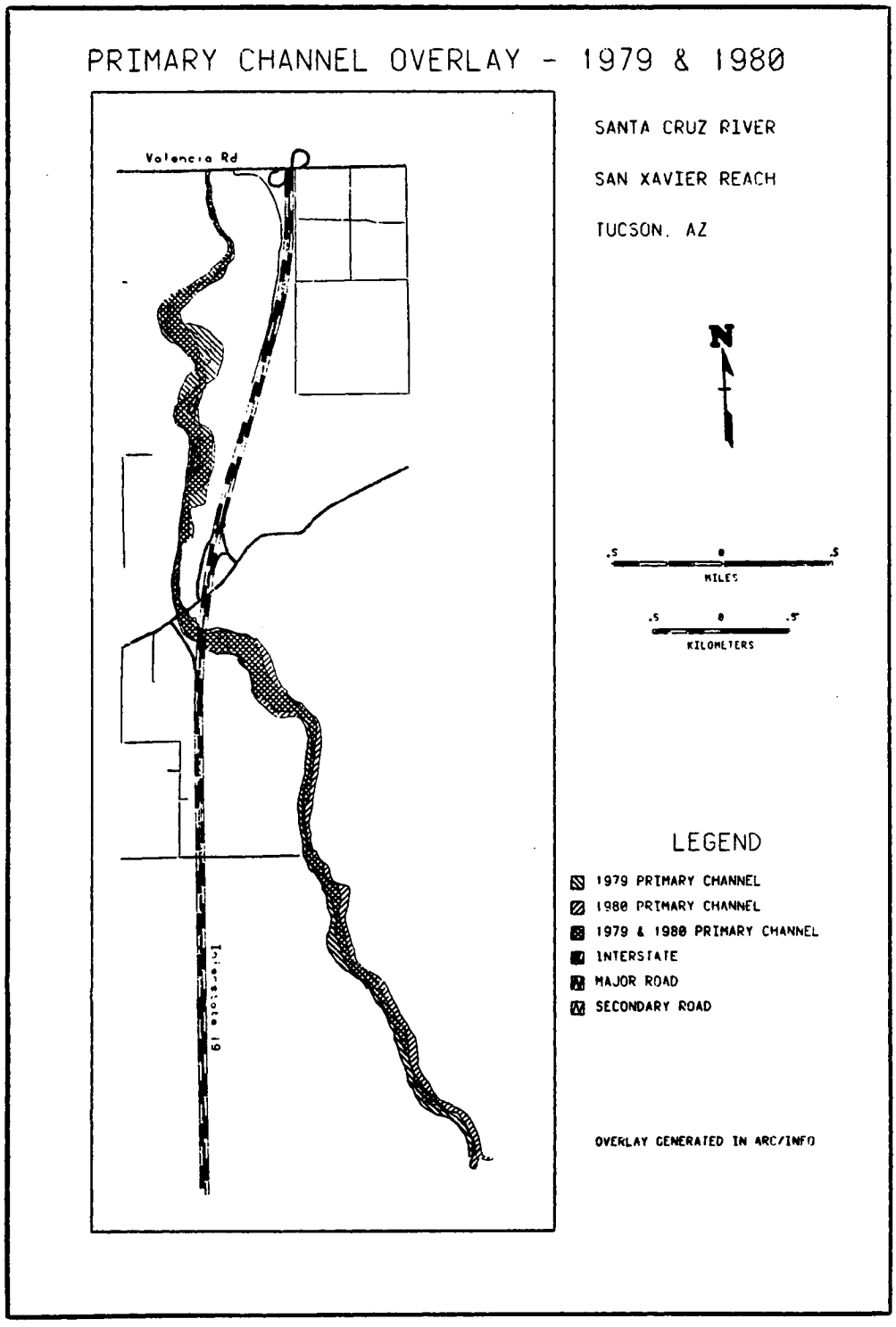
PRIMARY CHANNEL OVERLAY - 1979 & 1980
Valencia Rd
Interstate 19
SANTA CRUZ RIVER
SAN XAVIER REACH
TUCSON, AZ
N
.5 0 .5
MILES
.5 0 .5
KILOMETERS
LEGEND
1979 PRIMARY CHANNEL
1980 PRIMARY CHANNEL
1979 & 1980 PRIMARY CHANNEL
INTERSTATE
MAJOR ROAD
SECONDARY ROAD
OVERLAY GENERATED IN ARC/INFO

Figure 35

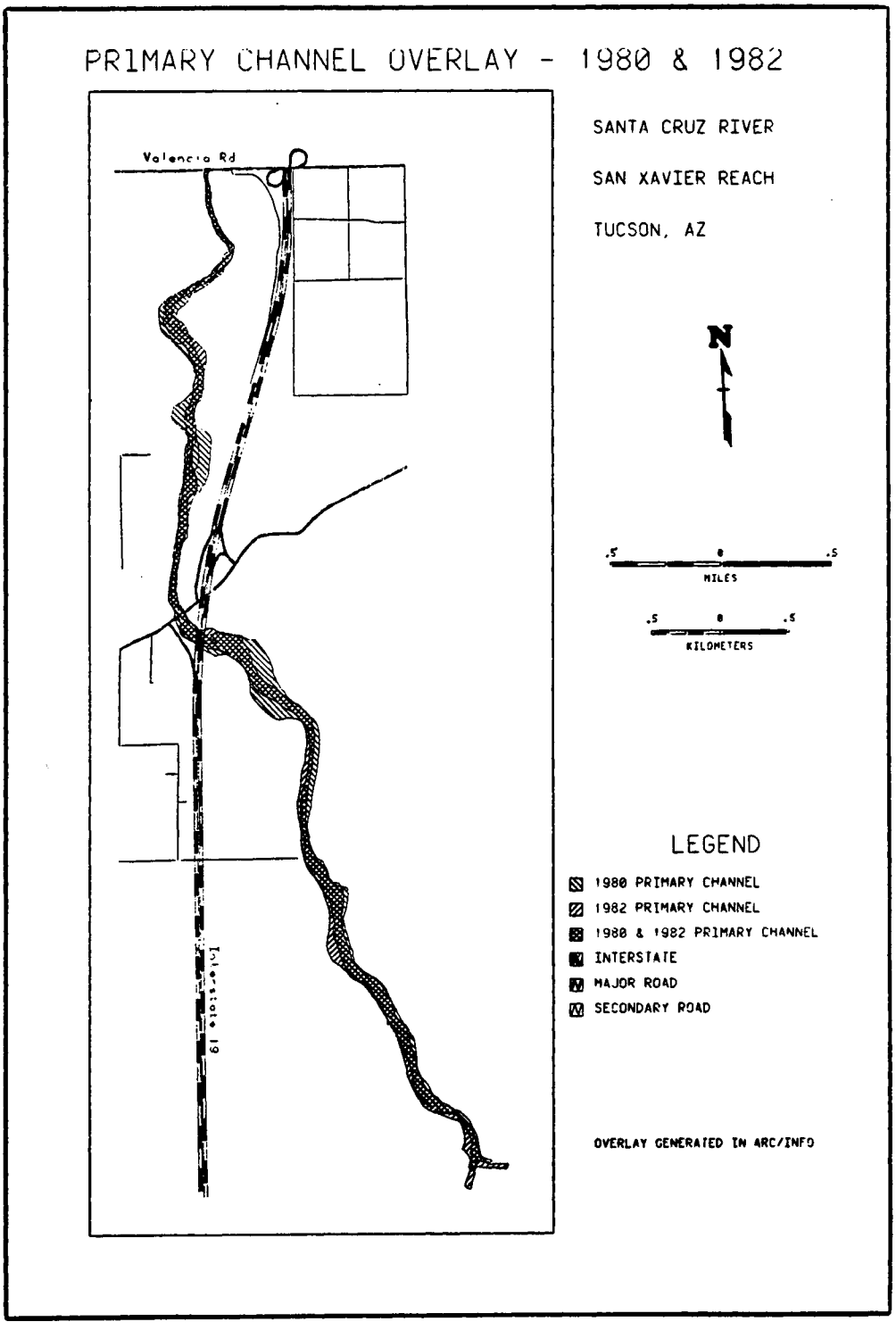
PRIMARY CHANNEL OVERLAY - 1980 & 1982
Valencia Rd
Interstate 19
SANTA CRUZ RIVER
SAN XAVIER REACH
TUCSON, AZ
N
.5 0 .5
MILES
.5 0 .5
KILOMETERS
LEGEND
1980 PRIMARY CHANNEL
1982 PRIMARY CHANNEL
1980 & 1982 PRIMARY CHANNEL
INTERSTATE
MAJOR ROAD
SECONDARY ROAD
OVERLAY GENERATED IN ARC/INFO

1979 - 1982

The reaches that experienced channel widening in 1977 and 1978 are characterized by an almost equal amount of narrowing during the relaxation period between 1979 and 1982 (Figures 33, 34, and 35). Stable reaches through these floods also remain very stable through this relaxation period. Thus, channel narrowing dominantly occurred within the flood widened subreaches. Standard deviation for the 1982 channel (87.9 feet) is nearly 50 feet less than that for the 1979 channel (136.6 feet) (Figure 26). Further, the standard deviation for the 1982 channel is only about 30 feet greater then that for the 1976 channel. This trend indicates a rapid recovery (four years) of channel width to the flood events and a tendency for all cross sections tend toward an equilibrium condition.

The 10/2/83 Flood

The flood of 10/2/83 (48,850 cfs) caused the greatest amount of channel widening during the time frame of this study. As figure 36 indicates, channel widening of generally more then 100 feet occurred throughout the channel except at cross section 7. This anomaly is a result of bank reconstruction immediately

Figure 36

1982 and 1983 At-A-Section Widths

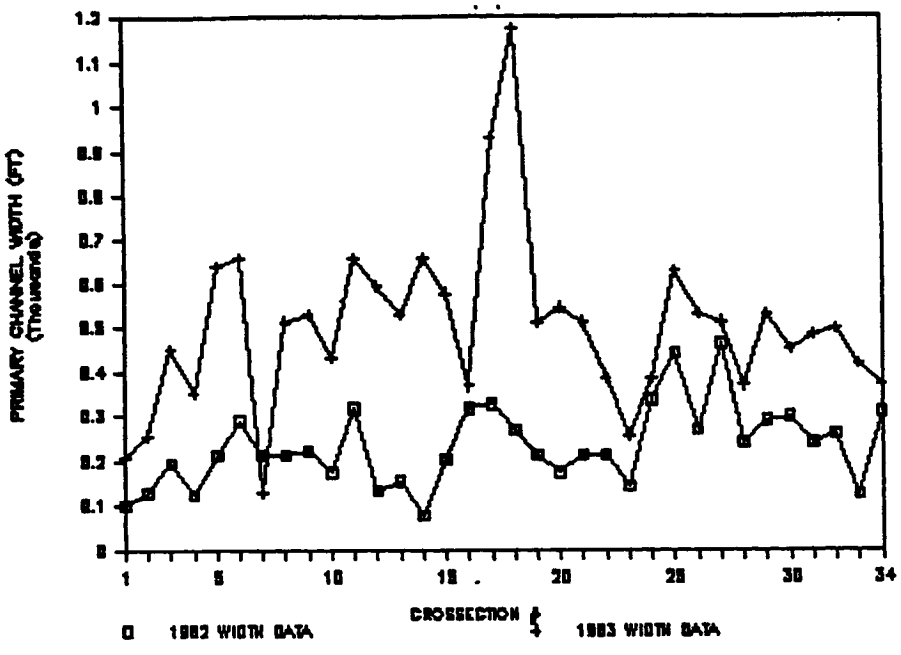

Figure 38

1983 and 1988 At-A-Section Widths

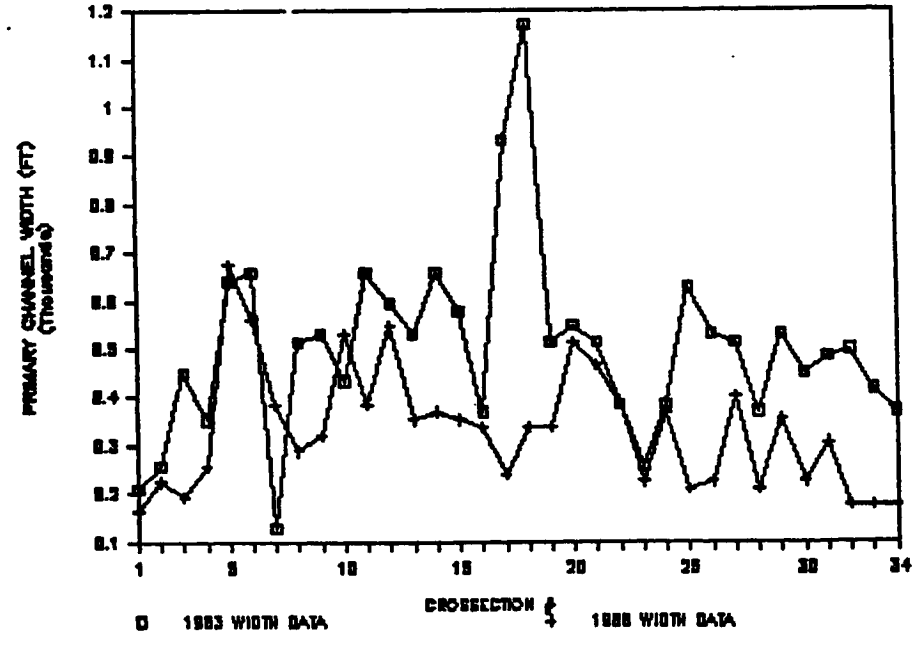

Figure 37

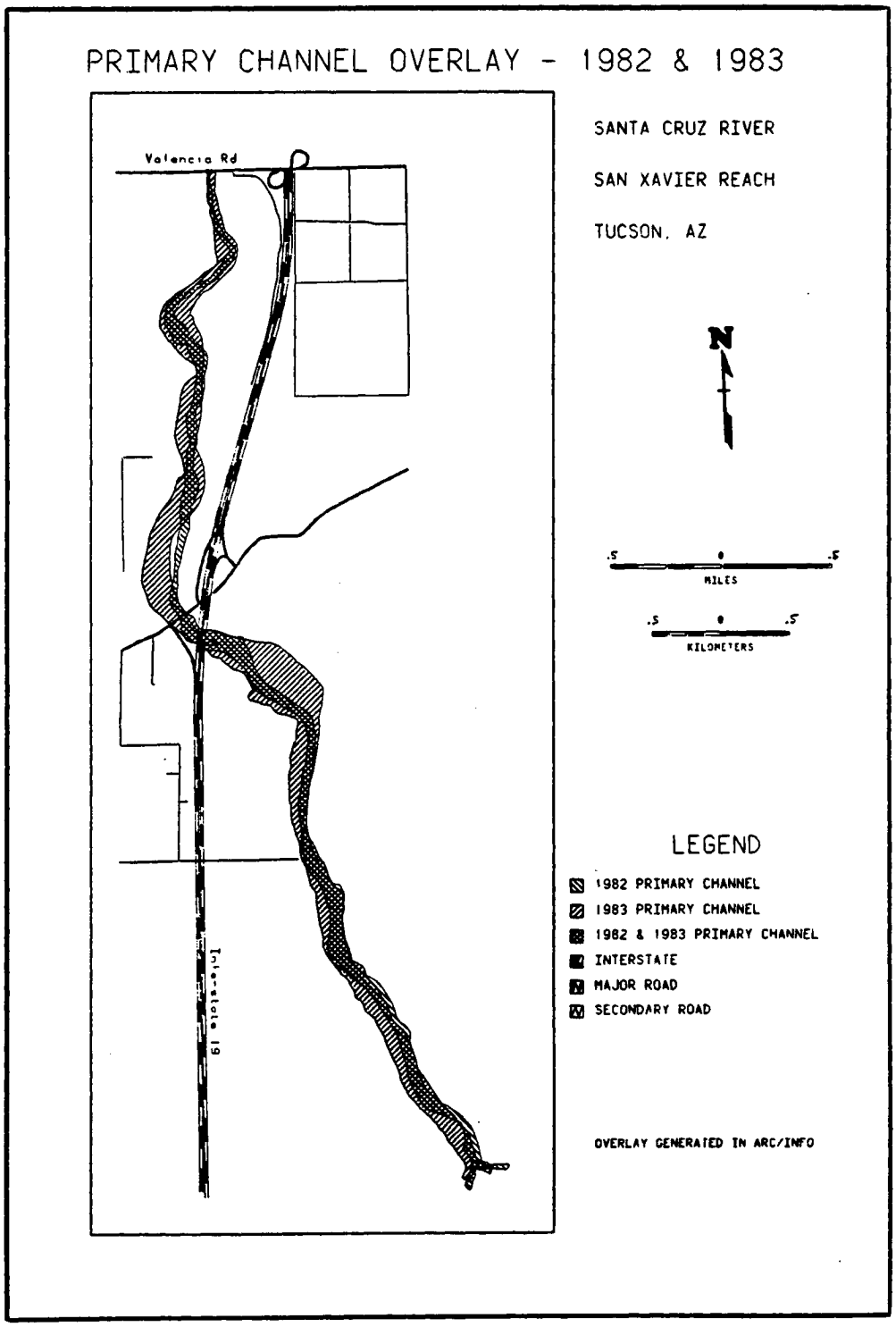
PRIMARY CHANNEL OVERLAY - 1982 & 1983
Valencia Rd
Interstate 19
SANTA CRUZ RIVER
SAN XAVIER REACH
TUCSON, AZ
N
.5 0 .5
MILES
.5 0 .5
KILOMETERS
LEGEND
1982 PRIMARY CHANNEL
1983 PRIMARY CHANNEL
1982 & 1983 PRIMARY CHANNEL
INTERSTATE
MAJOR ROAD
SECONDARY ROAD
OVERLAY GENERATED IN ARC/INFO

Figure 39

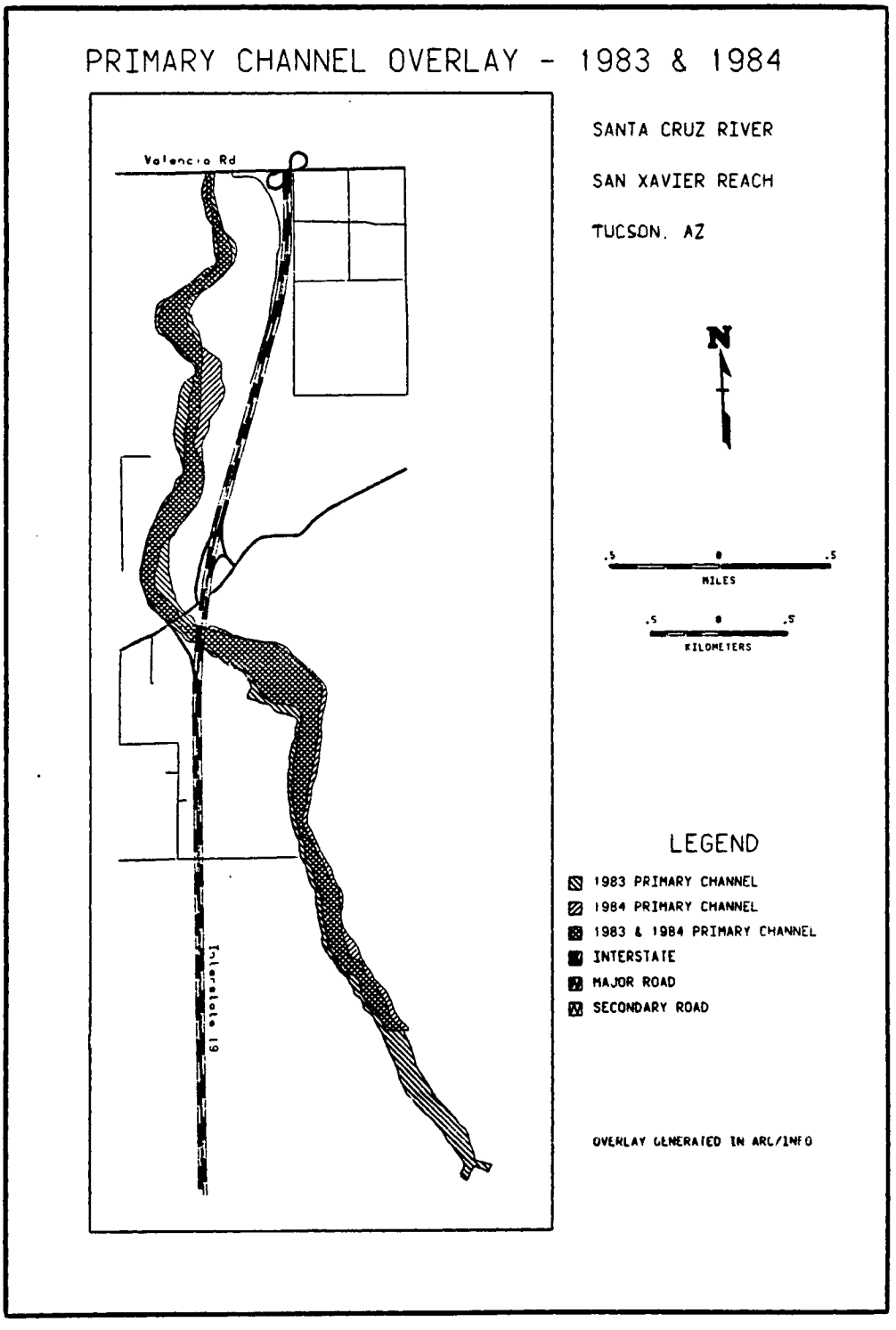
PRIMARY CHANNEL OVERLAY - 1983 & 1984
Valencia Rd
Interstate 19
SANTA CRUZ RIVER
SAN XAVIER REACH
TUCSON, AZ
N
.5 0 .5
MILES
.5 0 .5
KILOMETERS
LEGEND
1983 PRIMARY CHANNEL
1984 PRIMARY CHANNEL
1983 & 1984 PRIMARY CHANNEL
INTERSTATE
MAJOR ROAD
SECONDARY ROAD
OVERLAY GENERATED IN ARC/INFO

Figure 40

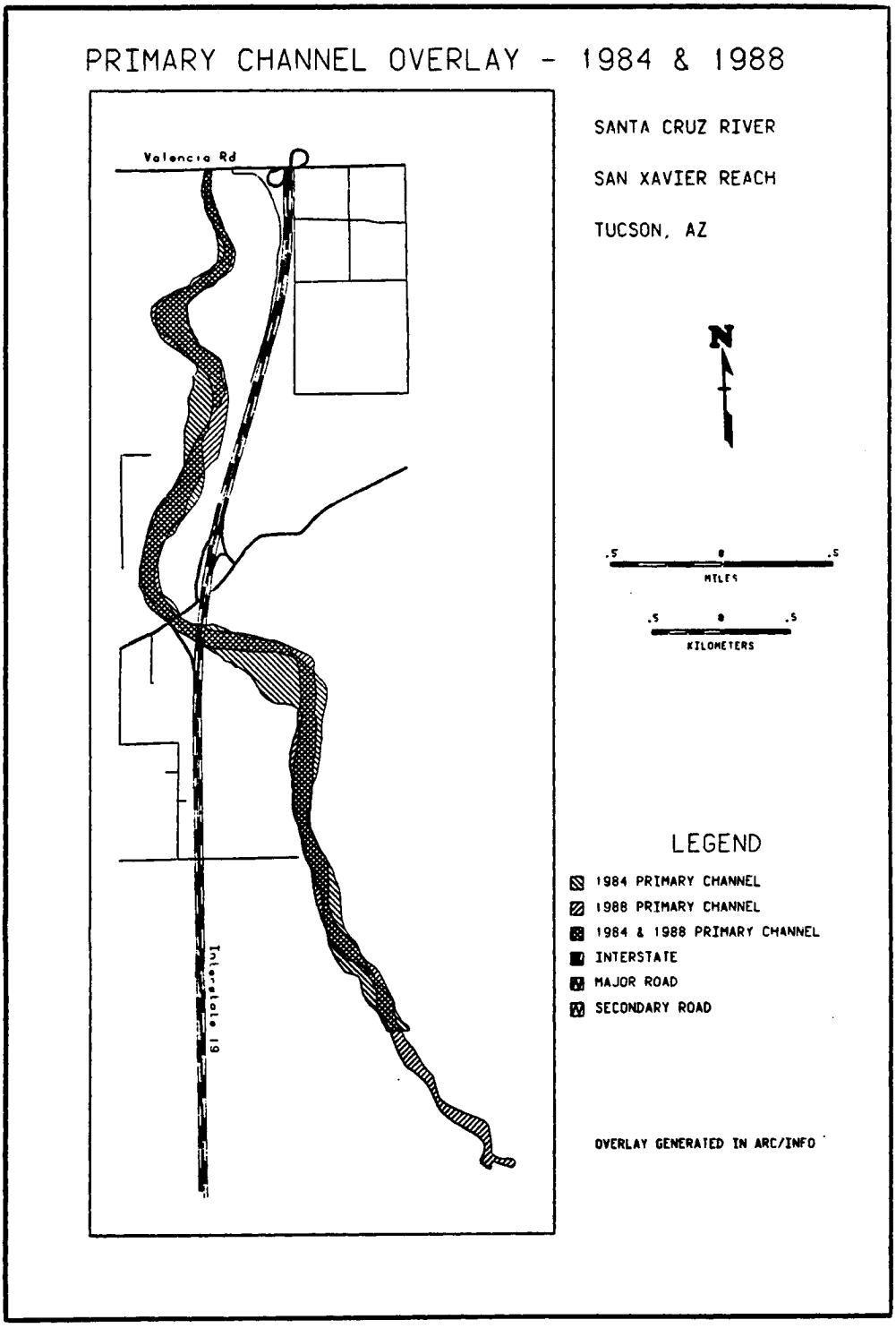
PRIMARY CHANNEL OVERLAY - 1984 & 1988
Valencia Rd
Interstate 19
SANTA CRUZ RIVER
SAN XAVIER REACH
TUCSON, AZ
N
.5 0 .5
MILES
.5 0 .5
KILOMETERS
LEGEND
1984 PRIMARY CHANNEL
1988 PRIMARY CHANNEL
1984 & 1988 PRIMARY CHANNEL
INTERSTATE
MAJOR ROAD
SECONDARY ROAD
OVERLAY GENERATED IN ARC/INFO

following the flood (between the flood and the date of the air photography). Figure 37 shows that the meander cutoff, instigated by the 1977 flood immediately south of Martinez Hill, was fully developed following the 1983 flow. Between cross sections 8 and 3, a meander bend around the west boundary of the gravel mining operation was completely washed out by the flow. During the interim between the event and the photographic coverage on 10/10/83 the meander bend was completely reconstructed to approximate its original form. During the flood, both the San Xavier Road bridge and the northbound bridge of I-19 collapsed as a result of arroyo widening along the east wall of this reach. The standard deviation of channel width for the 1983 channel (190 feet) increased by more than 100 feet compared to the 1982 value (Figure 26). Thus, channel widths for the 1983 channel are extremely variable throughout the reach. These observations all indicate that the 1983 flood may have caused catastrophic channel changes within the San Xavier reach.

1983 - 1988

Finally, the relaxation period between 1983 and 1988 is characterized by primary channel narrowing (Figures 38, 39, and 40). Excepting cross sections within

the mining district, channel narrowing occurs throughout the study reach. The subreaches most dramatically widened during the 1983 flood are generally narrowed by 100 or more feet during this period. Cross sections 17 and 18, associated with the meander cutoff, underwent the most change, each narrowing by more than 650 feet. The 1984 flow (11,600 cfs) smoothed the channel meander pattern between cross sections 9 and 6 where the banks had been reconstructed a year earlier (Figure 39). As a result, increases in width between 1983 and 1988 occur within this sub-reach. As the channel narrows through time, standard deviation values drop rapidly (Figure 26). A total change in standard deviation of approximately 65 feet between 1983 and 1988 indicates very rapid recovery to equilibrium conditions in the channel despite major channel changes caused by the 1983 flood.

Chapter 5

CONCLUSION

Based upon the results presented in this study, forces of equilibrium seem to dominantly control channel form along the San Xavier reach of the Santa Cruz River during the 17 year period between 1971 and 1988. Changes caused by flood events, including the "catastrophic" flood in 1983, are rapidly adjusted toward equilibrium conditions during years immediately following these flows. This trend indicates that channel form is controlled by floods only for very short time periods, possibly just for the duration of the events themselves. Trends in the data during subsequent relaxation periods manifest the dominance of an equilibrium conditions on controlling channel form. Contrary to results of a study of the Gila River in Arizona (Burkham, 1972), a system similar to the Santa Cruz River, relaxation periods for the San Xavier reach are apparently characterized by rapid adjustment toward equilibrium rather than slow adjustment spanning several decades.

Trends in hydraulic variables through time indicate that floods temporarily disrupt processes acting within the channel. Trends for channel width and planimetric channel area through time show that increases in these hydraulic variables are associated with floods in 1977, 1978, and 1983. Subsequent relaxation periods are consistently characterized by reductions for both width and area. Due to systematic measurement errors, adjusted for by the braid index, trends for raw wavelength and sinuosity data did not correlate well with the 1977 and 1978 floods. Large changes did, however, occur in association with the 1983 event. Temporal trends in the braid index variable, used to measure channel pattern, indicate that the channel became heavily braided in response to the three floods. Within four years following the 1978 event, the braided pattern had readjusted to a single channel through virtually all of the study reach. Rapid readjustment of channel pattern also followed the 1983 flood until 1988 (the present) when this study ends. In general, rapid adjustment of hydraulic variables to equilibrium conditions occurs during the relaxation periods.

The braid index defined in this study provided a variable to account for systematic errors created by measuring hydraulic variables in a channel which changes

pattern through time. Using this variable as a second independent variable in regression analyses allowed for simplified measurements of hydraulic variables, particularly sinuosity and wavelength which become difficult to define in a braided system. Results of multivariate regressions using braid index as the second independent variable consistently explained more of the covariation among the regressed variables then did simple regression analyses based on peak discharge alone.

Strong relationships between the independent variables of braid index and peak discharge, and each of the dependant variables (average channel width, planimetric channel area, average channel wavelength, and channel sinuosity) through time indicate the apparent dominance of an equilibrium state on controlling channel form during this study. These strong relationships between hydraulic variables indicate that the same fluvial processes are controlling the channel form between 1971 and 1988 despite the wide range of peak discharges associated with this period. Even the channel resulting from the flow of 10/2/83, considered catastrophic by most standards (Saarinen et. al., 1984), was reasonably well fitted to the multiple regression model. Since, in theory, fluvial processes in a channel controlled by catastrophic flows should be redefined by each

catastrophic flood, such a channel should exhibit poor relationships between hydraulic variables through time. As indicated, this is not the case in the San Xavier reach during the 17 years of channel history analyzed in this study.

The three major floods during the time frame of this study caused channel pattern changes similar to those observed by Burkham (1972) and Pearthree and Baker (1987) in other river reaches in Arizona. A braided system resulted from the floods probably due to deposition of large amounts of coarse grained sediments within the channel during receding flood stages. Following the 1978 and 1983 events, vegetation was reestablished along the sides of, and on bars within, the primary channel. As vegetation matured, braided channels were abandoned, sinuosity increased, and the braided system slowly moved toward a single channel pattern. The rate of channel pattern development occurred very rapidly within the San Xavier reach. A short period of four years is sufficient for redefinition of the braided 1978 system back to a single channel pattern. The recovery time necessary for the 1984 braided system to return to a single channel cannot be defined because the channel is still readjusting at the time of this study. However, the trend again indicates a very rapid recovery

rate, much quicker then that observed in other similar systems. Again, the rapid recovery rate supports the argument that an equilibrium condition is controlling channel form.

Although the results manifest that channel form is controlled dominantly by equilibrium conditions in the San Xavier reach, time frame limitations of this study inhibit the identification of these conditions. To justify observations of the equilibrium conditions would require a timeframe extending back into the 1960s and through the 1990s. If results similar to those obtained in this study hold true over longer time periods, then unequivocal conclusions might be drawn about the period necessary for equilibrium conditions to be met within the system. Thus, based upon this study, the San Xavier reach between 1971 and 1988 is best not thought of as a system in equilibrium, but rather a system constantly and rapidly adjusting toward equilibrium conditions.

The initial purpose of this study was to determine the extent to which the San Xavier reach is a result of catastrophic flows. Assumptions based on previous studies of fluvial systems in arid and semi-arid climates indicate that catastrophic flows are dominant controls of channel form over time periods similar to those of this study. However, results of this study

indicate that these assumptions do not hold true for the San Xavier reach of the Santa Cruz River. For this reason, I suggest that future studies of arid and semi-arid fluvial systems consider both frameworks of equilibrium and catastrophism as interrelated to one another. Integration of both frameworks is necessary to fully understand the nature of channel change through time for any given system. "Present form is the product of both past and present processes and conditions." (Knighton, 1984, p.162). Also, I suggest that measurement errors inherent in defining hydraulic variables may be critical sources of inconsistency in previous studies attempting to assess the nature of equilibrium between form and process in ephemeral systems. Attempts to account for such errors by using variables, such as the braid index employed in this study, might prove useful in subsequent studies of channel change through time.

APPENDIX 1

Hydraulic Variable Data

PRIMARY CHANNEL DATA
Entire Study Reach

YEAR	DISCHARGE	WAVELENGTH (ft)	AREA (sq ft)	AVE WIDTH (ft)	SINUOSITY	BRAID INDEX
1971	6880	3111.1	28868.05	157.5129	1.268975	1
1972	8000	3052.1	44548.61	222.8235	1.286835	1
1974	7930	3379.904	33111.11	164.7868	1.232145	1.029411
1976	2760	3029.925	28819.44	130.1858	1.17881	1.088235
1978	25100	3239.929	37798.61	192.4732	1.15003	1.235294
1979	14750	3152.091	54548.61	260.7117	1.158455	1.205882
1980	5760	3169.887	51958.33	257.5095	1.1678	1.117647
1982	2660	2930.570	44715.27	232.3451	1.183	1.029411
1983	48850	4070.766	99930.55	501.5867	1.10374	1
1984	1900	4979.175	83798.61	438.0048	1.1302	1.965517
1986	11600	4230.533	68708.33	343.9372	1.15441	1.67647
1988	2000	3944.433	64208.33	331.5573	1.163575	1.352941

PRIMARY CHANNEL CROSSECTIONAL WIDTH (ft.)

	XSECTION	1971	1972	1974	1976	1978	1979	1980	1982	1983	1984	1986	1988	STD DEV. AT X-SECT
1	1	42.394	105.0216	86.718	77.08	104.068	97.3136	83.8246	101.1676	208.7683	144.626	126.4666	180.6833	41.02657
	2	90.669	174.3936	110.8025	86.3865	141.6346	103.0945	76.163	126.1455	256.9333	126.4666	180.6833	224.8166	52.91126
	3	66.4816	330.4606	183.066	120.4375	146.462	117.647	79.007	193.6635	449.6333	272.9916	353.2833	192.7	114.0466
	4	96.36	269.76	125.255	125.255	120.4376	240.676	164.16	125.255	353.2833	256.9333	289.05	256.9333	81.63746
5	5	173.43	211.97	96.35	240.675	308.32	443.21	269.76	211.97	642.3333	513.8666	658.3916	674.45	197.9210
	6	144.626	173.43	183.795	77.08	164.16	676.1	366.13	269.05	658.3916	481.75	433.575	562.0416	191.6206
	7	164.16	173.43	144.626	77.08	231.24	639.56	211.97	211.97	126.4666	497.6083	369.3416	385.4	144.6166
	8	125.255	211.97	183.795	115.62	173.43	385.4	192.7	211.97	513.8666	610.2166	272.9916	289.05	149.1602
	9	134.89	202.335	164.16	125.255	250.61	376.765	289.05	221.605	529.925	449.6333	481.75	321.1666	132.7483
10	10	183.065	327.59	221.605	86.715	231.24	289.05	346.86	173.43	433.575	353.2833	545.9833	529.925	135.0971
	11	164.16	183.795	192.7	86.715	221.605	462.48	414.305	317.955	658.3916	529.925	272.9916	385.4	164.9341
	12	134.89	260.146	96.35	134.89	228.4225	163.795	173.43	134.89	594.1583	465.6916	658.3916	545.9833	197.4327
	13	77.08	250.61	279.416	86.715	183.065	202.335	134.89	154.16	529.925	433.575	321.1666	353.2833	133.6673
	14	173.43	289.76	173.43	77.08	183.065	116.62	125.255	77.08	658.3916	240.875	369.3416	369.3416	166.9126
15	15	202.335	231.24	192.7	96.35	240.675	125.255	134.89	202.335	578.1	417.5166	289.05	353.2833	131.7338
	16	154.16	250.61	211.97	144.625	366.13	337.225	366.13	317.955	369.3416	385.4	289.05	337.225	81.28603
	17	327.59	250.61	250.61	86.715	202.335	433.575	587.735	327.59	931.3833	931.3833	272.9916	240.875	263.7566
	18	134.89	134.89	154.16	144.625	134.89	491.385	684.085	269.76	1172.258	1156.2	529.926	337.225	366.9382
	19	105.986	231.24	183.065	115.62	183.065	250.61	366.13	211.97	513.8666	417.5166	497.6083	337.225	133.9976
20	20	144.626	173.43	173.43	96.35	192.7	183.065	231.24	173.43	545.9833	481.75	497.6083	513.8666	163.0294
	21	183.065	134.89	164.16	154.16	183.795	183.065	211.97	211.97	513.8666	417.5166	449.6333	465.6916	138.4487
	22	211.97	211.97	173.43	144.625	166.6125	202.335	250.61	211.97	385.4	305.1083	305.1083	385.4	77.89107
	23	144.626	154.16	125.255	173.43	105.986	134.89	116.62	144.626	256.9333	240.876	272.9916	224.8166	66.12609
	24	250.61	221.605	240.875	173.43	144.626	231.24	289.76	337.225	385.4	337.225	369.3416	369.3416	77.21880
25	25	327.59	250.61	173.43	125.255	183.795	317.955	423.94	443.21	626.275	465.6916	208.7583	208.7583	146.3679
	26		134.89	96.35	96.35	116.62	173.43	211.97	269.76	529.925	449.6333	272.9916	224.8166	136.7938
	27		250.61	183.795	96.35	144.625	433.575	279.416	462.48	513.8666	545.9833	224.8166	401.4583	150.6244
	28		337.225	154.16	154.16	231.24	250.61	250.61	240.876	369.3416	385.4	176.6416	208.7583	77.49801
	29		221.605	192.7	115.62	240.875	192.7	269.76	269.05	529.925	385.4	240.875	353.2833	107.7253
30	30		289.05	173.43	154.16	173.43	260.146	269.05	298.685	449.6333	0	256.9333	224.8166	88.07403
	31		231.24	134.89	96.35	211.97	154.16	183.795	240.875	481.75	0	465.6916	305.1083	101.9236
	32		279.416	173.43	183.795	164.16	134.89	366.13	260.146	497.6083	0	385.4	176.6416	113.6472
	33		250.61	96.35	356.495	231.24	116.62	183.795	125.255	417.5166	0	176.6416	176.6417	77.08735
34	34		211.97	192.7	211.97	298.685	144.626	202.335	308.32	369.3416	0	192.7	176.6416	81.38770

	MEAN 71	MEAN 72	MEAN 74	MEAN 76	MEAN 78	MEAN 79	MEAN 80	MEAN 82	MEAN 83	MEAN 84	MEAN 86	MEAN 88
	187.6129	222.6236	164.7868	130.1868	192.4732	260.7117	267.6098	232.3461	601.5867	438.0048	343.9372	331.5873
STD DEV	87.90870	86.79907	44.91610	55.29840	86.84918	136.8818	134.3771	87.92869	190.0071	202.4174	136.3725	126.7748

APPENDIX 2

Arroyo Surface Classification Maps

SANTA CRUZ RIVER ARROYO SURFACES 1971

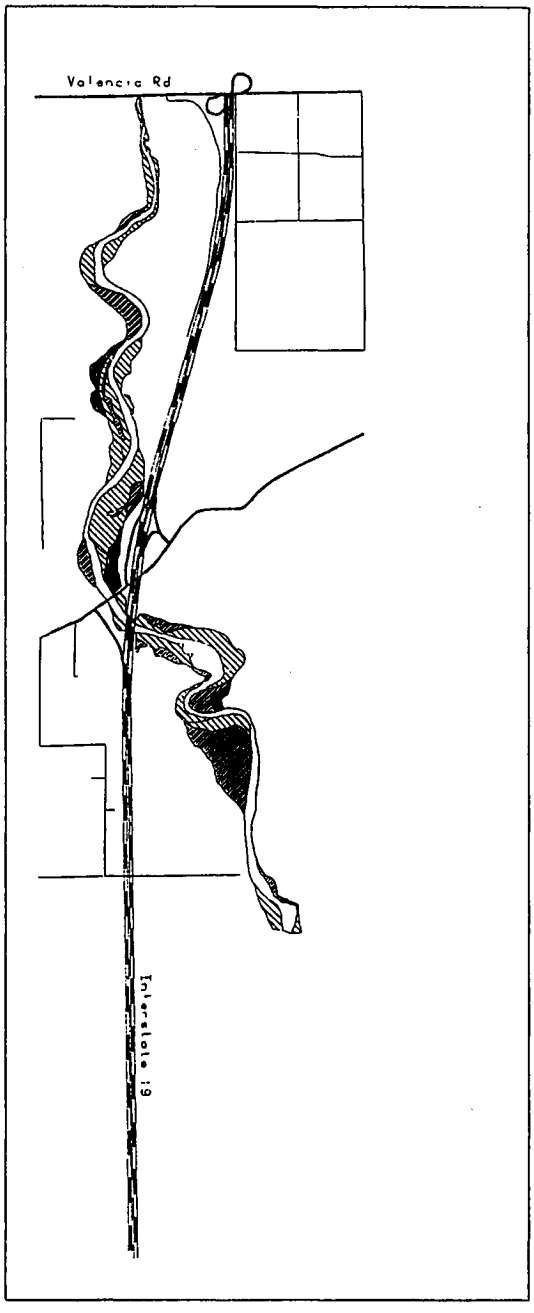

SANTA CRUZ RIVER

SAN XAVIER REACH

TUCSON, AZ

N

.5 0 .5
MILES

.5 0 .5
KILOMETERS

LEGEND

- PRIMARY CHANNEL
- NEWLY VEGETATED TERRACE
- SCRUB SURFACE
- MATURELY VEGETATED SURFACE

- INTERSTATE
- MAJOR ROAD
- SECONDARY ROAD

ARROYO SURFACES INTERPRETED FROM 1971 COOPER AERIAL COVERAGE - 1:12,000

SANTA CRUZ RIVER ARROYO SURFACES 1972

SANTA CRUZ RIVER

SAN XAVIER REACH

TUCSON, AZ

N

.5 0 .5
MILES

.5 0 .5
KILOMETERS

LEGEND

- PRIMARY CHANNEL
- NEWLY VEGETATED TERRACE
- SCRUB SURFACE
- MATURELY VEGETATED SURFACE

- INTERSTATE
- MAJOR ROAD
- SECONDARY ROAD

ARROYO SURFACES INTERPRETED FROM 1972 COOPER AERIAL COVERAGE - 1:30,000

SANTA CRUZ RIVER ARROYO SURFACES 1974

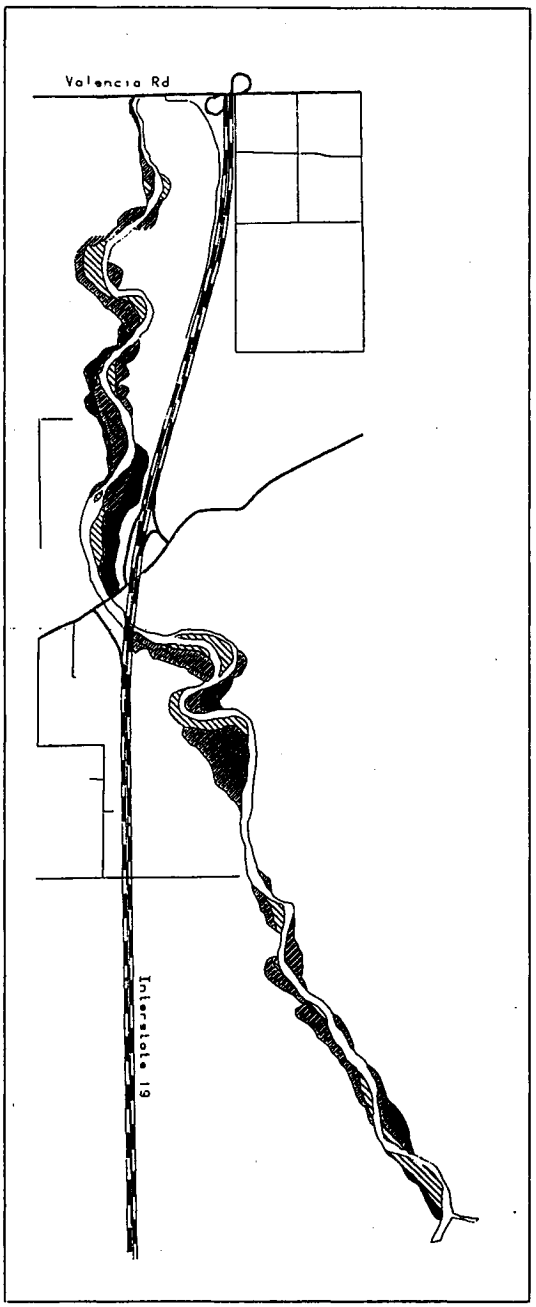

SANTA CRUZ RIVER

SAN XAVIER REACH

TUCSON, AZ

N

.5 0 .5
MILES

.5 0 .5
KILOMETERS

LEGEND

- PRIMARY CHANNEL
- NEWLY VEGETATED TERRACE
- SCRUB SURFACE
- MATURELY VEGETATED SURFACE
- INTERSTATE
- MAJOR ROAD
- SECONDARY ROAD

ARROYO SURFACES INTERPRETED

FROM 1974 COOPER AERIAL

COVERAGE - 1:20,500

SANTA CRUZ RIVER ARROYO SURFACES 1976

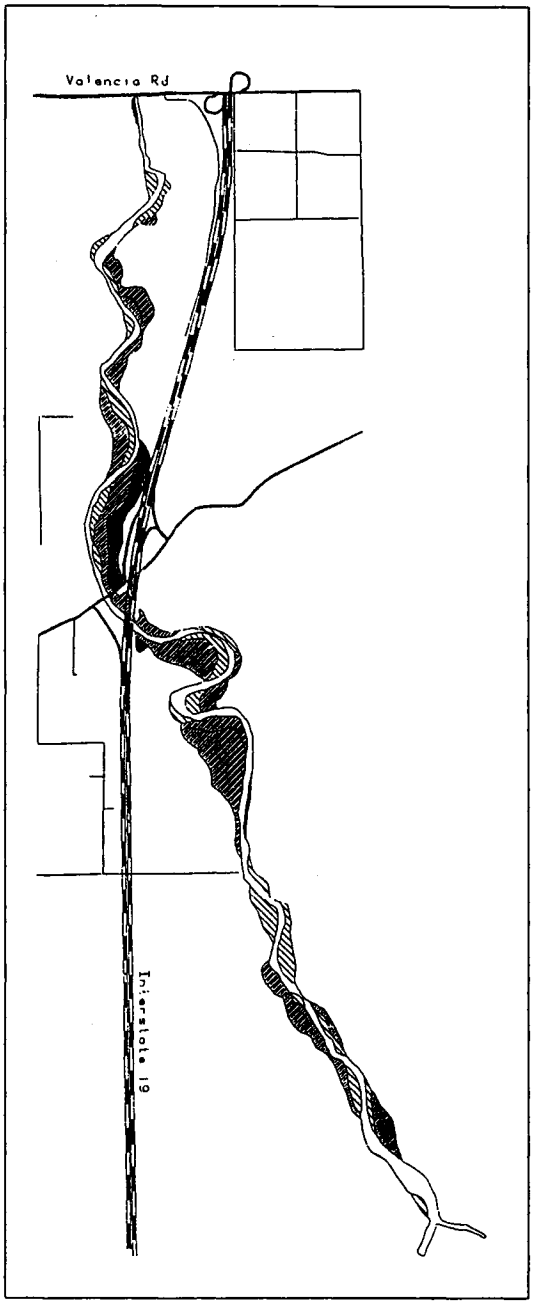

SANTA CRUZ RIVER

SAN XAVIER REACH

TUCSON, AZ

N

.5 0 .5
MILES

.5 0 .5
KILOMETERS

LEGEND

- PRIMARY CHANNEL
- NEWLY VEGETATED TERRACE
- SCRUB SURFACE
- MATURELY VEGETATED SURFACE

- INTERSTATE
- MAJOR ROAD
- SECONDARY ROAD

ARROYO SURFACES INTERPRETED FROM 1976 COOPER AERIAL COVERAGE - 1:20,500

SANTA CRUZ RIVER ARROYO SURFACES 1978

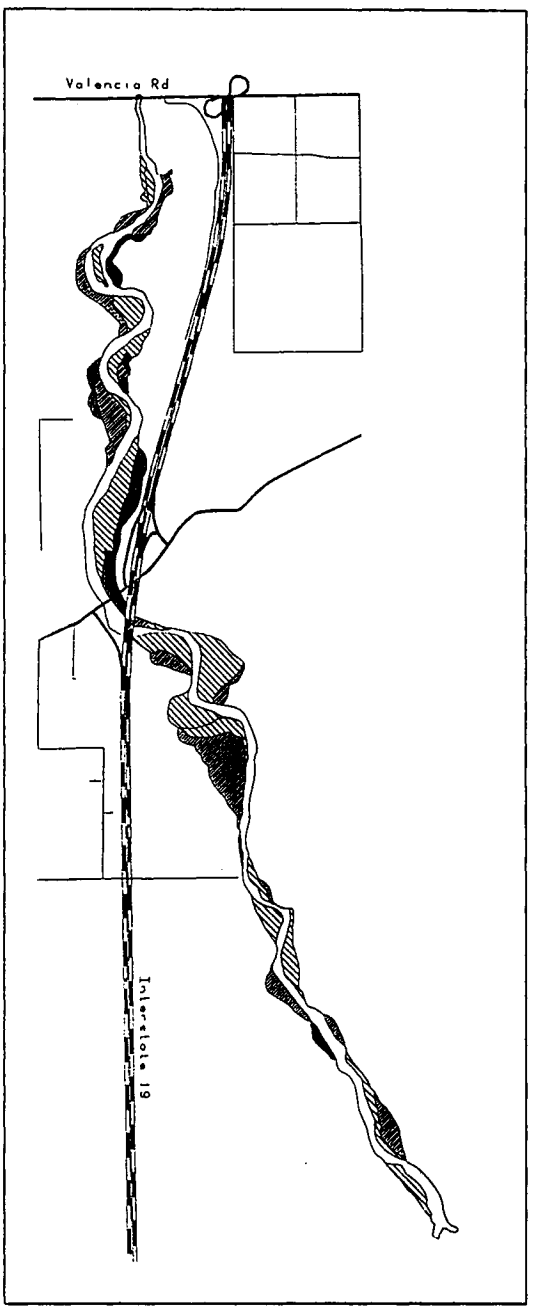

SANTA CRUZ RIVER

SAN XAVIER REACH

TUCSON, AZ

N

.5 0 .5
MILES

.5 0 .5
KILOMETERS

LEGEND

- PRIMARY CHANNEL
- NEWLY VEGETATED TERRACE
- SCRUB SURFACE
- MATURELY VEGETATED SURFACE

- INTERSTATE
- MAJOR ROAD
- SECONDARY ROAD

ARROYO SURFACES INTERPRETED FROM 1978 COOPER AERIAL COVERAGE - 1:21,500

SANTA CRUZ RIVER ARROYO SURFACES 1979

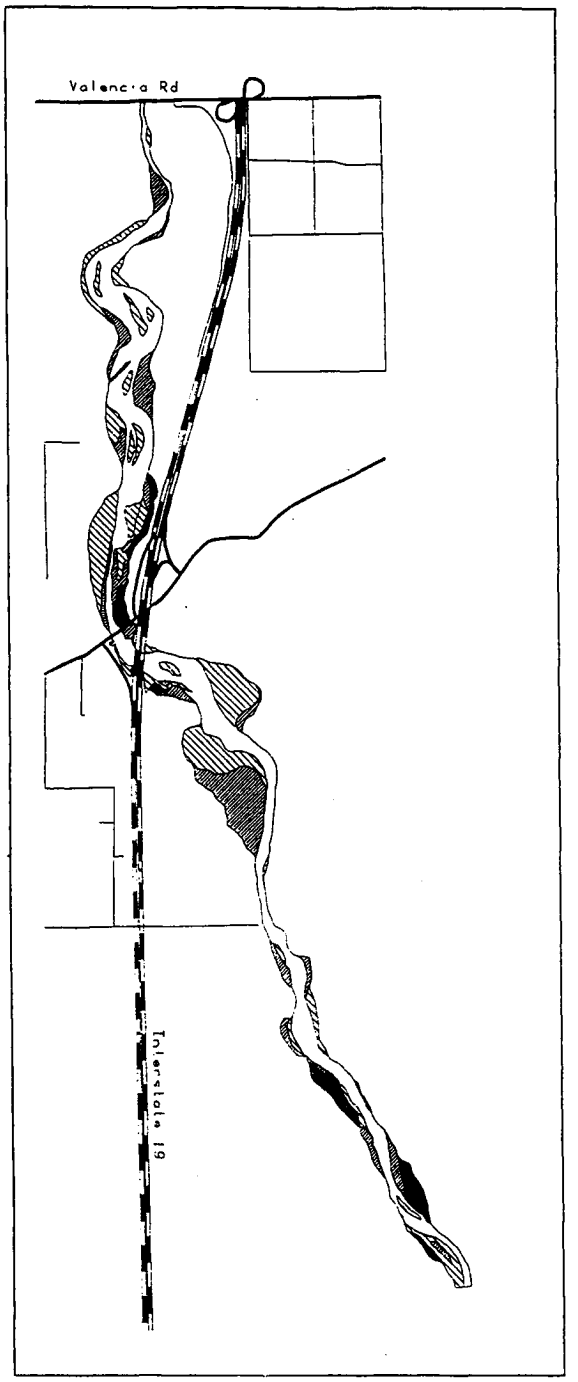

SANTA CRUZ RIVER

SAN XAVIER REACH

TUCSON, AZ

N

.5 0 .5
MILES

.5 0 .5
KILOMETERS

LEGEND

- PRIMARY CHANNEL
- NEWLY VEGETATED TERRACE
- SCRUB SURFACE
- MATUPELY VEGETATED SURFACE
- MAN-MADE FEATURE
- INTERSTATE
- MAJOR ROAD
- SECONDARY ROAD

ARROYO SURFACES INTERPRETED FROM 1979 COOPER AERIAL COVERAGE - 1 :2 000

SANTA CRUZ RIVER ARROYO SURFACES 1980

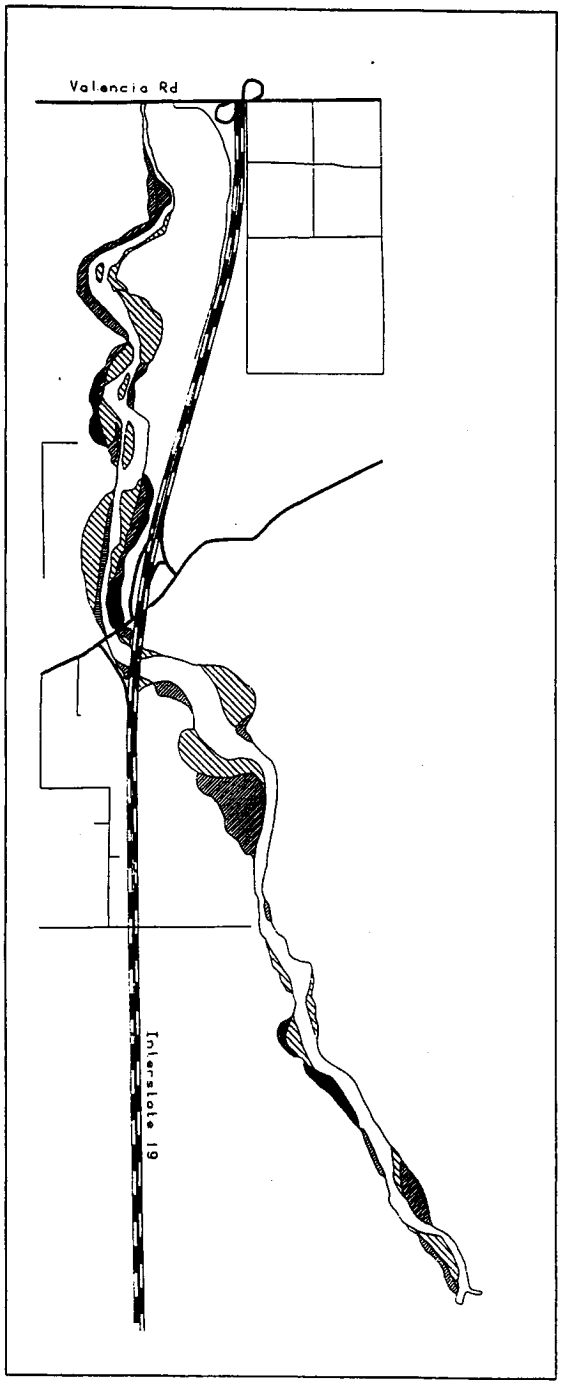

SANTA CRUZ RIVER

SAN XAVIER REACH

TUCSON, AZ

N

.5 0 .5
MILES

.5 0 .5
KILOMETERS

LEGEND

- PRIMARY CHANNEL
- NEWLY VEGETATED TERRACE
- SCRUB SURFACE
- MATURELY VEGETATED SURFACE
- MAN-MADE FEATURE
- INTERSTATE
- MAJOR ROAD
- SECONDARY ROAD

ARROYO SURFACES INTERPRETED FROM 1980 COOPER AERIAL COVERAGE - 1 20,000

SANTA CRUZ RIVER ARROYO SURFACES 1982

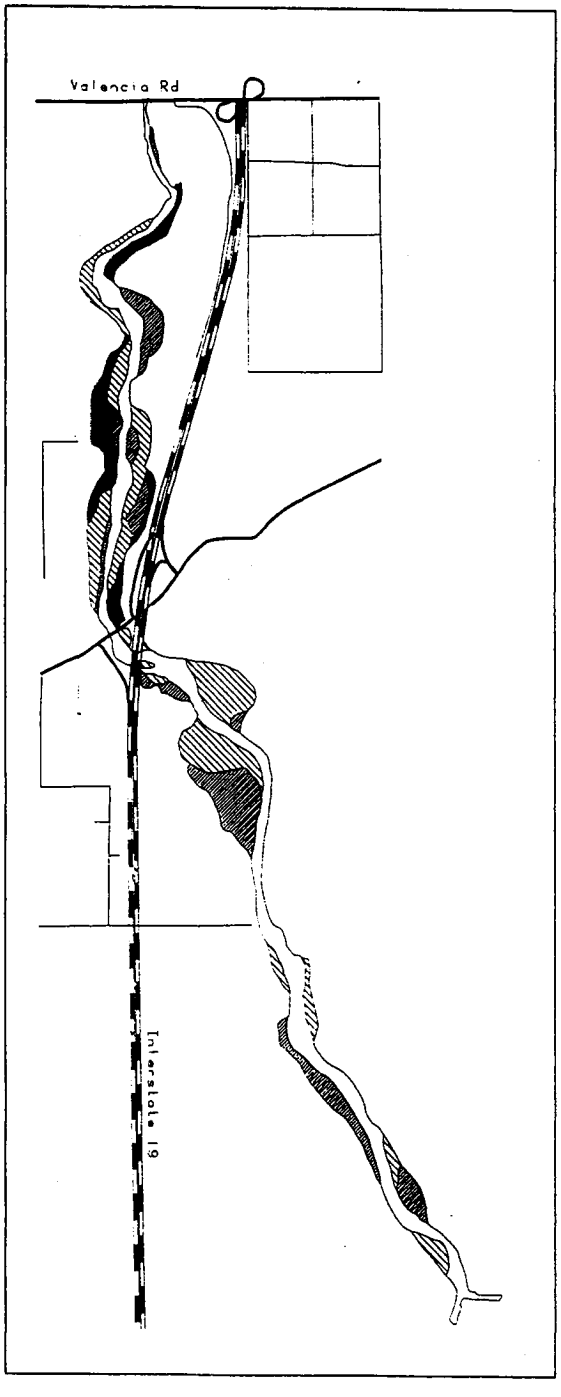

SANTA CRUZ RIVER

SAN XAVIER REACH

TUCSON, AZ

N

.5 0 .5
MILES

.5 0 .5
KILOMETERS

LEGEND

- PRIMARY CHANNEL
- NEWLY VEGETATED TERRACE
- SCRUB SURFACE
- MATURELY VEGETATED SURFACE
- MAN-MADE FEATURE
- INTERSTATE
- MAJOR ROAD
- SECONDARY ROAD

ARROYO SURFACES INTERPRETED FROM 1982 COOPER AERIAL COVERAGE - 1 30,000

SANTA CRUZ RIVER ARROYO SURFACES 1983

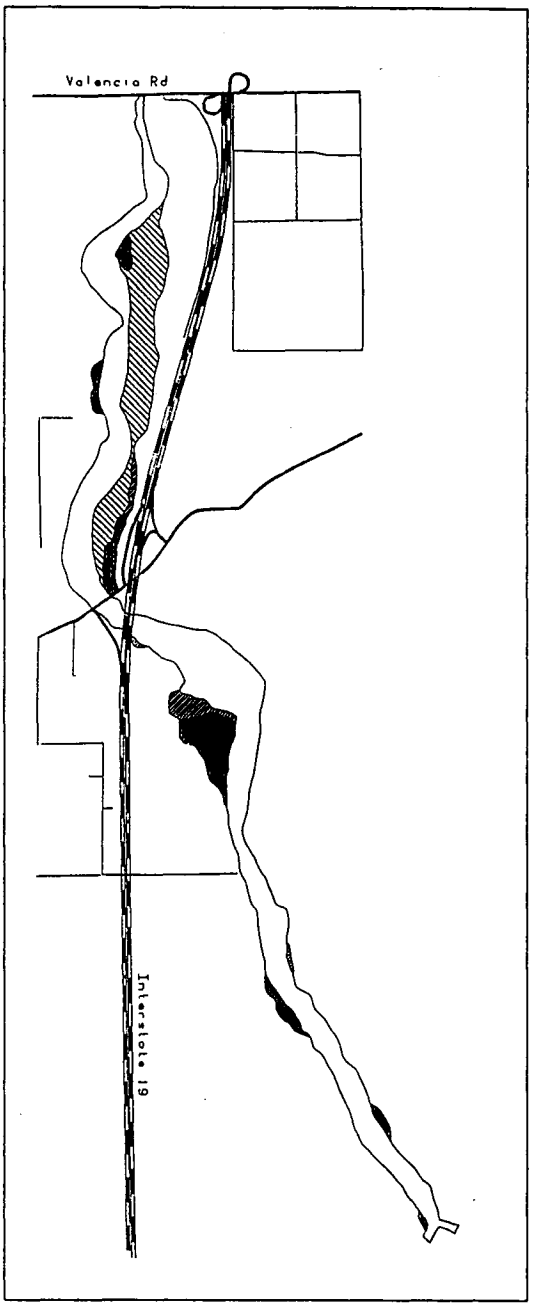

SANTA CRUZ RIVER

SAN XAVIER REACH

TUCSON, AZ

N

.5 0 .5
MILES

.5 0 .5
KILOMETERS

LEGEND

- PRIMARY CHANNEL
- NEWLY VEGETATED TERRACE
- SCRUB SURFACE
- MATURELY VEGETATED SURFACE
- INTERSTATE
- MAJOR ROAD
- SECONDARY ROAD

ARROYO SURFACES INTERPRETED FROM 1983 COOPER AERIAL COVERAGE - 1:12,000

SANTA CRUZ RIVER ARROYO SURFACES 1984

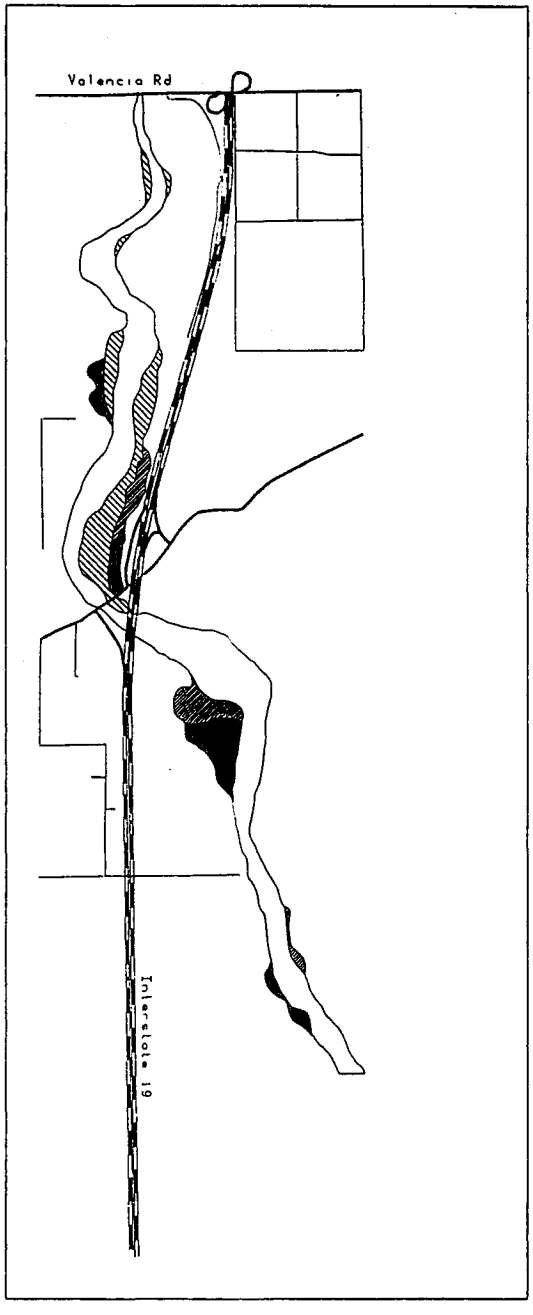

SANTA CRUZ RIVER

SAN XAVIER REACH

TUCSON, AZ

N

.5 0 .5
MILES

.5 0 .5
KILOMETERS

LEGEND

- PRIMARY CHANNEL
- NEWLY VEGETATED TERRACE
- SCRUB SURFACE
- MATURELY VEGETATED SURFACE

- INTERSTATE
- MAJOR ROAD
- SECONDARY ROAD

ARROYO SURFACES INTERPRETED FROM 1984 COOPER AERIAL COVERAGE - 1:15,000

SANTA CRUZ RIVER ARROYO SURFACES 1986

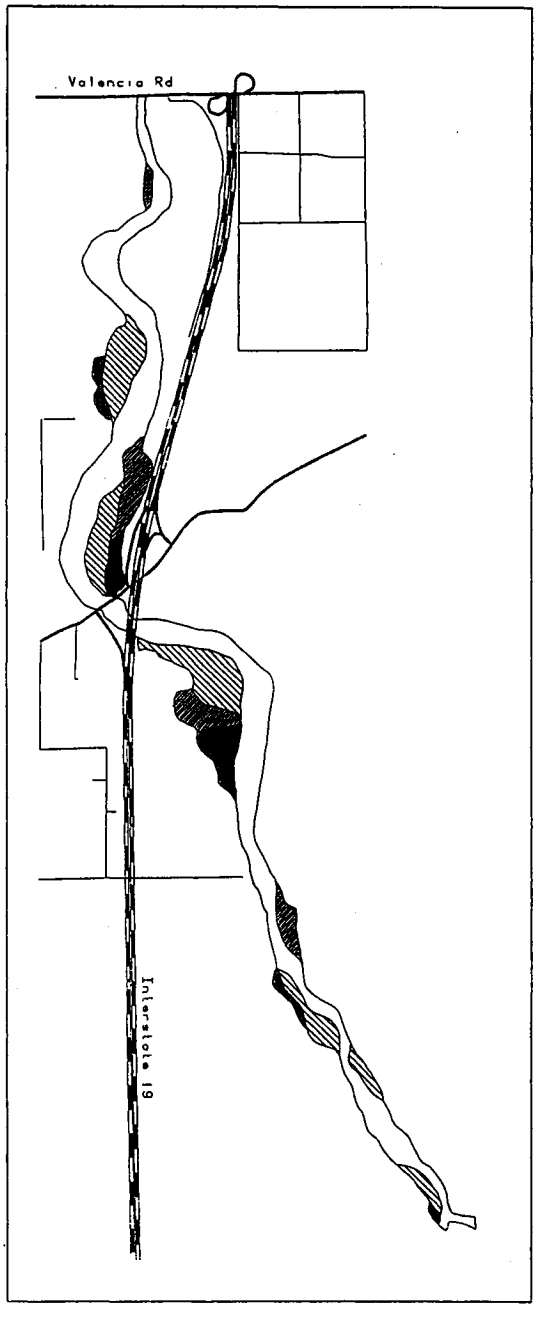

SANTA CRUZ RIVER

SAN XAVIER REACH

TUCSON, AZ

N

.5 0 .5
MILES

.5 0 .5
KILOMETERS

LEGEND

- PRIMARY CHANNEL
- NEWLY VEGETATED TERRACE
- SCRUB SURFACE
- MATURELY VEGETATED SURFACE

- INTERSTATE
- MAJOR ROAD
- SECONDARY ROAD

ARROYO SURFACES INTERPRETED

FROM 1986 COOPER AERIAL

COVERAGE - 1:24,000

SANTA CRUZ RIVER ARROYO SURFACES 1988

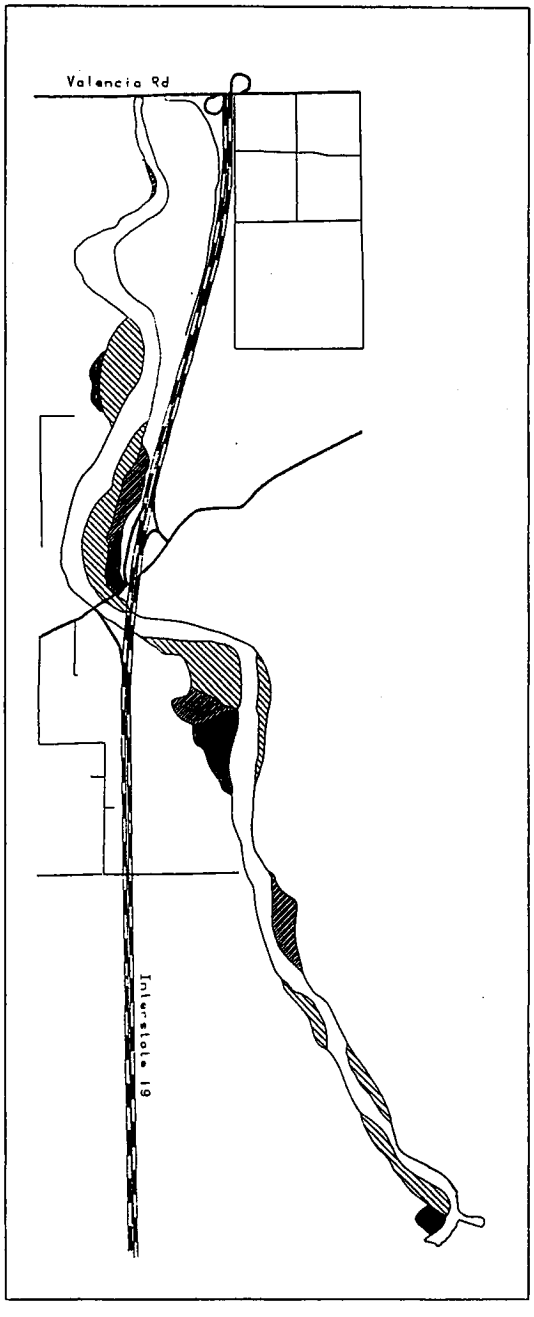

SANTA CRUZ RIVER

SAN XAVIER REACH

TUCSON, AZ

N

.5 0 .5
MILES

.5 0 .5
KILOMETERS

LEGEND

- PRIMARY CHANNEL
- NEWLY VEGETATED TERRACE
- SCRUB SURFACE
- MATURELY VEGETATED SURFACE

- INTERSTATE
- MAJOR ROAD
- SECONDARY ROAD

ARROYO SURFACES INTERPRETED FROM 1988 COOPER AERIAL COVERAGE - 1:40,000

LIST OF REFERENCES

Ambrosia, Vincent and Whiteford, Gary T. 1983. Areal photograph interpretation in remote sensing. Chapter 4 in Richason, Benjamin F. Jr. ed. 1983. Introduction to Remote Sensing of the Environment. Dubuque, Iowa: Kendall/Hunt Publishing Company.

Baker, Victor R. 1977. Stream-channel response to floods, with examples from central Texas. Bulletin of the United States Geological Society 88:1057-1071.

Betancourt, Julio L. and Turner, Raymond M. 1985. Historic arroyo-cutting and subsequent channel changes at the Congress Street crossing, Santa Cruz River, Tucson, Arizona. Arid Lands, Today and Tomorrow: Proceedings of the International Arid Lands Research and Development Conference, October 1985.

Burkham, D.E. 1972. Channel changes of the Gila River in Safford Valley, Arizona 1846-1970. United States Geological Survey Professional Paper 655G:G1-G24.

Chorley, Richard J. 1962. Geomorphology and general systems theory. United States Geological Survey Professional Paper 500B:B1-B10.

Cooke, Ronald U. and Reeves, Richard W. 1976. Arroyos and Environmental Change in the American South-West. Oxford: Clarendon Press.

Dury, G.H. 1964. Principles of underfit streams. United States Geological Survey Professional Paper 452A:A1-A67.

Environmental Systems Research Institute. 1987. ARC/INFO Users Manual. Redlands California: ESRI.

Graf, William L. 1979. Catastrophe theory as a model for change in fluvial systems. in Rhodes, Dallas D. and Williams Garnett P. eds. 1979. Adjustments of the Fluvial System. Dubuque, Iowa: Kendall/Hunt Publishing Company. pp. 13-32.

--------. 1981. Channel instability in a braided, sand bed river. Water Resources Research 17(4):1087-1093.

Haynes, C. Vance Jr. and Huckell, Bruce. 1986. Sedimentary Successions of the Prehistoric Santa Cruz River, Tucson, Arizona. Unpublished manuscript. University of Arizona and Arizona State Museum.

Gupta, Avijit and Fox H. 1974. Effects of high-magnitude floods on channel form: A case study in Maryland Piedmont. Water Resources Research 10(3):499-509.

Jens, Stifel W. and McPherson, M.B. 1964. Hydrology of urban areas. in Chow, V.T. ed. Handbook of Applied Hydrology. New York: McGraw Hill Book Company.

Knighton, A. David. 1977. Short term changes in hydraulic geometry. in Gregory, K.J. ed. River Channel Changes. New York: John Wiley & Sons.

Knighton, David. 1984. Fluvial Forms and Processes. London: Edward Arnold Ltd.

Langbein, Walter B. and Leopold, Luna B. 1964. Quasi-equilibrium states in channel morphology. American Journal of Science 262:782-794.

Leopold, L.B., Emmett, W.W. and Myrick, R.M. 1966. Channel and hillslope processes in a semi-arid area, New Mexico. United States Geological Survey Professional Paper 352G:153-253.

Leopold, L.B. and Miller, J.P. 1956. Ephemeral streams - hydraulic factors and their relation to the drainage net. United States Geological Survey Professional Paper 282A.

Leopold, Luna B., Wolman, M. Gordon and Miller, John P. 1964. Fluvial Processes in Geomorphology. San Francisco: W. H. Freeman and Company.

Maddock, Thomas. 1969. The behavior of straight open channels with movable beds. United States Geological Survey Professional Paper 622A:A1-A70.

Nordin, C.F. and Beverage, J.P. 1965. Sediment transport in the Rio Grande New Mexico. United States Geological Survey Professional Paper 462F:F1-F35.

Pearthree, Marie Slezak and Baker, Victor R. 1987. Channel Change along the Rillito Creek System of Southeastern Arizona 1941 through 1983: Implications for Floodplain Management. Arizona Bureau of Geology and Mineral Technology Geological Survey Branch, Special Paper 6.

Ritter, Dale F. 1986. Process Geomorphology. Dubuque, Iowa: Wm. C. Brown Publishers.

Saarinen, T.F., Baker, V.R., Durrenberger, R., Maddock, T., Jr. 1984. The Tucson, Arizona Flood of October 1983. Washington D.C.: National Academy Press.

Schumm, S.A. 1961. Effect of sediment characteristics on erosion and deposition in ephemeral-stream channels. United States Geological Survey Professional Paper 352C:31-70.

Schumm, S.A. and Lichty, R.W. 1963. Channel widening and flood-plain construction along Cimarron River in Southwestern Kansas. United States Geological Survey Professional Paper 352D:71-88.

----------. 1965. Time, space, and causality in geomorphology. American Journal of Science 263:110-119.

Sellers, Willaim D., Hill, Richard H. and Sanderson-Rae, Margaret. 1985. Arizona Climate: The First Hundred Years. Tucson: University of Arizona Press.

Stewart, John H. and LaMarche, Valmore C. Jr. 1967. Erosion and deposition produced by the flood of December 1964 on Coffee Creek Trinity County, California. United States Geological Survey Professional Paper 422K:K1-K22.

Waters, Michael R. 1988. Holocene alluvial geology and geoarchaeology of the San Xavier reach of the Santa Cruz River, Arizona. Bulletin of the Geological Society of America 100:479-491.

Webb, Robert H. September 1988. Personal Communication.

Webb, Robert H. and Betancourt, Julio L. 1987. Flood Frequency and Erosion Potential in Ephemeral-Stream Channels: A case Study of the Santa Cruz River, Pinal, Pima, and Santa Cruz Counties, Arizona. Unpublished Project Proposal, United States Geological Survey, Water Resources Division, Arizona District.

Wolman, M. Gordon and Miller, John P. 1960. Magnitude and frequency of forces in geomorphic processes. Journal of Geology 68:54-74.